UC Irvine
UC Irvine Electronic Theses and Dissertations

Title

The Effect of Organics on Particle Formation and Growth from Methanesulfonic Acid, Amines and Water

Permalink

https://escholarship.org/uc/item/7t2569fx

Author

Arquero, Kristine Dahl

Publication Date

2017

Copyright Information

Peer reviewed|Thesis/dissertation

UNIVERSITY OF CALIFORNIA,
IRVINE

The Effect of Organics on Particle Formation and Growth from Methanesulfonic Acid, Amines
and Water

DISSERTATION

submitted in partial satisfaction of the requirements
for the degree of

DOCTOR OF PHILOSOPHY

in Chemistry

by

Kristine Dahl Arquero

Dissertation Committee:
Professor Barbara J. Finlayson-Pitts, Chair
Assistant Professor Craig Murray
Professor Sergey A. Nizkorodov

2017

DEDICATION

To my parents and my first teachers, Aquilino and Dahlia, for their sacrifices and unconditional love.

To my Kuyas, Daryl and Jason, for always having my back.

To my love, Mark, for being an equal partner.

To our son, Joaquin, for his smiles and laughter that encouraged me as I completed this work.

"If your dreams do not scare you, they are not big enough." –Ellen Johnson Sirleaf

"It is impossible to live life without failing at something, unless you live so cautiously that you might as well not have lived at all – in which case, you fail by default." – J. K. Rowling

TABLE OF CONTENTS

LIST OF FIGURES

viii

ACKNOWLEDGEMENTS

First and foremost, thank you to my love, Mark, I could not have done this without you. Thank you for understanding and for always knowing what to say. I love you.

Professor Finlayson-Pitts, thank you for your mentorship, time and investment in my growth. On a personal level, your support and leadership both inside and outside the lab has helped shape me into a more confident woman, scientist and scholar. I will be forever grateful.

To my committee members, Professor Nizkorodov and Professor Murray, thank you for your support. Professor Nizkorodov, you have been an amazing ally and I appreciate your help in getting me to the next stage of my career. Professor Murray, with every run-in, whether on the 3rd floor or on ring road, you provided words of wisdom that were comforting as I completed this dissertation.

Thank you to my collaborators Professor R. Benny Gerber, Dr. Mychel Varner and Dr. Jing Xu for your help in making sense of my experimental results. I appreciate your awesome work.

A huge thank you to all members of the Finlayson-Pitts group (past, present and extended), especially to Mike Ezell, Dr. Véronique Perraud and Dr. Lisa Wingen. Thank you for teaching me the ropes. On numerous occasions you dropped what you were working on to answer a question or check something out. I will always remember your generosity in helping me work through experimental challenges.

Michelle Fairhurst and Allison Vander Wall, it has been an honor sharing an office and building a safe space between the three of us. Truly, no one else knows or fully understands our adventures of graduate school. Thank you for providing a laughter filled oasis when I needed it most and for practicing Shine Theory like a boss. This experience would not have been the same without you two.

As an undergraduate I had the privilege of finding strong female mentors who helped me navigate the big and often scary world of Cal. Thank you to the "Superwomen of Chemistry," Dr. Michelle Douskey, Dr. Christina Stuart, Anna del Rosario, Hemamala Karunadasa and Tatiana Lim. You supported me as I pursued my B.S. and planted the Ph. D. seed.

Thank you to my high school chemistry teacher, Mr. Langdale. You first introduced me to chemistry, encouraged me to tutor and started me on the path to my career as a chemist and educator.

Thank you to the friendships that have sustained me. To my friends from 2nd grade, junior high, high school, college, NYC and beyond thank you for being my confidants, for your emotional support and for your time. Your intelligence, strength, courage, wisdom and independence inspire me.

Words cannot fully express my immense gratitude for my family for supporting me in ways big and small. Momma, Daddy, Kuya Daryl and Kuya Jason, thank you for being my foundation. A special thank you to Daddy for sparking my interest in finding out how things work. Joaquin, I may have birthed you, but you have given me life in unexpected ways, thank you. I am so proud to be your Momma. Thank you to our family and friends who comprise the village that is helping us raise Joaquin and, by extension, has supported my graduate studies.

CURRICULUM VITAE
KRISTINE DAHL ARQUERO

EDUCATION

University of California, Irvine   Irvine, California
Ph.D. in Chemistry   2017
GPA: 3.97
Advisor: Professor Barbara J. Finlayson-Pitts

City University of New York – Lehman College   Bronx, New York
M.Ed. in Science Education   2010
GPA: 3.90
Thesis: Experiencing Regents Chemistry: A Hands-On Approach to Abstract Concepts

University of California, Berkeley   Berkeley, California
B.S. in Chemistry with Honors   2008
GPA: 3.62

RESEARCH EXPERIENCE

University of California, Irvine   Irvine, California
Graduate Research Assistant, Finlayson-Pitts Group   2013 – 2017
Advisor: Professor Barbara J. Finlayson-Pitts
- Researched the mechanism of new particle formation and growth from methanesulfonic acid, amines, water, and organics in an aerosol flow reactor system

University of California, Berkeley   Berkeley, California
Undergraduate Research Assistant, Long Group   2006 – 2007
Advisor: Professor Jeffrey R. Long
- Researched the magnetic properties of cyano-ligated chromium complexes

TEACHING EXPERIENCE

University of California, Irvine   Irvine, California
Instructional Design Teaching Assistant, Chemistry 12   Mar 2016 – June 2016
Supervisor: Dr. Renee Link
- Aided in the design and development of an updated general chemistry course for non-science majors that will transition to a massive open online course

Lab Teaching Assistant, AirUCI Summer Workshop   July 2014
Supervisors: Professor Sergey Nizkorodov & Dr. Mickey Laux
- Led an experiment to determine the concentration of additives in gasoline using Fourier transform infrared spectroscopy for 20 high school science teachers

Discussion Teaching Assistant, Chemistry 1B   Jan 2014 – June 2014
Supervisor: Professor Sergey Nizkorodov
- Led four discussion sections for 171 undergraduates in introductory chemistry
- Guided students through problems and supported their learning with careful questioning

Analytical Lab Teaching Assistant, Chemistry 151L/2LB/3LC   Sep 2012 – June 2013
Supervisors: Professor Rob Corn & Dr. Kim Edwards
- Assisted in transitioning the upper division analytical lab (151L) to a lower division analytical lab (3LC) by testing suitability of select experiments

iMentor   New York City, New York
Program Coordinator, Lower East Side Preparatory High School   Aug 2011 – July 2012
- Conducted weekly lessons on topics ranging from social media to college prep for 80 recent Chinese immigrants
- Facilitated mentor-mentee relationships between students and professionals by guiding them through language and generational barriers

Mott Hall Bronx High School   Bronx, New York
Chemistry Teacher, International Baccalaureate & Regents Chemistry   Sep 2008 – June 2011
- Designed and implemented challenging, interactive, and scaffolded Regents chemistry curriculum for 150 high school students in grades 10 – 12

University of California, Berkeley – College of Chemistry   Berkeley, California
Undergraduate Student Instructor, Chem 1A   July 2007 – May 2008
Supervisors: Dr. Michelle Douskey & Dr. Christina Stuart
- The only undergraduate student instructor amongst dozens of graduate student instructors
- Facilitated discussion for class of thirty undergraduates during weekly four-hour laboratory sessions

PUBLICATIONS

Arquero, K. D.; Xu, J.; Gerber, R. B.; Finlayson-Pitts, B. J. Particle Formation and Growth from Oxalic Acid, Methanesulfonic Acid, Trimethylamine and Water: A Combined Experimental and Theoretical Study. *Phys. Chem. Chem. Phys.*, Under review.

Arquero, K. D.; Gerber, R. B.; Finlayson-Pitts, B. J. The Role of Oxalic Acid in New Particle Formation from Methanesulfonic Acid, Methylamine, and Water. *Environ. Sci. Tech.*, **2017**, 2124-2130.

Chen, H.; Ezell, M. J.; Arquero, K. D.; Varner, M. E.; Dawson, M. L.; Gerber, R. B.; Finlayson-Pitts, B. J. New Particle Formation and Growth from Methanesulfonic Acid, Trimethylamine, and Water. *Phys. Chem. Chem. Phys.*, **2015**, 13699-13709.

Ezell, M. J.; Chen, H.; Arquero, K. D.; Finlayson-Pitts, B. J. Aerosol Fast Flow Reactor for Laboratory Studies of New Particle Formation. *J. Aerosol Sci.*, **2014**, 78, 30-40.

Dawson, M. L.; Perraud, V.; Gomez, A.; Arquero, K. D.; Ezell, M. J.; Finlayson-Pitts, B. J. Measurement of gas-phase ammonia and amines in air by collection onto an ion exchange resin and analysis by ion chromatography. *Atmos. Meas. Tech. Discuss.*, **2014**, 7, 1573-1602.

Nishino, N.; Arquero, K. D.; Dawson, M. L.; Finlayson-Pitts, B. J. Infrared Studies of the Reaction of Methanesulfonic Acid with Trimethylamine on Surfaces and Atmospheric Implications. *Environ. Sci. Technol.*, **2014**, 48 (1), 323-330.

Karunadasa, H. I.; Arquero, K. D.; Berben, L. A.; Long, J. R. Enhancing the magnetic anisotropy of cyano-ligated Cr(II) and Cr(III) complexes via heavy-halide ligand effects. *Inorg. Chem.*, **2010**, 49, 4738-4740.

PRESENTATIONS

*Presenting author(s)

*Arquero, K. D.; Xu, J.; Gerber, R. B.; Finlayson-Pitts, B. J. The Role of Oxalic Acid in New Particle Formation from Methanesulfonic Acid, Methylamine, and Water. 34th Informal Symposium on Kinetics and Photochemical Processes in the Atmosphere. University of California, San Diego. May 12, 2017. Poster Presentation.

*Arquero, K. D.; *Perraud, V.; *Xu, J. "Particles Through the Looking Glass." Science and Societal Impacts of Air Quality and Climate Issues: Past, Present, and Future. The Arnold and Mabel Beckman Center, Irvine, CA. April 18, 2017. Oral Presentation.

*Arquero, K. D.; Xu, J.; Gerber, R. B.; Finlayson-Pitts, B. J. "Investigating the Effect of Organics on New Particle Formation and Growth from Methanesulfonic Acid, Methylamine, and Water." 33rd Informal Symposium on Kinetics and Photochemical Processes in the Atmosphere. University of California, Irvine. March 24, 2016. Poster Presentation.

*Arquero, K. D.; Xu, J.; Varner, M. E.; Gerber, R. B.; Finlayson-Pitts, B. J. "New Particle Formation in the Atmosphere." 16th Annual Orange County Achievement Rewards for College Scientists Scholar Awards Dinner. The Arnold and Mabel Beckman Center, Irvine, CA. March 23, 2016. Invited Talk.

*Arquero, K. D.; *Xu, J.; Gerber, R. B.; Finlayson-Pitts, B. J. "Investigating the Effect of Organics on New Particle Formation and Growth from Methanesulfonic Acid, Methylamine, and Water." 251st American Chemical Society National Meeting and Exposition: Computers in Chemistry. San Diego Convention Center. March 16, 2016. Poster Presentation.

*Arquero, K.D.; Ezell, M.J.; *Varner, M.E.; Gerber, R.B.; Finlayson-Pitts, B.J. "Exploring the Effect of Organics on New Particle Formation and Growth from Methanesulfonic Acid, Amines, and Water." 32nd Informal Symposium on Kinetics and Photochemical Processes in the Atmosphere. California State University, Northridge. April 3, 2015. Poster Presentation.

*<u>Arquero, K. D.</u>; Ezell, M. J.; Finlayson-Pitts, B. J. "New Particle Formation and Growth from Methanesulfonic Acid, Amines, Water, and Organics." American Geophysical Union 47th Annual Fall Meeting. Moscone Center, San Francisco, CA. December 16, 2014. Poster Presentation.

*<u>Arquero, K. D.</u>; Ezell, M. J.; Finlayson-Pitts, B.J. "New Particle Formation and Growth from Methanesulfonic Acid, Trimethylamine, Water, and Organics." 2014 Ford Conference. University of California, Irvine, CA. September 27, 2014. Oral Presentation.

*<u>Arquero, K. D.</u>; Ezell, M. J.; Finlayson-Pitts, B.J. "New Particle Formation and Growth from Methanesulfonic Acid, Trimethylamine, Water, and Organics." 2nd Annual Air UCI Retreat. University of California, Irvine, CA. September 2, 2014. Invited Talk.

*<u>Arquero, K. D.</u>; Nishino, N.; Dawson, M. L.; Finlayson-Pitts, B. J. "Heterogeneous Reaction of Methanesulfonic Acid with Trimethylamine on Surfaces: Implications for Laboratory and Atmospheric Measurements." 31st Informal Symposium on Kinetics and Photochemical Processes in the Atmosphere. University of California, Riverside, CA. March 12, 2014. Poster Presentation.

*<u>Arquero, K.D.</u>; Nishino, N.; Dawson, M.L.; Finlayson-Pitts, B.J. "Heterogeneous Reaction of Methanesulfonic Acid with Trimethylamine on Surfaces: Implications for Laboratory and Atmospheric Measurements." 10th Annual Collaborative Workshop in Chemistry at Interfaces. AirUCI. Surf and Sand Hotel, Laguna Beach, CA. January 22-23, 2014. Poster Presentation.

HONORS & AWARDS

Pedagogical Fellowship, *Fellow*   Apr 2015 – Mar 2016
An advanced pedagogical, pre-professional program that prepares graduate students for a faculty position

Ford Foundation Predoctoral Fellowship, *Fellow*   Sep 2014 – June 2017
A three-year long fellowship that supports graduate students who show promise of achievement as future scholars and teachers and are committed to advancing diversity in the academia

Achievement Rewards for College Scientists Foundation, *Scholar*   Sep 2014 – May 2016
A scholarship that rewards doctoral students who have achieved academic success and exhibit outstanding promise as scientists, researchers and leaders

Michael E. Gebel Award, *Recipient*   May 2014
An award that recognizes excellence in graduate environmental chemistry research and a non-traditional trajectory to graduate studies

New York City Teaching Fellows, *Science Fellow*   June 2008 – May 2010
A two-year long fellowship that trains and supports college graduates for a career in primary or secondary public education in high needs areas of New York City

SERVICE

AirUCI Atmospheric Integrative Research, Irvine, California   2013 – 2017
- Conducted outreach to local primary and secondary school students to expose them to research opportunities
- Connected with primary and secondary school educators to support their efforts to promote STEM education

Iota Sigma Pi National Honor Society for Women in Chemistry, Irvine, California
                                                                                               2012 – 2017
- Participated in outreach to local youth to encourage and pique interest in the sciences

Center for Engaged Instruction, Irvine, California   Sep 2015, Sep 2016
- Designed and led the Teaching Assistant Professional Development Program for chemistry graduate students

PROFESSIONAL DEVELOPMENT

Center for Engaged Instruction   Irvine, California
Pedagogical Fellow   May 2015 – Feb 2016
- Studied pedagogy and best practices in Advanced Higher Education Pedagogy courses
- Incorporated strategies from University Studies courses in workshops for training of chemistry teaching assistants

American Chemical Society, *Member*   Jan 2015 – Present

American Geophysical Union, *Member*   Aug 2014 – Aug 2015

ABSTRACT OF THE DISSERTATION

The Effect of Organics on Particle Formation and Growth from Methanesulfonic Acid, Amines
and Water

By

Kristine Dahl Arquero

Doctor of Philosophy in Chemistry

University of California, Irvine, 2017

Professor Barbara J. Finlayson-Pitts, Chair

Atmospheric particles negatively affect human health, limit visibility and impact climate. Their

deleterious effects are known, but the mechanism of how particles form and grow in the

atmosphere is not fully understood. Sulfuric acid (H_2SO_4) is a large contributor to particle

formation, but nucleation of H_2SO_4-H_2O cannot explain atmospheric observations. Ammonia

(NH_3) can form particles with sulfuric acid, yet the ternary nucleation of H_2SO_4-NH_3-H_2O still

does not match measurements, indicating the participation of other precursors. Amines have

been shown to enhance particle formation and, despite their lower concentrations in air, can

displace NH_3 in clusters. As the use of sulfur-based fossil fuels is phased out, and consequently

H_2SO_4 concentrations are reduced, methanesulfonic acid (MSA) is expected to become a more

important source of particles. MSA does not form particles efficiently with water alone, but does

so with amines and water. The reaction of MSA and ammonia/amines is dependent on relative

humidity, basicity and amine structure. In this dissertation, the effect of four organic compounds

on the reaction of methanesulfonic acid, amines and water is investigated. Experiments are

conducted in a small volume aerosol flow reactor at ambient temperature and atmospheric

pressure (294 K, 1 atm). Early experiments show that the aerosol flow reactor is sensitive to

order of addition of reactants. Laboratory results are interpreted along with results of theoretical

calculations of initial clusters completed by the Gerber group. Results show that particle

formation is influenced by proton transfer, hydrogen bonding capacity and basicity. Molecular

structure can also impact particle formation and growth by influencing how initial clusters grow

to detectable particles. Particle formation from organics and amines with and without water is

inefficient in this system. Results show that, in the atmosphere, water likely overwhelms the

effect of organics. Theoretical calculations give insight on how experimentally unobservable

initial clusters of these systems correlates with detectable particles. The results of this work

could aid atmospheric models in more accurately predicting the impact of particles on a regional

and global level.

CHAPTER 1 INTRODUCTION

1.1 NEW PARTICLE FORMATION AND GROWTH

Atmospheric particles have wide reaching effects; they impact human health,[1-8] visibility,[9, 10] and the climate.[11-13] If inhaled deep into the lungs, particles can cause pulmonary issues[6] and are correlated with higher morbidity and premature mortality.[1, 3, 5, 7] There is also evidence that particles can indirectly impact health. A study in Tehran, Iran showed that inhibited visibility of the sun, due to particles, was associated with vitamin D deficiency in adolescents.[2] Loss of visibility occurs when particles are large enough (>100 nm) to scatter light/solar radiation, an example of their direct effect on climate.[9, 10] Particles can also indirectly affect climate by acting as cloud condensation nuclei and altering cloud properties.[14, 15] Atmospheric particles play a critical role in the balance of global radiation, but are one of the least understood radiative forcing agents.[13] There is a large uncertainty in the contribution of atmospheric particles to radiative forcing, which is propagated in the overall uncertainty in the total climate budget.[13] The current understanding of how particles form and grow in the atmosphere must be improved for more accurate predictions of particle impacts.[16-19]

Sulfuric acid (H_2SO_4) has long been recognized as a large contributor to atmospheric particles.[20-28] H_2SO_4 is formed by the oxidation of sulfur dioxide (SO_2), which has both biogenic (*e.g.,* released by volcanic eruptions)[29] and anthropogenic sources (*e.g.,* a byproduct of fossil fuel combustion).[30] However, nucleation involving H_2SO_4 and water alone cannot fully explain atmospheric observations of particle formation.[11, 22, 31-35]

1

Ammonia (NH_3) and amines are ubiquitous in the atmosphere.[36-40] Sources of ammonia/amines range from animal husbandry to vegetation, with estimated annual emissions of 50,000 Gg N for NH_3 and ~100 Gg N each for mono-, di- and trimethylamine.[37] The inclusion of ammonia with sulfuric acid and water enhances particle formation,[41-45] but laboratory studies show that ternary nucleation rate of NH_3-H_2SO_4-H_2O is too slow to match atmospheric measurements.[41, 42, 44, 45] Modelling studies that include NH_3, H_2SO_4 and H_2O nucleation also do not accurately reproduce observed data.[45-47] Although ambient amine concentrations are lower than those of NH_3,[37, 48-51] amines can displace ammonia in ammonium sulfate/bisulfate clusters.[52-55] Amines form particles with sulfuric acid,[44, 56-65] and have been shown to more efficiently enhance particle formation compared to NH_3.[44, 59, 60, 62-65] Theoretical studies of H_2SO_4-NH_3/amine[66-69] and H_2SO_4-NH_3/amine-H_2O[70-75] clusters not only support experimental results but also provide insight on the initial steps of particle formation and growth.

The discrepancy between atmospheric models and observations of particle formation suggests that additional precursors must be involved in the process.[16, 17, 76-78] Organics are found in particles measured from around the world and are likely candidates to contribute to particle formation.[79] It has been proposed that organics participate in the initial stages of nucleation with H_2SO_4,[76-78, 80] but some field studies have found organics to form particles on their own.[81-85] Organics[76-78, 82, 86-91] and organic salts[63, 92, 93] (formed by organic acids and amines) may also play a role in stabilizing initial clusters and growing them to detectable particles.

Methanesulfonic acid (CH_3SO_3H, MSA) is another potential source of atmospheric particles in certain locations. In Alaska, a correlation between particle number concentration and the
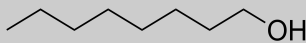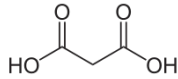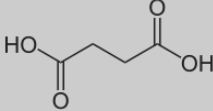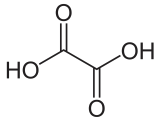
methanesulfonate anion was observed over a three year period.[94] In the Arctic, particle growth was associated with MSA and trimethylamine ($(CH_3)_3N$, TMA) during the summer.[95] MSA is typically associated with particles in/near marine areas[96-104] but has been measured in particles as much as ~100 miles inland.[105-109] Formed in the oxidation of organosulfur compounds,[110-113] with diverse sources including the ocean,[114-116] animal husbandry[117] and human breath,[118] MSA concentrations can be $10^5 - 10^7$ molecules cm^{-3} (~10 – 100% relative to sulfuric acid concentrations).[119-124] MSA may currently be a minor contributor to particle formation, but its relative importance will likely increase as the use of sulfur-based fossil fuels is reduced.[125]

MSA and water do not form a significant amount of particles alone.[126-129] However, MSA and water with ammonia/amines have been shown to efficiently form particles; this reaction is sensitive to relative humidity (RH), amine basicity and amine structure.[130-133] Relative to sulfuric acid, MSA is less studied, experimental and theoretical studies of particle formation including MSA are limited.[125-137] To the best of our knowledge, the effect of organics on the system of MSA, amines and water had not been studied prior to the work presented here.

Table 1.1 shows properties of the four organic compounds that are investigated in this work: 1-octanol ($C_8H_{17}OH$, octanol), malonic acid ($CH_2(COOH)_2$, MaA), succinic acid ($HOOC-CH_2-CH_2-COOH$, SuA) and oxalic acid ($(COOH)_2$, OxA). The series spans a range of vapor pressures, functional groups and chain lengths. Octanol has been measured from emissions from agricultural crops and other plant species.[138, 139] Additionally, octanol is considered a representative partially oxidized compound, which has been proposed to coat aqueous particles.[140] Dicarboxylic acids have been measured in urban, rural and Arctic particles,[141-152] as

well as in biomass burning plumes.[153] OxA was determined to be the most abundant dicarboxylic acid measured, followed by MaA and/or SuA.[142-153] Samples of vehicle exhaust emissions suggest that dicarboxylic acids are products of incomplete combustion of hydrocarbons.[142, 144] Studies that measured dicarboxylic acids in particles in remote areas or found diurnal/seasonal variation in their concentration support the pathway for their production by photochemical oxidation of volatile organic compounds.[142, 143, 146-148, 150]

Table 1.1 Properties of the organics investigated in this dissertation.

Organic	Vapor Pressure at 298 K (Pa)	Categorization[154-157]	Structure
1-octanol (octanol)	11.0^{158}	IVOC[a]	
malonic acid (MaA)	1.7×10^{-4} [159]	SVOC[b]	
succinic acid (SuA)	7.7×10^{-5} [159]	SVOC	
oxalic acid (OxA)	1.4×10^{-2} [159]	IVOC	

[a] "IVOC" indicates an intermediate volatility organic compound.
[b] "SVOC" indicates a semi-volatile organic compound.

Theoretical studies propose that ammonium/alkylaminium dicarboxylates, including OxA-NH$_3$ with and without water,[160-162] OxA-dimethylamine-H$_2$O,[163] and SuA-dimethylamine,[164] are involved in nucleation of atmospheric particles. Yet, others suggest that particle formation from dicarboxylic acids will occur with sulfuric acid and water[165] or ammonia.[166]

Dicarboxylic acids have multiple opportunities for hydrogen bonding, which are important for cluster stabilization, particle formation and growth in the MSA-ammonia/amine-H_2O system.[130-133] Furthermore, OxA, MaA and SuA have been measured in particles along with MSA and ammonia/amines.[149, 167, 168] OxA, MaA and SuA are polar in nature and differ in vapor pressure and carbon chain length; these dicarboxylic acids are good candidates to investigate participation of gas phase organics in particle formation and growth.

1.2 RESEARCH GOALS

The main goal of this research is to elucidate the mechanism of particle formation and growth from the gas phase reaction of organics, MSA, amines and water. Previous studies have shown that the reaction of MSA and amines efficiently forms new particles and that the amine structure and relative humidity affect particle formation. However, to the best of our knowledge, laboratory studies of the effect of organics on the MSA-amine and MSA-amine-H_2O system had not been explored until this project. Organics with different functional groups, varying vapor pressures and hydrogen bonding capacity are chosen to help identify the properties that affect how particles form and grow in air. The results of this work will lead to an improved understanding of the fundamental chemistry of nucleation and growth of new particles in air. Ultimately, these results can be incorporated into atmospheric models to better predict particle impacts on a regional and global scale. A series of experiments are performed on a custom-built small volume aerosol flow tube reactor that can achieve reaction times within the system ranging from 0.8 to 12 s. Experimental results are interpreted in light of results of initial clusters, calculated by the Gerber group in Chapter 3 – 5, of the organic-MSA-amine and organic-MSA-amine-H_2O systems.

1.3 EXPERIMENTAL METHODS

1.3.1 Small Volume Aerosol Flow Reactor

Experiments were performed in a small volume (~6.6 L) aerosol flow reactor (Figure 1.1, Figure 1.2), which was modeled after another flow tube in this lab.[169] The reactor was custom built and designed to monitor the formation and growth of particles as a function of reaction time. It is made of borosilicate glass to protect from corrosion due to long-term exposure to acids and has three fixed ring inlets, three spoke inlets, and a movable sample line. The three ring inlets (ring #1, ring #2, and ring #3), roughly two cm apart, are perforated hollow tubes housed in the upstream end cap. The upstream end cap also guides three concentric tubes (92 cm long) that terminate in four perforated hollow tubes, these spoke inlets (spoke #1, spoke #2, spoke #3) are two cm apart and are movable as a unit. Perforations on the inlets were designed to insure sufficient mixing of reactants at the spokes (Figure 1.3). A ¼″ stainless steel sample line, 142 cm in length, is held at the other end of the flow tube by the downstream end cap. Attached to the sample line are ¼″ stainless steel bellows (172.7 cm) that terminate in one of three detectors used in these studies. The portion of the total gas/particle flow that is not sampled is vented through an exhaust from the downstream end cap.

All experiments were performed at atmospheric pressure, 1 atm, and ambient lab temperature, 294 K with a total flow of 17 standard liters per minute (Lpm) in the aerosol flow reactor. The total flows from each of the inlets was consistent between experiments, unless noted otherwise (Table 2.1, Expts. 1, 2) with 10 Lpm through ring #1, 2 Lpm each through ring #2 and ring #3,

6

and 1 Lpm each through spokes #1 – #3. All air flows were controlled by mass flow controllers

(Alicat) and verified with bubble meters (Gilibrator 2, Sensidyne).
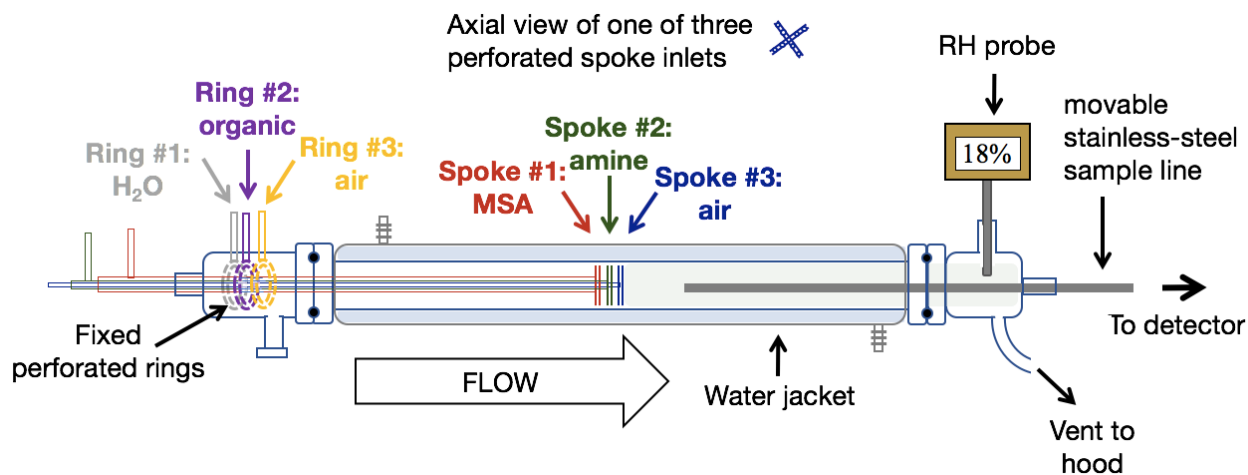
Figure 1.1 Schematic of small volume aerosol flow reactor.
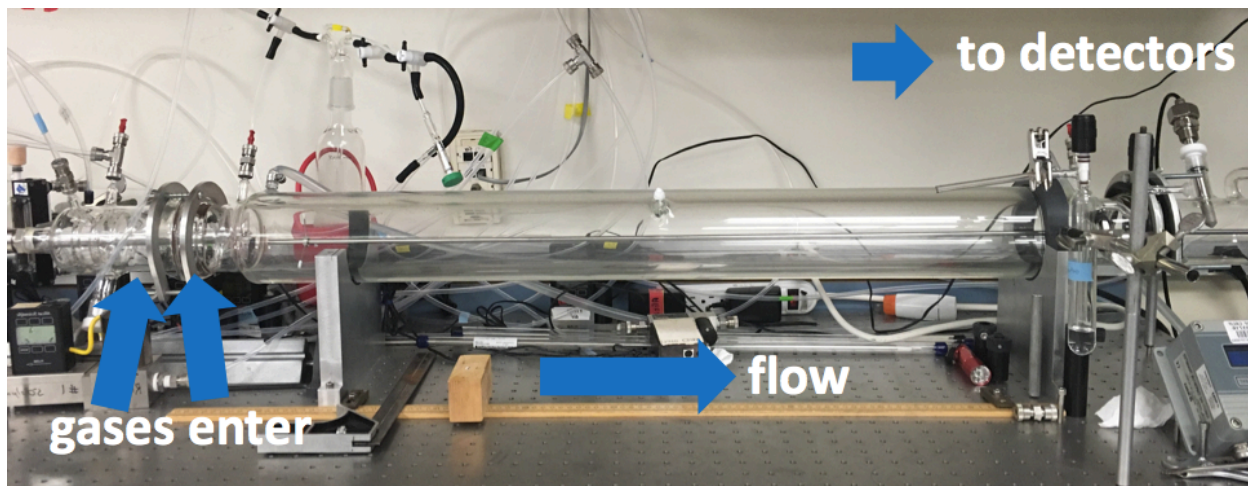
Figure 1.2 Photo of small volume aerosol flow reactor.
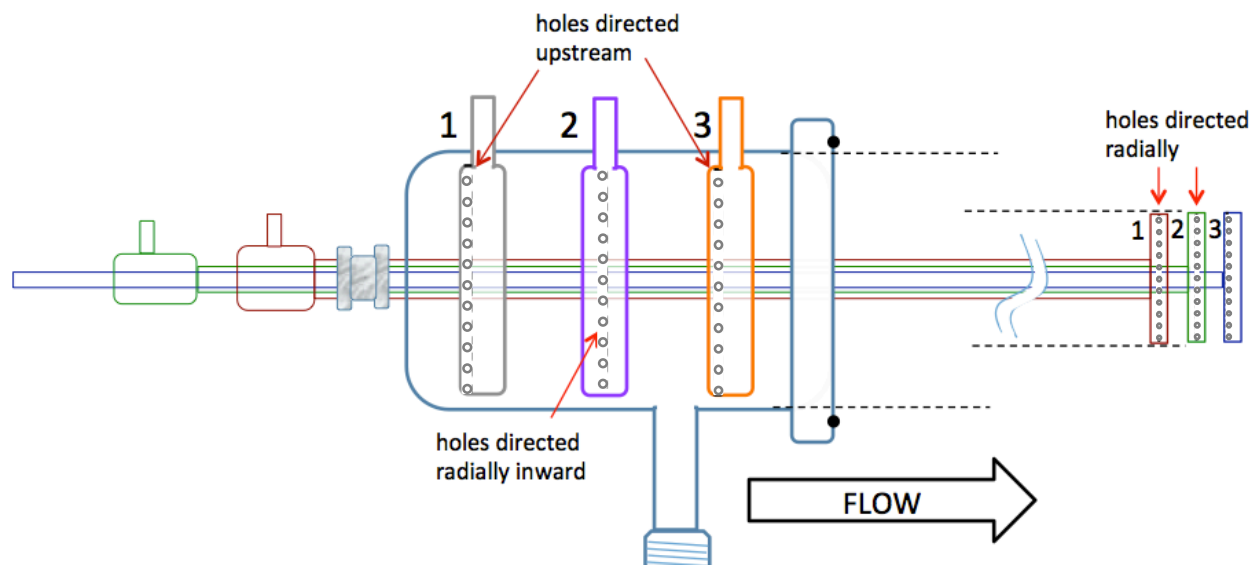
Figure 1.3 Detail of ring and spoke inlets.

To characterize the residence times in the flow tube, a small volume of colorless NO was added to the system through spoke #1, which was quickly oxidized by O_2 to NO_2, a brown gas (Figure 1.4). Residence times were determined by measuring the time to reach maximum absorbance of NO_2, monitored at $\lambda = 420.43$ nm with UV-visible spectroscopy (Ocean Optics, model HR4000CG-UV-NIR) at different spoke inlet positions. This procedure closely follows that described in Ezell *et al.*[169]
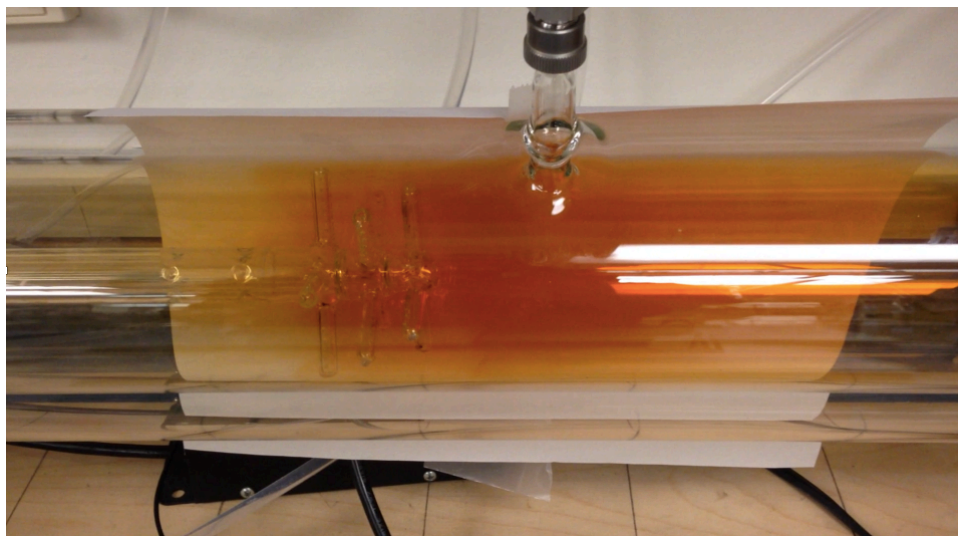
Figure 1.4 NO, introduced through spoke #3, oxidized to NO_2 upon exposure to O_2 in the flow reactor.

Reaction times can be adjusted by altering the distance between the sample line and the inlets. The defined $t = 0$ is at the inlet from which MSA (when present) is introduced because, as results will show, the reaction between MSA and the amine is most efficient at forming particles. Within the flow tube reaction times range from 0.8 s up to 14.2 s, which does not include the total 3.1 s residence time in the sample line to the detectors. Reaction times within the system assume that reactions have been completed by the time particles reach the sample inlet and that wall loss of gas phase species in the sample inlet is fast. If the time in the sample line were to be included, the data would be displaced by 3.1 s; this would not affect the results or conclusions presented since only peak particle number concentrations and geometric mean diameters are considered. Note that the time dependence of detectable particle formation is very sensitive to the nature and concentrations of the reactants as discussed by Chen *et al.*[130] For example, reaching a plateau at longer reaction times is typically indicative of depletion of the limiting reagent.

In Chapter 2 and part of Chapter 3, measurements were made in order of decreasing reaction time from 14.2 s to 0.8 s for the "base case" with MSA and TMA only (Section 1.3.4) and in order of increasing reaction time from 0.8 to 14.2 s in the presence of octanol, MaA or SuA. In part of Chapter 3 and all of Chapters 4 and 5, to minimize a potential sampling time bias, measurements were done in the following order of reaction times: 12.4 s, 7.6 s, 3.8 s, 1.3 s, 0.8 s, 2.5 s, 5.1 s, and 10.1 s for both the base case (MSA-amine or MSA-amine-H_2O) and in the presence of the variable reactant (MaA, SuA or OxA).

The aerosol flow reactor was cleaned frequently with 18.2 MΩ cm water (Thermo Scientific, Model 7146) and isopropyl alcohol then dried overnight with dry air from a purge air generator (Parker-Balston, Model 75-62). The flow reactor was then conditioned with MSA, unless the effect of MSA was being investigated, for at least two days to passivate the tubing, inlets, and walls of the system.[130] The water and air used throughout all experiments was 18.2 MΩ cm water and dry purge air.

1.3.2 Gas Phase Reactants

1.3.2.1 *Methanesulfonic Acid*

Gas phase MSA was produced by flowing dry air over the pure liquid (Fluka, 99.0%) that was kept in a trap at room temperature. Two methods were used to quantify MSA. For both methods, gas phase MSA was collected for 10 minutes onto a 0.45 μm Durapore filter (Millex-HV) placed prior to the entrance of the reactor. With the first method, the filter was extracted with 10 mL of water and then analyzed by ultra-high pressure liquid chromatography tandem mass spectrometry (Waters). For the second method, the filter was extracted with 10 mL of

water (J.T. Baker, LC-MS grade), diluted by half with methanol (J.T. Baker, LC-MS grade) and then analyzed by electrospray ionization mass spectrometry in negative mode (Waters, Xevo TQ-S). Reported MSA concentrations were calculated from the concentration out of the trap and the total flow of air in the aerosol reactor, these values represent upper limits because of potential losses in the inlets and tubing.

1.3.2.2   *Amines*

Two sources of gas phase TMA were used. In Chapter 2 and part of Chapter 3, a custom mixture of TMA in a gas cylinder (Airgas, 1 ppm in N_2) was used as provided from the manufacturer. It was discovered later that, as the tank was emptied, an ammonia impurity become more and more prominent and contributed to inconsistent particle number concentration measurements. The ammonia contamination was likely below the limits of detection of a less sensitive instrument that was used for quantification of the amine at that time. As a result, use of amine tanks was discontinued in favor of permeation tubes. In part of Chapter 3 and all of Chapter 5, gas phase TMA was generated by flowing dry air over pure TMA in a permeation tube (VICI Metronics, 993 ng/min) that was held in a water bath at room temperature. In Chapter 4, air was flowed over pure MA in permeation tubes (VICI Metronics, 72 ng/min or 1003 ng/min) that were kept in a water bath at ambient temperature to generate gas-phase MA. All amines were quantified by a technique developed in this lab.[170] TMA/MA was collected onto a weak cation exchange resin, which was placed prior to its point of entry into the flow reactor, extracted with 10 mL of oxalic acid (Fluka, 0.1 M) and then analyzed by ion chromatography (IC; Metrohm, model 850 or Dionex, ICS-1100). Purity of the amines generated by the permeation tubes was confirmed by

IC, neither the TMA nor the MA permeation tube had NH_3 or other amine contamination (Table 1.2).

Table 1.2 Summary of amine sources.

Amine	Source	Note
trimethylamine (TMA)	gas cylinder	NH_3 contamination
TMA	permeation tube	no contamination
methylamine (MA)	permeation tube	no contamination

1.3.2.3   *Organics*

To generate gas phase octanol (Sigma-Aldrich, anhydrous 99%), air flowed over the liquid that was held in a trap and kept at room temperature. The gas phase dicarboxylic acids were each produced by flowing dry air over the respective pure solids, which were heated in a water bath to 340 K for MaA (Alfa Aesar, 99%), 343K for SuA (Sigma-Aldrich, $\geq$ 99%) and 303 K for OxA (Aldrich, 98%). Presence of the gas phase dicarboxylic acid was confirmed by atmospheric pressure chemical ionization tandem mass spectrometry (Waters, Xevo TQ-S). Due to losses in the sampling line, quantitative measurements of the organics were not possible, so the concentrations of 1-octanol, MaA and OxA were calculated based on their respective vapor pressure.[158, 159] As a result, the reported concentrations represent an upper limit.

1.3.2.4   *Water*

Humid conditions were obtained by flowing dry air through a bubbler filled with 18.2 MΩ cm water, which was held in a water bath at ambient temperature to offset the decrease in

temperature due to evaporative cooling. Relative humidity (RH) was measured by an RH probe (Vaisala, Type HMP 234) positioned in the downstream end cap. Note that for experiments done under dry conditions, the RH probe in the reactor measured < 3% RH.

1.3.3   Detectors

Time dependencies of particle size distributions and number concentrations were measured with a scanning mobility particle sizer (SMPS; TSI, classifier model 3080, nano differential mobility analyzer (nano DMA) model 3085, and condensation particle counter (CPC) model 3776) attached to the sample line. During experiments the SMPS took three scans at each reaction time. Reported SMPS values were averaged over the three scans and errors (2σ) were calculated from the triplicate measurements. For some experiments, number concentrations were measured directly with the n-butanol based CPC in place of the SMPS. CPC data represent measurements taken over a 60 s or 120 s sample time with a 1 s average interval. In Chapters 3 – 5, number concentrations including the smallest of detectable particles were obtained using a diethylene glycol based particle size magnifier (PSM; AirModus, Model A10); the cutoff diameter is roughly 1.4 nanometers for ammonium sulfate particles. Measurements with the PSM were taken over a 60 s sample time.

TSI specifies a 2.5 nm cutoff, but studies have shown that CPC detection efficiency is dependent on particle composition.[171-175] It is expected that the MSA-amine particles formed in this system are similar in composition to the ammonium sulfate particles used for PSM calibration and there is no data that suggest the MSA-amine or organic-MSA-amine particles with and without water behave differently in the PSM. However, as demonstrated in Chapter 2, in the presence of water

the organic-MSA-amine particles may be different than the sucrose particles used for CPC

calibration, which has implications for detection efficiency in the CPC. In most cases, particles

were larger than 2.5 nm and the CPC and PSM produced similar data.

1.3.4   Measurement Scheme

The effect of a single gas phase component (organic, MSA, amine, H_2O) was investigated by

comparing particle number concentrations and size distributions when the selected species was

added to a "base case" that had two (typically MSA + amine) or three components (typically

MSA + amine + H_2O). Note that the selected components were present during particle

formation, not added after particles had been formed from the base case reactants. This

juxtaposition of number concentrations and particle sizes measured with and without the variable

reactant isolates the effect of the reactant and obviates the challenge of attaining identical

conditions in the aerosol flow reactor from day to day, which is experimentally challenging.

CHAPTER 2   THE EFFECT OF 1-OCTANOL ON THE REACTION OF MSA AND TMA WITH AND WITHOUT WATER

2.1   RESEARCH GOALS

Previous work done in this lab showed that MSA and TMA form a significant number of particles and that particle formation is enhanced with increased RH.[130, 133] The goal of this work is to investigate the effect, if any, of octanol on particle formation and growth on the reaction of MSA, TMA and water. With six total inlets, order of addition of the acid, base and organic can be manipulated to determine if reactant sequence affects particle formation and growth in the aerosol reactor. The first studies done with the newly built aerosol reactor also focused on determining the sensitivity of the system to the order of addition of reactants. Results of this study are summarized in Table 2.1 presented at the end of Section 2.2.

2.2   INITIAL RESULTS AND DISCUSSION

It is important to note that the TMA used in this set of experiments came from a gas cylinder that was later determined to be contaminated with NH_3. Previous work has shown large enhancement of particle formation with sulfuric acid and mixtures of ammonia and amines compared to sulfuric acid and the amine alone.[60, 64] A comparison of particle formation from MSA and TMA from the contaminated gas cylinder versus TMA from the permeation tube confirms that, at the same concentration of acid and "amine," the TMA/NH_3 mixture is more efficient than the comparable rate of particle formation from MSA and TMA alone (similar to results from the analogous sulfuric acid reactions). The biggest effect the contamination has on

the data presented here is on the particle number concentrations from MSA and "TMA," which are likely elevated due to the presence of NH_3.

Figure 2.1 shows the size distributions of the base case with MSA and TMA alone compared to those in the presence of octanol. With all three reactants added through the spokes (Figure 2.1b), number concentrations decreased in the presence of octanol compared to the base case and particles did not grow.
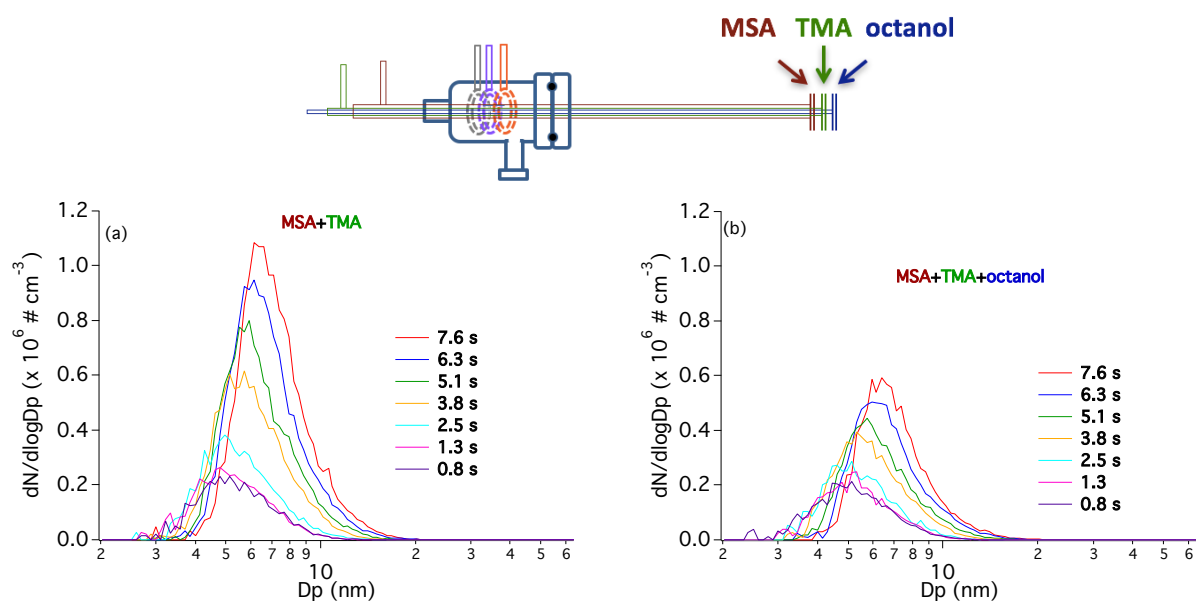
Figure 2.1 Average size distributions from triplicate measurements with the SMPS comparing the base case reaction of (a) MSA (~14 ppb) + TMA (1.0 ppb) (b) with octanol (5.9 ppm) where all reactants were added through the spokes as shown; errors excluded for clarity. Reaction times indicated in the figure corresponds to the time reactants interacted in the reactor, with t = 0 corresponding to the time MSA is introduced at spoke #1. See Table 2.1, Expt. 1.

To determine the expected time it takes for TMA to react with MSA, the hard sphere collision rate was calculated from Equation 2.1 where k_B is the Boltzmann constant, T is the temperature, and the radii of MSA and TMA were estimated from the largest distance between atoms in the respective molecule.

$$k = \pi(r_{MSA} + r_{TMA})^2 \sqrt{\frac{8k_BT}{\pi\mu}}$$ **Equation 2.1**

This approach is based off work done by Dawson et al.[133] who successfully reproduced

experimentally observed particles from MSA and TMA with a diffusion-controlled kinetics

model. The lifetime of TMA with respect to reaction with MSA ($\tau = 0.01$ s) is smaller than the

time between spokes (0.25 s), so it is expected that MSA and TMA reacted prior to meeting

octanol. However, results did not change when the spoke inlets for TMA and octanol were

switched. Such results indicate that order of addition was inconsequential when all three

reactants came through the spokes, perhaps due to the effective mixing at the spokes facilitated

by the radially directed inlet perforations (Figure 1.3).

The order of addition to the flow reactor was changed to allow MSA and TMA to enter through

the ring inlets and react upstream, roughly 4 s before meeting octanol, which was introduced

through spoke #1. This configuration was intended to probe the effect of octanol on particle

growth. In Figure 2.2, a small decrease (< 20% reduction) in the size distributions is observed in

the octanol, MSA, TMA system, but this is not considered significant. The presence of octanol

does not significantly affect particle number concentration or particle size compared to the base

case of MSA and TMA alone. When octanol was introduced after MSA and TMA reacted,

particles only grew to ~6 – 7 nm.
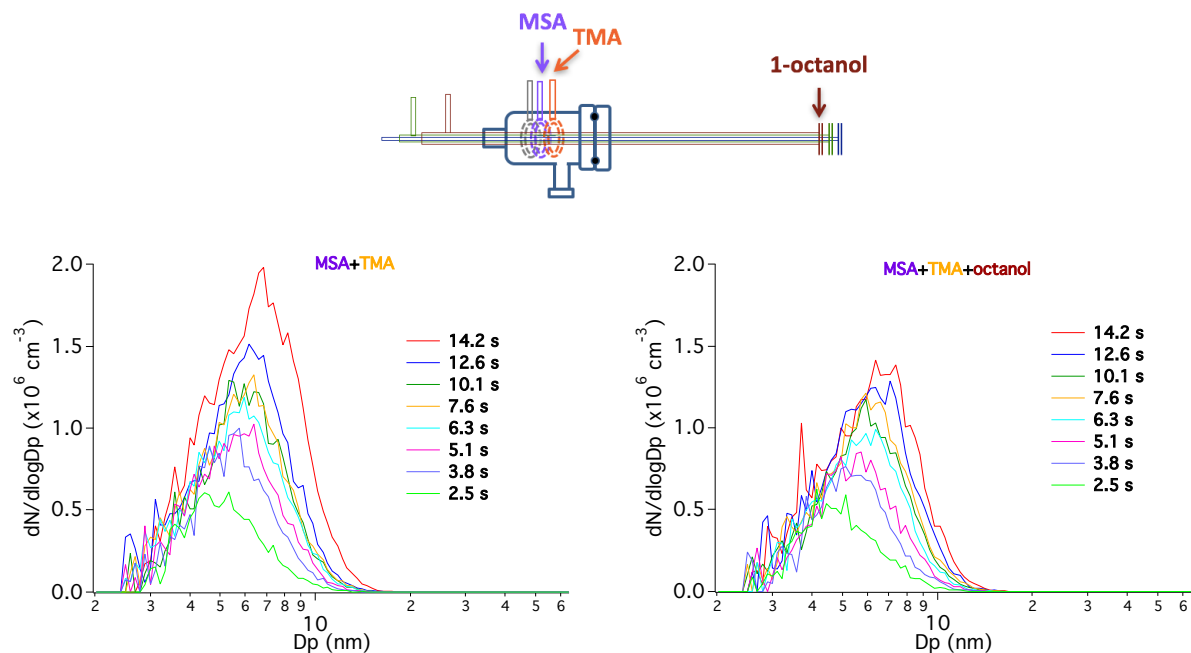
Figure 2.2 Average size distributions from triplicate measurements with the SMPS comparing the base case reaction of (a) MSA (8.4 ppb) + TMA (1.5 ppb) (b) with octanol (29 ppb) where all reactants were added through the inlets in the reactor as shown; errors excluded for clarity. Reaction times indicated in the figure corresponds to the time reactants interacted in the reactor, with t = 0 corresponding to the time MSA is introduced at ring #2. See Table 2.1, Expt. 6.

Particles were expected to grow via condensation of octanol, which is affected by opposing forces: (1) the Kelvin effect, an increase of vapor pressure due to particle curvature, and (2) Raoult's law, a decrease of vapor pressure due to the solute effect. To explain this stunted growth, a Köhler curve (Figure 2.3), derived from the balance between the Kelvin effect and Raoult's law, was calculated for the growth of a 6 nm MSA-TMA particle in octanol (Figure 2.2). It must be noted that the Kelvin effect and Raoult's law depend on bulk liquid properties, therefore the Köhler curve is used here as an approximation for the growth (or lack thereof) of an MSA-TMA particle in the presence of octanol in the aerosol reactor.[11]
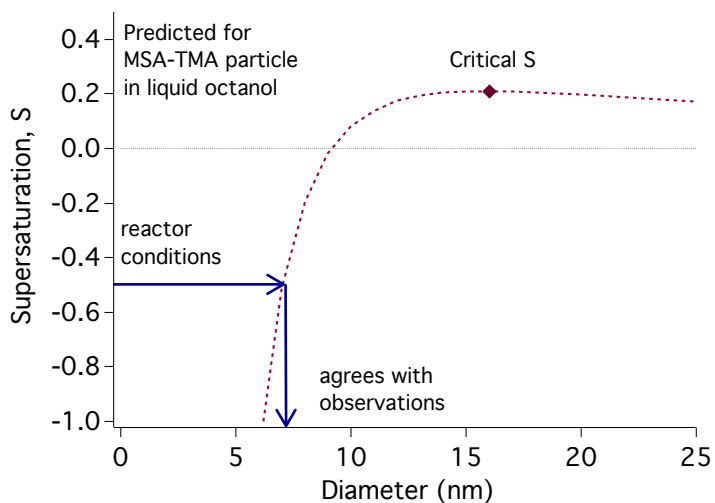
Figure 2.3 Köhler curve calculated for growth of a 6 nm MSA-TMA particle in octanol with critical supersaturation, S, relative to the vapor pressure of 1-octanol.

The effective saturation in the aerosol flow reactor under these conditions was determined to be roughly –0.5, which may explain why in Figure 2.2 the mean diameter is only 6 – 7 nm. According to the Köhler curve in Figure 2.3, critical supersaturation (~0.2) is achieved at ~16 nm. MSA-TMA particle growth was likely restricted to 6 – 7 nm in the presence of octanol because, within the reactor, supersaturation was not high enough to support further condensation of octanol onto particles.

The order of addition was repeated under humid conditions and results are shown in Figure 2.4. Octanol had no effect on particle formation and did not promote particle growth compared to the base case of MSA + TMA + H_2O. It has been shown that compared to the MSA-TMA base case, particle formation is enhanced and particle size is increased in the presence of water.[130, 133] In these studies water provided additional hydrogen bonding sites that aided in the growth of clusters to detectable sizes.[130, 133] In Chen *et al.*[130] particle formation from MSA, TMA and water was very sensitive to the order of addition to the flow reactor. When water was present

with MSA and TMA, particle formation was more efficient and particle sizes were larger than the dry base case scenario.[130] However, water had no effect on particle formation and a small effect on particle growth when it was added ~12 s after MSA and TMA had time to react.[130] Octanol was expected to act similarly to water and provide hydrogen bonding opportunities for growth of MSA-TMA-H_2O clusters. In Figure 2.4 the amount of water vapor (2.1×10^{17} molecules cm^{-3}) is orders of magnitude larger than that of octanol (2.5×10^{12} molecules cm^{-3}), perhaps drowning out any effect of the octanol. This configuration shows that once MSA-TMA-H_2O clusters are formed there is no effect with octanol.
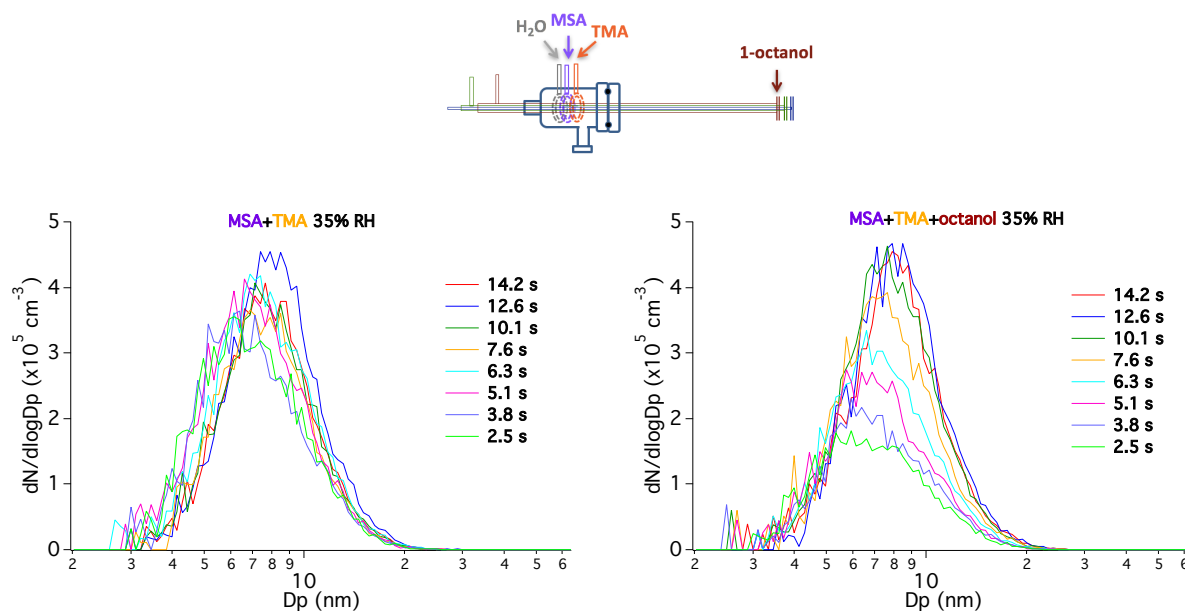
Figure 2.4 Average size distributions from triplicate measurements with the SMPS comparing the reaction of (a) MSA (2.8 ppb) + TMA (2.1 ppb) (b) with H_2O (35% RH) and (c) with octanol (100 ppb) where all reactants were added through the inlets in the reactor as shown; errors excluded for clarity. Reaction times indicated in the figure corresponds to the time reactants interacted in the reactor, with t = 0 corresponding to the time MSA is introduced at ring #2. See Table 2.1, Expt. 14.

With the last configuration tested, water was introduced through ring #1, octanol through ring #2, MSA through spoke #1, and TMA through spoke #2; it was presumed that all reactants met at the same time, similar to the configuration in Figure 2.1. Figure 2.5 shows suppression of

particle formation in the presence of octanol. This configuration (Figure 2.5) was only measured once, but these results combined with Table 2.1 Expts. 1, 2 (done without water) may suggest that octanol slightly suppresses particle formation if octanol, MSA and TMA (and water) are introduced at the same time.
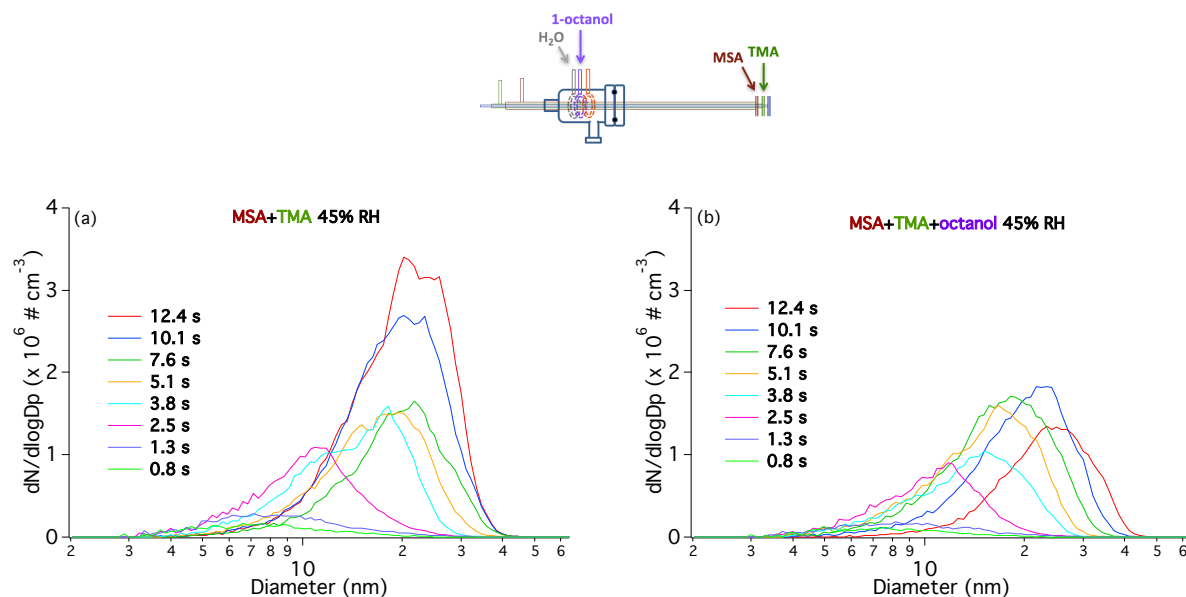
Figure 2.5 Average size distributions from triplicate measurements with the SMPS comparing the base case reaction of (a) MSA (2 ppb) + TMA (0.6 ppb) + H_2O (45% RH) (b) with octanol (100 ppb) where all reactants were added through the inlets in the reactor as shown; errors excluded for clarity. Reaction times indicated in the figure corresponds to the time reactants interacted in the reactor, with t = 0 corresponding to the time MSA is introduced at spoke #1. See Table 2.1, Expt. 17.

The set of experiments conducted in this series is incomplete, but results from Table 2.1 show that under both dry and humid conditions, octanol does not have a significant effect on number concentration or particle size when added after MSA and TMA have reacted. However, if octanol, MSA and TMA (and water) are introduced at the same time, results suggest that octanol does not grow particles and suppresses particle formation. These initial results warranted a closer look to determine if observations were truly due to the presence of octanol or were due to a systematic error.

Table 2.1 Conditions and results for MSA + TMA and MSA + TMA + H_2O experiments done with and without octanol.

Expt.	Ring #1	Ring #2[a,b]	Ring #3[a]	Spoke #1[a,b]	Spoke #2[a,b]	Spoke #3[a,b]	Result
1a	dry air	-	-	~14 ppb MSA	1.0 ppb TMA	dry air	base case
1b	dry air	-	-	~14 ppb MSA	1.0 ppb TMA	5.9 ppm octanol	<[c]
2a	dry air	-	-	~7 ppb MSA	dry air	1.0 ppb TMA	base case
2b	dry air	-	-	~7 ppb MSA	2.9 ppm octanol	1.0 ppb TMA	<
3a	dry air	7.2 ppb MSA	2.7 ppb TMA	dry air	dry air	dry air	base case
3b	dry air	7.2 ppb MSA	2.7 ppb TMA	59 ppb octanol	dry air	dry air	0[d]
4a	dry air	6.9 ppb MSA	3 ppb TMA	dry air	dry air	dry air	base case
4b	dry air	6.9 ppb MSA	3 ppb TMA	29 ppb octanol	dry air	dry air	< (21% decrease)
5a	dry air	23.1 ppb MSA	2.3 ppb TMA	dry air	dry air	dry air	base case
5b	dry air	23.1 ppb MSA	2.3 ppb TMA	29 ppb octanol	dry air	dry air	0
6a	dry air	8.4 ppb MSA	1.5 ppb TMA	dry air	dry air	dry air	base case
6b	dry air	8.4 ppb MSA	1.5 ppb TMA	29 ppb octanol	dry air	dry air	0
7a	dry air	7.8 ppb MSA	5.1 ppb TMA	dry air	dry air	dry air	base case
7b	dry air	7.8 ppb MSA	5.1 ppb TMA	29 ppb octanol	dry air	dry air	0
8a	dry air	2 ppb MSA	10.2 ppb TMA	dry air	dry air	dry air	base case
8b	dry air	2 ppb MSA	10.2 ppb TMA	5.9 ppm octanol	dry air	dry air	X[e]
9a	dry air	2.8 ppb MSA	10.2 ppb TMA	dry air	dry air	dry air	base case
9b	dry air	2.8 ppb MSA	10.2 ppb TMA	100 ppb octanol	dry air	dry air	X
10a	dry air	1.9 ppb MSA	31.8 ppb TMA	dry air	dry air	dry air	base case

							>[f] (20% increase)
10b	dry air	1.9 ppb MSA	**31.8 ppb TMA**	100 ppb octanol	dry air	dry air	>[f] (20% increase)
11a [g]	40% RH	**5 ppb MSA**	3.5 ppb TMA	dry air	dry air	dry air	base case
11b	40% RH	**5 ppb MSA**	3.5 ppb TMA	5.9 ppm octanol	dry air	dry air	0
12a	45% RH	**3.1 ppb MSA**	1.6 ppb TMA	dry air	dry air	dry air	base case
12b	45% RH	**3.1 ppb MSA**	1.6 ppb TMA	100 ppb octanol	dry air	dry air	< (27% decrease)
13a	40% RH	1.7 ppb MSA	**31.8 ppb TMA**	dry air	dry air	dry air	base case
13b	40% RH	1.7 ppb MSA	**31.8 ppb TMA**	100 ppb octanol	dry air	dry air	0
14a	35% RH	2.8 ppb MSA	2.1 ppb TMA	dry air	dry air	dry air	base case
14b	35% RH	2.8 ppb MSA	2.1 ppb TMA	100 ppb octanol	dry air	dry air	0
15a	35% RH	5.8 ppb MSA	5.1 ppb TMA	dry air	dry air	dry air	base case
15b	35% RH	5.8 ppb MSA	5.1 ppb TMA	29 ppb octanol	dry air	dry air	0
16a	dry air	dry air	dry air	2.3 ppb MSA	1.8 ppb TMA	dry air	base case
16b	dry air	100 ppb octanol	dry air	2.3 ppb MSA	1.8 ppb TMA	dry air	0
17a	45% RH	dry air	dry air	dry air	0.6 ppb TMA	dry air	base case
17b	45% RH	100 ppb octanol	dry air	**2 ppb MSA**	0.6 ppb TMA	dry air	<

[a] Concentrations of MSA and TMA are measured prior to their entrance to the reactor. These concentrations account for dilution in the reactor and, due to potential losses in the entrance lines, represent the maximum concentration of each species during reaction. Values are in bold-face font when in excess.

[b] Octanol concentration is calculated from its vapor pressure at 298 K[158] taking into account dilution in the flow reactor. As discussed in the text, this is the maximum concentration of octanol during reaction.

[c] "<" means at least a 20% decrease in particle number concentration was observed compared to the base case.

[d] "0" means the change in particle number concentration was < 20% increase or decrease compared to the base case.

[e] "X" means there was large variability and consequently large error in particle number concentration compared to the base case.

[f] ">" means at least a 20% increase in particle number concentration was observed compared to

the base case.

[g] Blue highlight indicates experiment was done with water.

2.3 DATA VERIFICATION

To determine whether the suppression of particle formation from octanol + MSA + TMA (+ H_2O) was a result of a reduced CPC counting efficiency, both gas phase octanol and water vapor were added to the sheath air of the nano DMA as shown in Figure 2.6. In this set of experiments only MSA and TMA were added through ring #2 and #3, respectively, to the reactor. To achieve humid conditions in the reactor, water vapor was added through ring #1, otherwise only dry air was added through all other inlets to maintain a total flow of 17 Lpm. The formed MSA-TMA particles were charged in the classifier and simultaneously size selected and introduced to octanol and/or water vapor in the nano DMA then counted by the CPC 3776, an n-butanol based CPC.
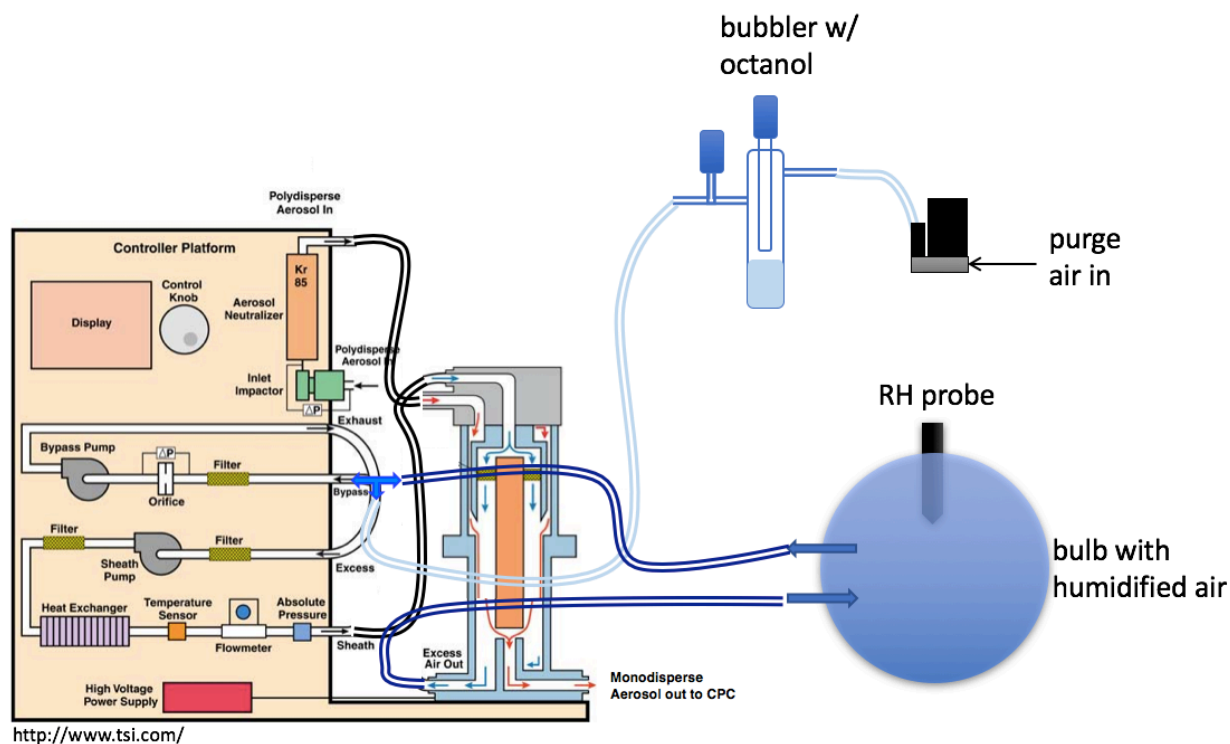
Figure 2.6 Schematic of addition of octanol and water vapor to the DMA.

In Figure 2.7 the MSA-TMA particle number concentration was not steady even after 70 minutes of conditioning in the flow reactor. With added octanol in the DMA, particle number decreased and continued to do so once water vapor (< 50% RH) was added to the DMA and after water vapor (40% RH) was added through ring #1 of the reactor. The geometric mean diameter was unaffected by the addition of octanol and water to the nano DMA, but particle growth is observed in the presence of water with MSA and TMA in the reactor.
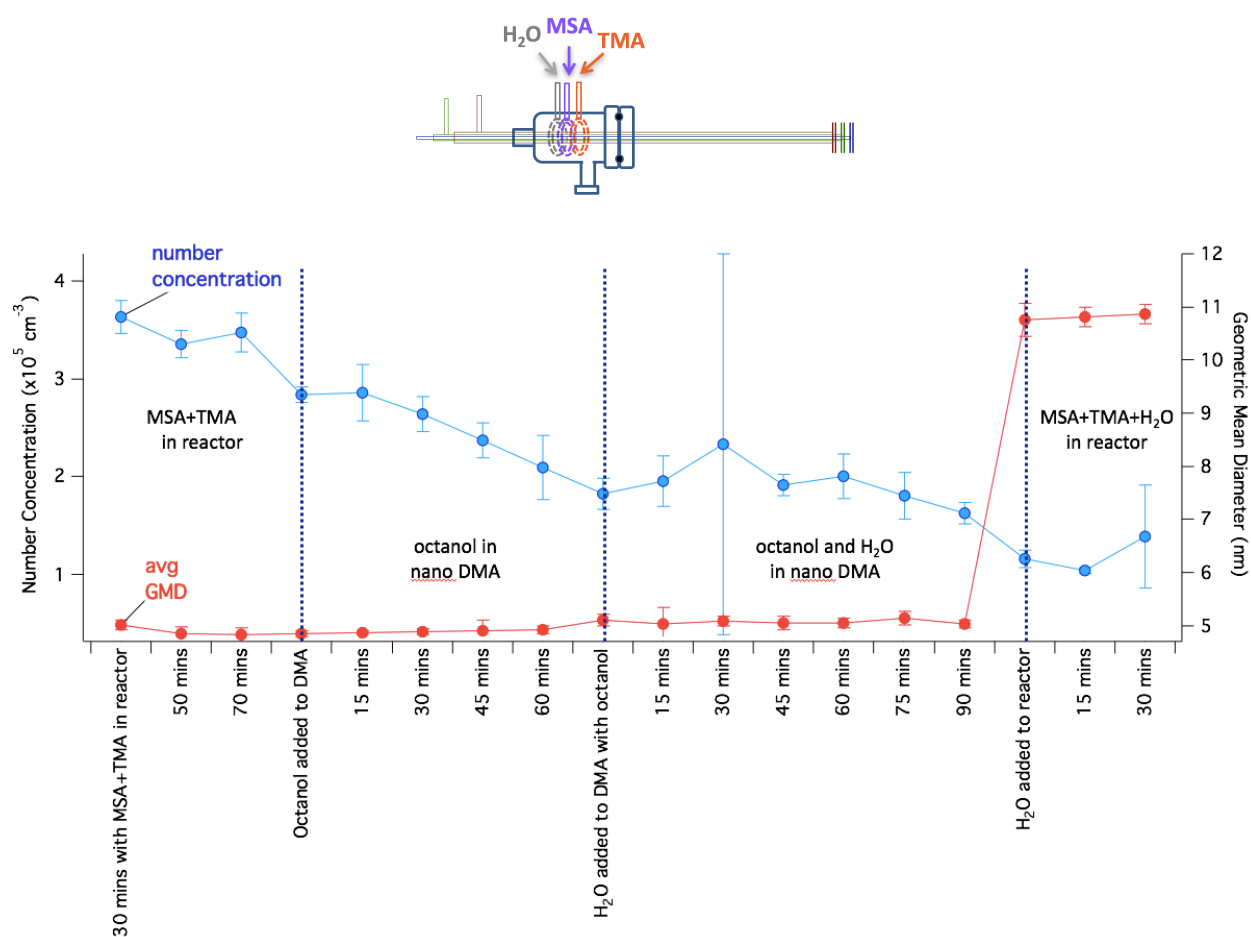
Figure 2.7 Average particle number concentrations and geometric mean diameters (GMD) from triplicate measurements with the SMPS of MSA (5.1 ppb), TMA (3.6 ppb), and H_2O (40% RH) where all reactants were added through the inlets in the reactor as shown and with added octanol and water in the nano DMA; errors are (2σ).

As seen in previous studies[130, 133] and in Figure 2.8 the SMPS measured larger MSA-TMA-H_2O particles and enhanced particle formation with water, compared to the base case (MSA and TMA only). Particle formation enhancement with water is not seen in Figure 2.7 indicating that the larger sized particles may be from coagulation of clusters/particles. At these time scales coagulation is expected if particle concentration exceeds 10^7 particles cm^{-3},[9] which is $1 - 2$ orders of magnitude higher than the particle concentrations measured in these experiments. This observed particle growth and absence of particle enhancement with added water in ring #1 of the reactor was reproducible. It is possible that coagulation occurred in the humidified DMA.
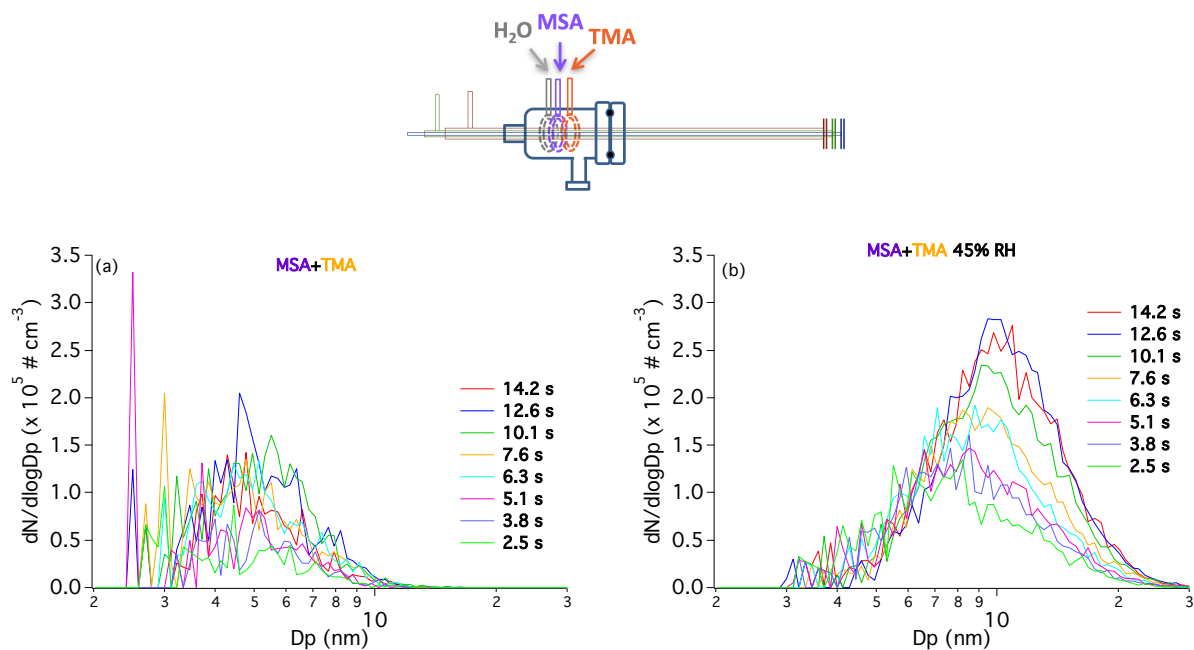
Figure 2.8 Average size distributions from triplicate measurements with the SMPS comparing the reaction of (a) MSA (3.1 ppb) + TMA (1.6 ppb) (b) with H_2O (45% RH) where all reactants were added through the inlets in the reactor as shown; errors excluded for clarity.

The sample line of the aerosol reactor was directly connected to the CPC to further investigate the effect of octanol and/or water on the CPC's ability to count octanol-MSA-TMA or octanol-MSA-TMA-H_2O particles. Figure 2.9 shows the MSA + TMA particle number concentration

steadily decreased over 60 minutes of conditioning and proceeded to go down in the presence of octanol for an additional 60 minutes. Once water was added through ring #1, the CPC did not detect any particles. Particle number concentration rebounded as soon as water was removed from the system. In Figure 2.10a, with MSA and TMA only, a burst of octanol was quickly added to and removed from the reactor within the 120 s sample time, but the number concentration did not change.

It is unclear if octanol alone influences the CPC's ability to count particles since particle concentrations with MSA and TMA were not steady in Figure 2.7 or in Figure 2.9. Octanol does not have a drastic effect on number concentrations in Figure 2.9 or Figure 2.10a when added to or removed from the system. However, it can take hours to purge octanol from the system so it is likely that octanol was not completely removed from the reactor in the time frame of the measurements, even if it was not actively added through spoke #1. In Figure 2.10b, after the burst of octanol, a burst of water was similarly added and removed from the reactor, which immediately reduced measured number concentrations. The CPC is sensitive to the effect of water in these measurements. With all four components (octanol, MSA, TMA and H_2O) in the reactor number concentrations drop and rebound within seconds of adding and removing water.
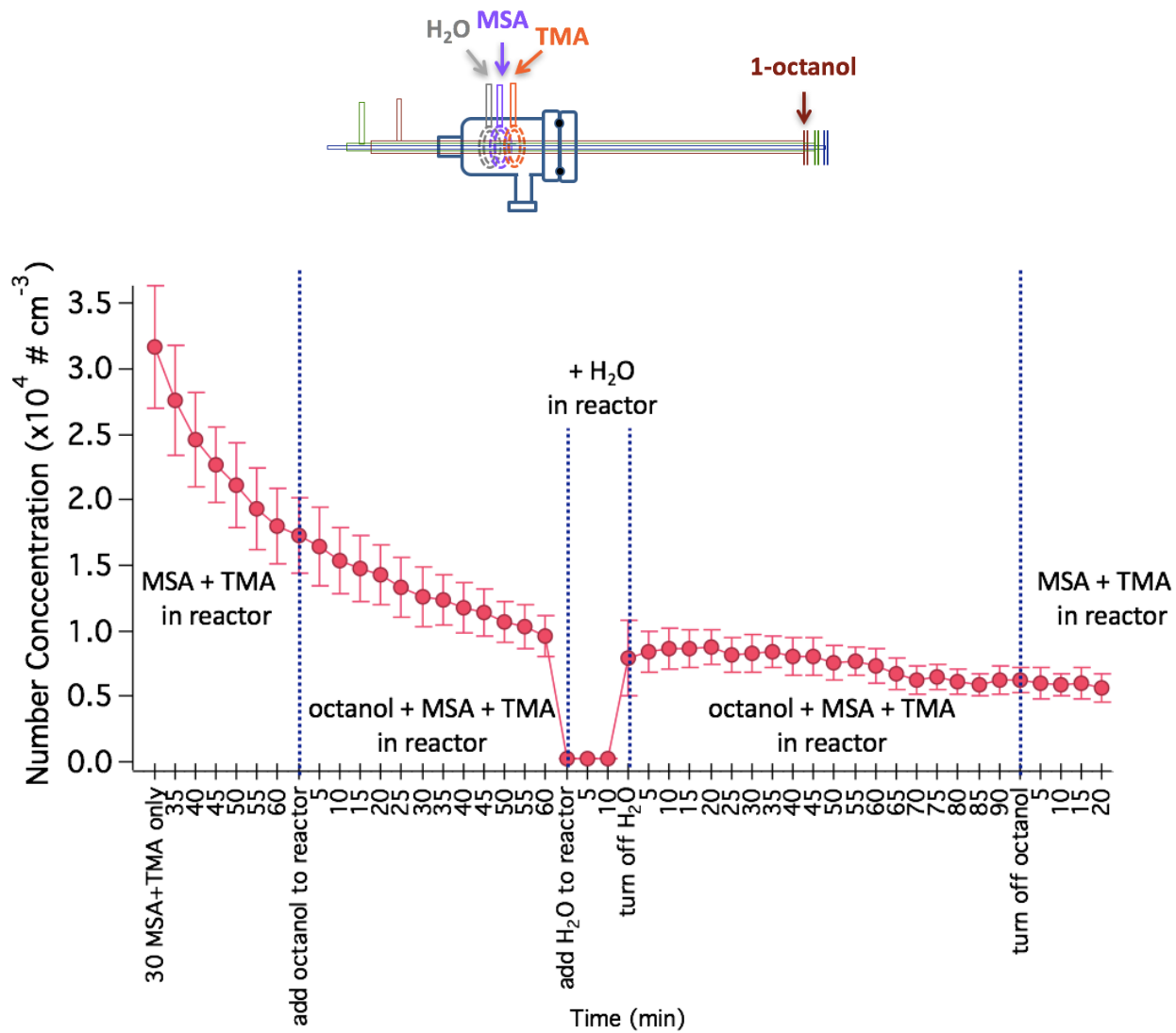
Figure 2.9 Particle number concentrations measured with the CPC with MSA (5.7 ppb), TMA (3.6 ppb), octanol (590 ppb) and water in the reactor where all reactants were added through the inlets as shown; errors (2σ) are from a two minute sample time with the CPC.
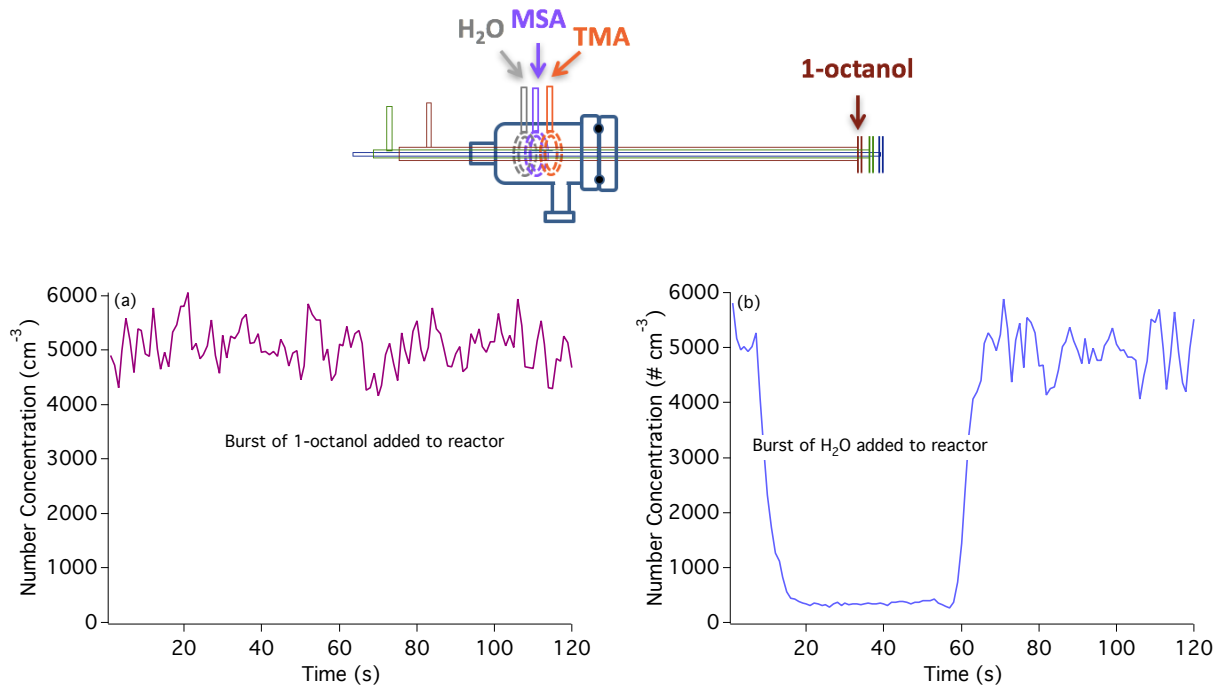
Figure 2.10 Particle number concentrations measured directly with the CPC with MSA (5.7 ppb), TMA (3.6 ppb) and (a) a burst of octanol (590 ppb) and then (b) a burst of H_2O (11% RH) in the reactor, where all reactants were added through the inlets as shown.

SMPS measurements show that octanol does not have an effect if it is added after MSA-TMA-H_2O particles form, the same configuration in the experiments for Figure 2.9 and Figure 2.10b. However, CPC measurements (Figure 2.9 and Figure 2.10b) suggest that the presence of water and octanol, which are always in excess of MSA and TMA, prevents efficient counting in the CPC. Note that the CPC water removal pump was not on during these measurements, which could pose issues for the butanol reservoir if experiments are done at large RHs.[176] However, the butanol reservoir was not contaminated with water at the RHs in any of the experiments done here.

Briefly, the portion of the CPC that is important for particle counting is composed of (1) a saturator, where n-butanol (the working fluid) is heated to create a supersaturated sheath air; (2)

a condenser, where the sampled particles meet the supersaturated butanol and grow by condensation of butanol; and (3) an optical detector that counts particles that have grown to droplet sizes. The Kelvin equation (Equation 2.2) relates the saturation ratio to the minimum particle diameter needed to support condensational growth of the supersaturated vapors, where p is the actual partial vapor pressure, p_s is the saturation vapor pressure, γ is the surface tension of the condensing fluid, M is the molecular weight of the condensing fluid, ρ is the density of the condensing fluid, R is the universal gas constant, T is the absolute temperature, and d is the Kelvin diameter.

$$\textbf{\textit{saturation ratio}} = \frac{p}{p_s} = \textbf{\textit{exp}}\left(\frac{4\gamma M}{\rho R T d}\right) \qquad \textbf{Equation 2.2}$$

The saturation ratio is sensitive to the temperature difference (ΔT) between the saturator (T_s = 312 K) and the condenser (T_c = 283 K).[176-178] A decrease in ΔT could be caused by (1) a decrease in T_s, lowering the amount of butanol vapor available for condensing, or (2) an increase in T_c, reducing the extent of supersaturation in the condenser; these effects would reduce the saturation ratio.[177, 178] A decrease in saturation ratio would shift the CPC cutoff diameter, D_{50}, to larger sizes.[177, 178] D_{50} is the size at which counting efficiency is 50%. Perhaps a brief increase in the CPC condenser temperature occurs in the presence of octanol with added H_2O that causes a shift in the saturation ratio and, consequently, an increase in the D_{50}. If the D_{50} increases, then particles at sizes typically activated in the condenser could not grow by condensation and would go undetected.

The counting efficiency of the CPC used in these experiments has been shown to be composition dependent (Table 2.2). The manufacturer used a nonpolar substance to determine the stated 2.5 nm cutoff diameter. However, other studies have shown larger D_{50} for the CPC 3776 for

different substances.[172, 175] The D_{50} is a function of the particle activation efficiency in the CPC condenser, which determines whether or not a particle will grow by condensation of the working fluid.[179] The differences in D_{50} indicate that particle activation in the CPC is dependent on chemical properties of the particle and the condensing working fluid.[172, 174, 175] With all four components in the flow reactor, it is likely that the particle composition is different than sucrose, which TSI used to calibrate the CPC.[176] If this were the case the octanol-MSA-TMA-H_2O particles would not activate in the condenser tube and would not grow large enough to be counted by the CPC optical detector.

Table 2.2 Counting efficiencies of the n-butanol based CPC 3776 (TSI) from the literature.

Substance	D_{50} (nm)
sucrose	$2.5^{[176]}$
NaCl	$4.1^{[172]}$
silver	$3.3^{[172]}$ $3.2^{[175]}$

2.4 EXPERIMENTAL IMPLICATIONS

Due to the challenging measurements with the CPC and octanol, MSA, TMA and H_2O, a less volatile organic with a different functional group was chosen for the next study presented in Chapter 3. These initial experiments described in this chapter are unfinished, but the results indicate that the flow reactor is affected by the order of addition of the reactants. The experimental practice of measuring the base case in order of descending reaction time (14.2 s down to 0.8 s) then turning on the octanol and measuring in order of increasing reaction time

(0.8 s up to 14.2 s) was intended to detect the immediate effect of the octanol at the shortest reaction time. This practice did not allow for a clear and consistent comparison of the effect of octanol at longer reaction times. Therefore, in part of Chapter 3 and all of Chapters 4 and 5, measurements were done at alternating reaction times (*i.e.* in the following order: 12.4 s, 7.6 s, 3.8 s, 0.8 s, 1.3 s, 5.1 s, 10.1 s) to avoid sampling bias with time. These initial experiments showed discrepancies in results obtained with the SMPS versus the CPC, results in Chapter 3 through Chapter 5 were done with at least two of the three detectors (SMPS, CPC, and PSM) to confirm the conclusions presented.

2.5 FUTURE DIRECTIONS

If this project were to be further explored, it is recommended that experiments be repeated. Most importantly, experiments should be repeated using pure TMA from a permeation tube to compare results reported here. Control experiments with octanol and water only in the reactor should be done with the CPC to test the validity of a temperature change in the condenser. The reactant order of addition to the flow reactor should be further tested with the CPC to determine if the CPC responds similarly when MSA, TMA and octanol are all added through the spokes.

CHAPTER 3 THE EFFECT OF MALONIC ACID ON THE REACTION OF MSA AND TMA WITH AND WITHOUT WATER

3.1 RESEARCH GOALS

Building off the work done in Chapter 2, an organic compound with a lower vapor pressure and more opportunities to hydrogen bond was selected for further experiments. Malonic acid (MaA) is a C4 dicarboxylic acid and is considered an SVOC at room temperature. Experiments on the effect of MaA on the reaction of MSA, TMA and water were carried out in the aerosol reactor. Reactant sequence effects were inconclusive from the octanol studies, so the effect of order of addition to the reactor were again investigated. Very preliminary experiments including another SVOC, succinic acid (SuA), were conducted as a comparison to MaA. Structures including clusters of MaA, SuA, MSA and TMA (from a collaboration with Professer R. Benny Gerber) were calculated and are presented in this chapter.

3.2 INITIAL RESULTS AND DISCUSSION

A majority of the experiments done here used TMA from the contaminated gas cylinder (italicized entries in Tables 3.1, 3.2, 3.3, and 3.5) and the remaining experiments generated gas phase TMA from a permeation tube (non-italicized entries in Table 3.2 and Table 3.4). As previously mentioned in Chapter 2, Section 2.2, particle formation was greatly enhanced from sulfuric acid and a mixture of ammonia and amines compared to that from sulfuric acid and pure amine.[60, 64] The biggest impact of the gas cylinder contamination is the increased rate of particle formation from MSA and TMA/NH_3. Table 3.1 shows control experiments with MaA and TMA in the absence and presence of water. Results confirm that, even with the NH_3 contamination,

33

MaA and TMA does not form particles without water and in the presence of water less than 50 particles cm^{-3} form.

Table 3.1 Control experiments, where no MSA was added, and results for the malonic acid (MaA), TMA (from the contaminated gas cylinder) and water system.

Expt.	Ring #1	Ring #3[a]	Spoke #1[b]	General Results
1	dry air	5 ppb TMA[c]	59 ppb MaA	no particles
2	dry air	24 ppb TMA	59 ppb MaA	no particles
3[d]	32% RH	5 ppb TMA	59 ppb MaA	< 50 particles cm^{-3}
4	32% RH	24 ppb TMA	59 ppb MaA	< 50 particles cm^{-3}

Note: Only dry air was added through ring #2, spoke #2 and spoke #3.
[a] Concentrations of TMA are measured prior to their entrance to the reactor. These concentrations account for dilution in the reactor and, due to potential losses in the entrance lines, represent the maximum concentration of each species during reaction.
[b] MaA concentration is calculated from its vapor pressure at 340 K[159] taking into account dilution in the flow reactor. As discussed in the text, this is the maximum concentration of malonic acid during reaction.
[c] Italicized entries indicate that the TMA source was the contaminated gas cylinder.
[d] Blue highlight indicates experiment was done with water.

In Figure 3.1, particle number concentrations from MSA, H_2O and the contaminated TMA/NH$_3$ gas cylinder are compared to those from MSA, H_2O and TMA from the permeation tube. The number concentration with the contaminated gas cylinder peaks at ~2 × 10^5 cm^{-3}. At the same concentration of TMA and roughly double the concentration of MSA, the number concentration with the permeation tube reaches ~2.5 × 10^4 particles cm^{-3}. There is nearly an order of magnitude difference due to the ammonia contamination in the TMA gas cylinder. Glasoe *et al.*[60] observed an enhancement of 20 – 100 times more particles with added NH$_3$ (200 ppt) to methylamine or dimethylamine, sulfuric acid and water. Under conditions with excess MSA and water, the MSA hydrate is expected to aid in particle formation and growth of MSA-TMA-H_2O particles.[130, 133] Therefore, it is even more jarring that the peak number concentration from 11

ppb MSA, 5 ppb TMA and water (20% RH) is lower than that from 6 ppb MSA, 5 ppb

TMA/NH₃ and water (23% RH). It is important to note that comparisons across experiments are

uncertain due to the variability of the reactor between days, but this elevated number

concentration from experiments done with the contaminated TMA gas cylinder is reproducible.
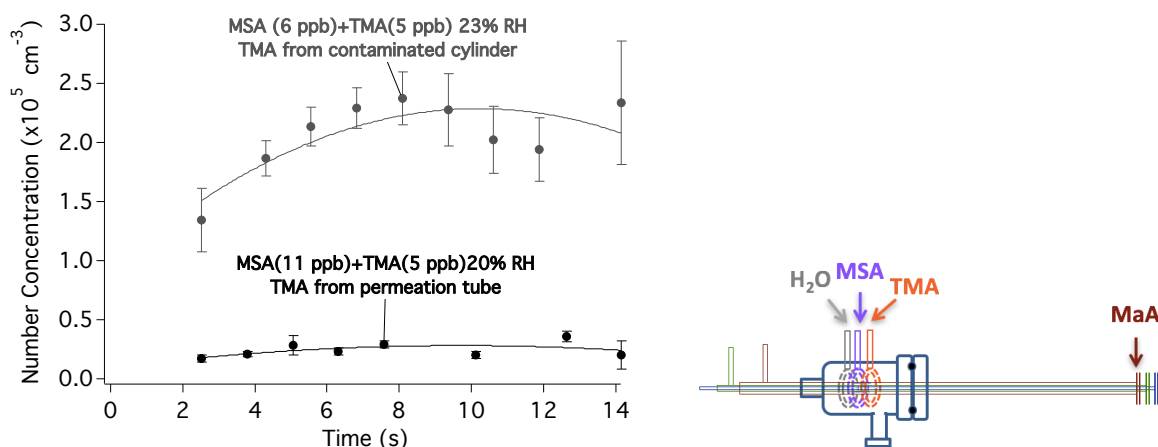
Figure 3.1 Particle number concentrations measured with the PSM with MSA (11 ppb), TMA (5 ppb, permeation tube) and water (20% RH) shown in black and MSA (6 ppb), TMA (5 ppb, contaminated gas cylinder) and water (23% RH) shown in gray; where all reactants were added through the inlets as shown; errors (2σ) are from one minute sample time. Reaction times indicated in the figure corresponds to the time reactants interacted in the reactor, with t = 0 corresponding to the time MSA is introduced at ring #2. Lines are intended to guide the eye. See Table 3.2, Expt. 16a and 21a.

In Table 3.2, Experiments 5 – 15 are too inconsistent to conclude the true effect of adding MaA

after MSA and TMA particles have formed under dry conditions. On the other hand, number

concentrations with MaA, are less than twice that of MSA, TMA and H_2O alone (Figure 3.2).

These results qualitatively agree with those done with octanol (Chapter 2, Section 2.2),

suggesting that MSA-TMA-H_2O particles will not hydrogen bond to an added IVOC alcohol or

SVOC dicarboxylic acid and subsequently grow in size. An attempt to test a less volatile

dicarboxylic acid was made, however, SuA could not be detected when introduced through the

spoke inlets, likely due to its lower volatility.
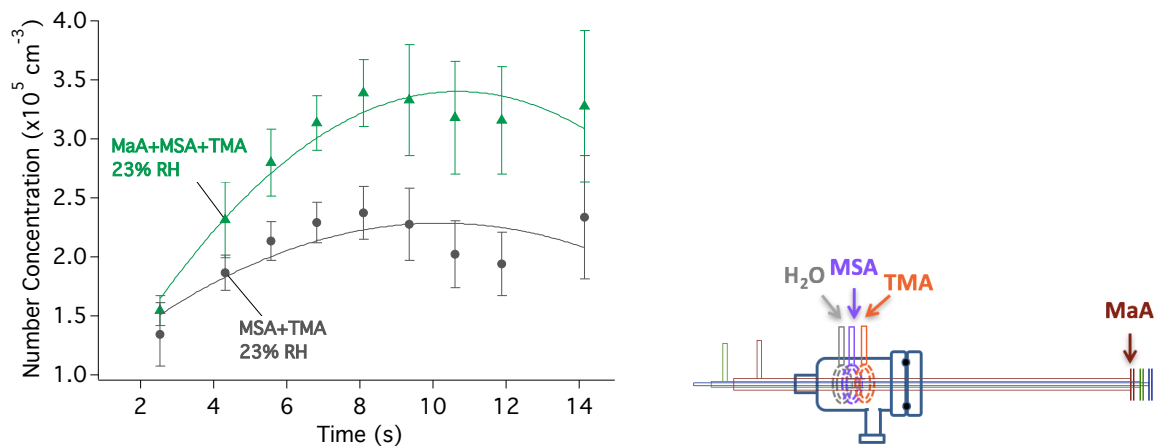
Figure 3.2 Particle number concentrations measured with the PSM with MSA (6 ppb), TMA (5 ppb, contaminated gas cylinder), malonic acid (59 ppb) and water (23% RH) in the reactor where all reactants were added through the inlets as shown; errors (2σ) are from one minute sample time. Note that number concentrations for MaA + MSA + TMA 23% RH may be underestimated due to higher coincidence in particle counting from the CPC above 3×10^5 cm^{-3}. Reaction times indicated in the figure corresponds to the time reactants interacted in the reactor, with t = 0 corresponding to the time MSA is introduced at ring #2. Lines are intended to guide the eye. See Table 3.2, Expt. 21.

Table 3.2 Conditions and results for experiments done with MSA added through ring #2, TMA (from either the contaminated gas cylinder or the permeation tube, indicated in the footnotes) added through ring #3 and with and without malonic acid (MaA) added through spoke #1.

Expt.	Ring #1	Ring #2[a]	Ring #3[a]	Spoke #1[b]	General Results	Conditioning Time (mins)
5a	*dry air*	***10 ppb MSA***	*2 ppb TMA* [c]	*dry air*	*base case*	
5b	*dry air*	***10 ppb MSA***	*2 ppb TMA*	*59 ppb MaA*	*0* [d]	*60*
6a	*dry air*	*5 ppb MSA*	*5 ppb TMA*	*dry air*	*base case*	
6b	*dry air*	*5 ppb MSA*	*5 ppb TMA*	*59 ppb MaA*	*−* [e]	*80*
7a	*dry air*	*5 ppb MSA*	*5 ppb TMA*	*dry air*	*base case*	
7b	*dry air*	*5 ppb MSA*	*5 ppb TMA*	*59 ppb MaA*	*+* [f]	*60*
8a	*dry air*	*5 ppb MSA*	*5 ppb TMA*	*dry air*	*base case*	
8b	*dry air*	*5 ppb MSA*	*5 ppb TMA*	*59 ppb MaA*	*−*	*60*
9a	*dry air*	*5 ppb MSA*	*5 ppb TMA*	*dry air*	*base case*	
9b	*dry air*	*5 ppb MSA*	*5 ppb TMA*	*59 ppb MaA*	*−*	*60*
10a	*dry air*	*4 ppb MSA*	*5 ppb TMA*	*dry air*	*base case*	
10b	*dry air*	*4 ppb MSA*	*5 ppb TMA*	*59 ppb MaA*	*−*	*30*
11a	*dry air*	*4 ppb MSA*	*4 ppb TMA*	*dry air*	*base case*	
11b	*dry air*	*4 ppb MSA*	*4 ppb TMA*	*59 ppb MaA*	*0*	*20*
12a	*dry air*	***7 ppb MSA***	*5 ppb TMA*	*dry air*	*base case*	
12b	*dry air*	***7 ppb MSA***	*5 ppb TMA*	*59 ppb MaA*	*0*	*0*
13a	*dry air*	***12 ppb MSA***	*5 ppb TMA*	*dry air*	*base case*	
13b	*dry air*	***12 ppb MSA***	*5 ppb TMA*	*59 ppb MaA*	*0*	*0*
14a	dry air	**10 ppb MSA**	7 ppb TMA[g]	dry air	base case	
14b	dry air	**10 ppb MSA**	7 ppb TMA	59 ppb MaA	0	0
15a	*dry air*	*1 ppb MSA*	***13 ppb TMA***	*dry air*	*base case*	
15b	*dry air*	*1 ppb MSA*	***13 ppb TMA***	*59 ppb MaA*	*−*	*0*
16a[h]	20% RH	**11 ppb MSA**	5 ppb TMA	dry air	base case	
16b	20% RH	**11 ppb MSA**	5 ppb TMA	59 ppb MaA	0	20
17a	20% RH	**13 ppb MSA**	5 ppb TMA	dry air	base case	
17b	20% RH	**13 ppb MSA**	5 ppb TMA	59 ppb MaA	0	10
18a	*19% RH*	*0.8 ppb MSA*	***24 ppb TMA***	*dry air*	*base case*	
18b	*19% RH*	*0.8 ppb MSA*	***24 ppb TMA***	*59 ppb MaA*	*0*	*50*
19a	*20% RH*	*6 ppb MSA*	***10 ppb TMA***	*dry air*	*base case*	
19b	*20% RH*	*6 ppb MSA*	***10 ppb TMA***	*59 ppb MaA*	*0*	*0*
20a	*16% RH*	*5 ppb MSA*	*4 ppb TMA*	*dry air*	*base case*	
20b	*16% RH*	*5 ppb MSA*	*4 ppb TMA*	*59 ppb MaA*	*0*	*40*
21a	*23% RH*	*6 ppb MSA*	*5 ppb TMA*	*dry air*	*base case*	

21b	*23% RH*	*6 ppb MSA*	*5 ppb TMA*	*59 ppb MaA*	*0*	*40*
22a	*17% RH*	*5 ppb MSA*	*4 ppb TMA*	*dry air*	*base case*	
22b	*17% RH*	*5 ppb MSA*	*4 ppb TMA*	*59 ppb MaA*	*0*	*35*

Note: Only dry air was added through spoke #2 and spoke #3.

[a] Concentrations of MSA and MA are measured prior to their entrance to the reactor. These concentrations account for dilution in the reactor and, due to potential losses in the entrance lines, represent the maximum concentration of each species during reaction. Values are in bold-face font when in excess.

[b] MaA concentration is calculated from its vapor pressure at 340 K[159] taking into account dilution in the flow reactor. As discussed in the text, this is the maximum concentration of malonic acid during reaction.

[c] Italicized entries indicate that the TMA source was the contaminated gas cylinder.

[d] "0" indicates the observed number concentration due to the added MaA was between 0.5 to 2 times the base case number concentration.

[e] "–" represents ≥ 0.5 times less particles were observed due to the added MaA.

[f] "+" represents ≥ 2 times more particles were observed due to the added MaA.

[g] Non-italicized entries indicate that the TMA source was the permeation tube.

[h] Blue highlight indicates experiment was done with water vapor.

Experiments were performed with MaA and TMA introduced through ring #2 and #3, respectively, and MSA in spoke #1. This configuration was intended to elucidate how MSA would react when meeting MaA and TMA at the same time. Results in Table 3.3 show that, with this configuration, there is no effect on particle formation. This configuration also further confirms that particles did not form from MaA and TMA/NH_3 before meeting MSA downstream.

Table 3.3 Conditions and results for experiments done with MSA added through spoke #1, TMA (from the contaminated gas cylinder) added through ring #3 and with and without malonic acid (MaA) added through ring #2.

Expt.	Ring #1	Ring #2[a]	Ring #3[b]	Spoke #1[b]	General Results	Conditioning Time (mins)
23a	*dry air*	*dry air*	*4 ppb TMA*[c]	***9 ppb MSA***	*base case*	
23b	*dry air*	*117 ppb MaA*	*4 ppb TMA*	***9 ppb MSA***	*0*[d]	*35*
24a	*dry air*	*dry air*	*4 ppb TMA*	***8 ppb MSA***	*base case*	
24b	*dry air*	*117 ppb MaA*	*4 ppb TMA*	***8 ppb MSA***	*0*	*0*
25a[e]	*20% RH*	*dry air*	*2 ppb TMA*	***7 ppb MSA***	*base case*	
25b	*20% RH*	*117 ppb MaA*	*2 ppb TMA*	***7 ppb MSA***	*0*	*0*
26a	*20% RH*	*dry air*	*3 ppb TMA*	***9 ppb MSA***	*base case*	
26b	*20% RH*	*117 ppb MaA*	*3 ppb TMA*	***9 ppb MSA***	*0*	*0*
27a	*20% RH*	*dry air*	*3 ppb TMA*	***9 ppb MSA***	*base case*	
27b	*20% RH*	*117 ppb MaA*	*3 ppb TMA*	***9 ppb MSA***	*0*	*0*

Note: Only dry air was added through spoke #2 and spoke #3.
[a] Malonic acid concentration is calculated from its vapor pressure at 340 K[159] taking into account dilution in the flow reactor. As discussed in the text, this is the maximum concentration of malonic acid during reaction.
[b] Concentrations of MSA and TMA are measured prior to their entrance to the reactor. These concentrations account for dilution in the reactor and, due to potential losses in the entrance lines, represent the maximum concentration of each species during reaction. Values are in bold-face font when in excess.
[c] Italicized entries indicate that the TMA source was the contaminated gas cylinder.
[d] "0" indicates the observed number concentration due to the added MaA was between 0.5 to 2 times the base case number concentration.
[e] Blue highlight indicates experiment was done with water vapor.

Table 3.4 shows results from experiments done with TMA generated from the permeation tube. Without water, results are inconclusive and show no effect of MaA with equal concentrations of MSA and TMA in the reactor. However, in conditions with excess MSA and excess TMA there is at least twice the amount of particles formed in the presence of MaA compared to the base case of MSA and TMA alone, suggesting a concentration dependence.

In a recent theoretical study, the requirements of an organic compound that favor cluster formation with sulfuric acid were investigated.[80] Calculated Gibbs free energies supported that organic compounds most efficiently stabilized sulfuric acid to form clusters if there were no internal hydrogen bonds present and if at least two carboxylic acid groups (with, ideally, $\geq$ three molecules between two –COOH groups) interacted directly with H_2SO_4.[80] Structures and energies calculated by Dr. Mychel Varner from the Gerber group are shown in Figure 3.3. Two isomers of MaA were found, one of which has an internal hydrogen bond and one free OH group available for addition of MSA or TMA (Figure 3.3); though MaA has two –COOH groups, there is only one carbon between them. Thus, MaA only partially meets the requirements proposed by Elm et al.,[80] which may help explain the inconsistent experimental results.

The most stable structures found by Elm et al.[80] show sulfuric acid with three hydrogen bonds to the organic; for a dicarboxylic acid, each of the –COOH groups has at least one hydrogen bond to H_2SO_4. The formation of a third hydrogen bond between sulfuric acid and MaA was found to strain the backbone of MaA and slightly destabilize the cluster compared to that with only two hydrogen bonds ($\Delta G_{3\text{-H-bonds}} = -5.4$ kcal mol^{-1} vs $\Delta G_{2\text{-H-bonds}} = -6.0$ kcal mol^{-}1).[80] There are only two hydrogen bonds between MaA and MSA in the MaA-MSA cluster (Figure 3.3). The

internal hydrogen bond on MaA prevents the possibility of a third hydrogen bond with MSA, which may serve to stabilize the MaA-MSA cluster as having only two hydrogen bonds does with MaA-H_2SO_4.[80] However, it is also possible that the other isomer of MaA (without the internal hydrogen bond) forms three hydrogen bonds with MSA, potentially straining MaA and weakening the MaA-MSA cluster.

Growth of these small clusters to detectable particles is expected to occur via hydrogen bonding.[130, 133] In the MaA-MSA cluster (Figure 3.3), MSA forms two hydrogen bonds with MaA and there is one free oxygen each on MSA and MaA that can participate in hydrogen bonding. The internal hydrogen bond on the MaA isomer reduces its hydrogen bonding capacity, thereby hindering additional growth of the MaA-MSA cluster. Under conditions of excess MSA, perhaps the hydrogen bonding sites available on the MaA-MSA cluster aids in particle formation and growth of MaA-MSA-TMA particles. As a tertiary amine, TMA has one available site for hydrogen bonding. Once TMA connects with MaA, TMA cannot form additional hydrogen bonds to grow the MaA-TMA cluster; growth must occur through MaA. A comparison of binding energies shows that the formation of the MaA-TMA cluster (-20 kcal mol^{-1}) is slightly more favorable than the MaA-MSA cluster (-17 kcal mol^{-1}). Perhaps, with excess TMA, the slightly stronger interaction between MaA and TMA promotes MaA-MSA-TMA particle formation and growth.

Between the two conformational isomers of MaA, there are multiple ways to form an MaA-MSA cluster. It is unclear if one isomer will lead to a more stable cluster than the other. The presence of an internal hydrogen bond on MaA can have opposing effects on cluster formation with MSA:

(1) to reduce the opportunities for hydrogen bonding with other species, which may impede cluster growth and (2) to prevent the formation of a third hydrogen bond with MSA, which potentially stabilizes the cluster. Considering the MaA isomer without the internal hydrogen bond, there are more possibilities for intermolecular hydrogen bonds, supporting growth, but three hydrogen bonds could form between MaA and MSA, likely destabilizing the cluster. The erratic experimental results may be a result of these conflicting effects.
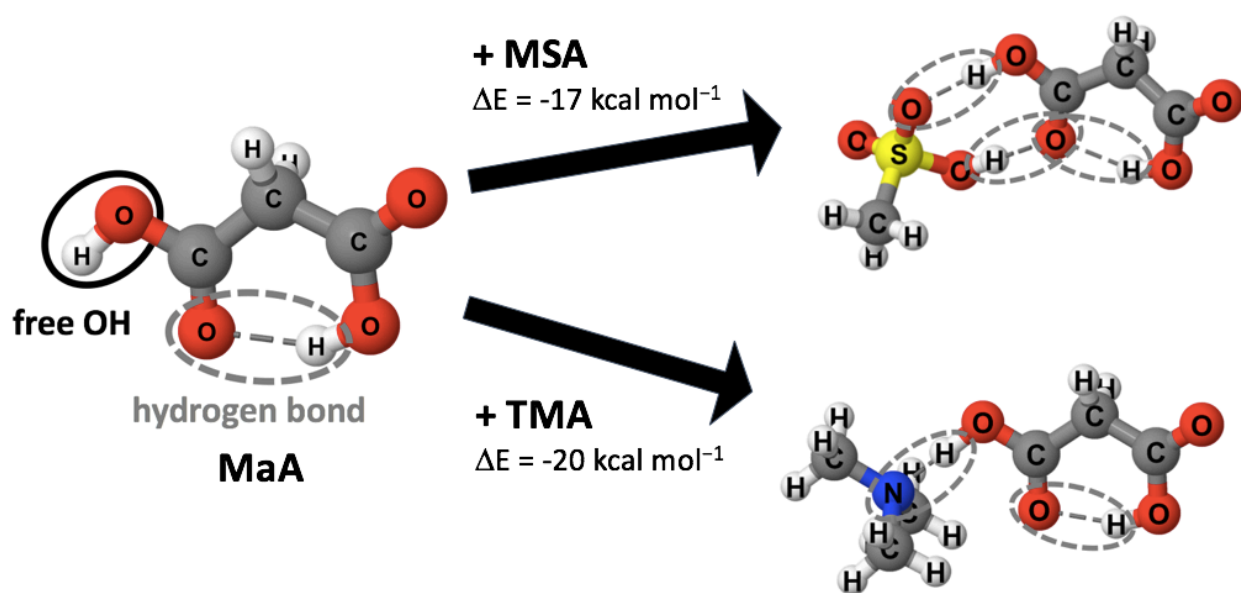
Figure 3.3 Structures and binding energies of MaA, MaA-MSA, and MaA-TMA calculated at the RIMP2/aug-cc-pV(D+d)Z level of theory by Dr. Mychel Varner from the Gerber group.

Table 3.4 Conditions and results for experiments done with MSA added through spoke #1, TMA (from the permeation tube) added through spoke #2 and with and without malonic acid (MaA) added through ring #2.

Expt.	Ring #1	Ring #2[a]	Spoke #1[b]	Spoke #2[b]	General Results	Conditioning Time (mins)
28a	dry air	dry air	**9 ppb MSA**	2 ppb TMA[c]	base case	
28b	dry air	20 ppb MaA	**9 ppb MSA**	2 ppb TMA	− [d]	0
29a	dry air	dry air	**12 ppb MSA**	2 ppb TMA	base case	
29b	dry air	20 ppb MaA	**12 ppb MSA**	2 ppb TMA	+ [e]	0
30a	dry air	dry air	**13 ppb MSA**	3 ppb TMA	base case	
30b	dry air	20 ppb MaA	**13 ppb MSA**	3 ppb TMA	+	0
31a	dry air	dry air	3 ppb MSA	**10 ppb TMA**	base case	
31b	dry air	20 ppb MaA	3 ppb MSA	**10 ppb TMA**	+	0
32a	dry air	dry air	5 ppb MSA	5 ppb TMA	base case	
32b	dry air	20 ppb MaA	5 ppb MSA	5 ppb TMA	0 [f]	0
33a	dry air	dry air	4 ppb MSA	4 ppb TMA	base case	
33b	dry air	20 ppb MaA	4 ppb MSA	4 ppb TMA	0	0
34a	dry air	dry air	3 ppb MSA	**10 ppb TMA**	base case	
34b	dry air	99 ppb MaA	3 ppb MSA	**10 ppb TMA**	+	20
35a[g]	18% RH	dry air	**11 ppb MSA**	3 ppb TMA	base case	
35b	18% RH	20 ppb MaA	**11 ppb MSA**	3 ppb TMA	0	0
36a	17% RH	dry air	**9 ppb MSA**	3 ppb TMA	base case	
36b	17% RH	20 ppb MaA	**9 ppb MSA**	3 ppb TMA	0	0
37a	20% RH	dry air	3 ppb MSA	**11 ppb TMA**	base case	
37b	20% RH	20 ppb MaA	3 ppb MSA	**11 ppb TMA**	+	0
38a	20% RH	dry air	0.6 ppb MSA	**11 ppb TMA**	base case	
38b	20% RH	20 ppb MaA	0.6 ppb MSA	**11 ppb TMA**	+	20
39a	17% RH	dry air	4 ppb MSA	4 ppb TMA	base case	
39b	17% RH	20 ppb MaA	4 ppb MSA	4 ppb TMA	0	0
40a	17% RH	dry air	3 ppb MSA	3 ppb TMA	base case	
40b	17% RH	20 ppb MaA	3 ppb MSA	3 ppb TMA	0	0

Note: Only dry air was added through ring #3 and spoke #3.

[a] MaA concentration is calculated from its vapor pressure at 340 K[159] taking into account dilution in the flow reactor. As discussed in the text, this is the maximum concentration of malonic acid during reaction.

[b] Concentrations of MSA and TMA are measured prior to their entrance to the reactor. These concentrations account for dilution in the reactor and, due to potential losses in the entrance lines, represent the maximum concentration of each species during reaction. Values are in bold-face font when in excess.

[c] Non-italicized entries indicate that the TMA source was the permeation tube.

Figure 3.4 shows no significant difference (< 2 times more particles) in number concentrations from MSA, TMA and water with and without MaA when MSA and TMA are at the same concentration. The same is true when MSA is in excess. Under conditions with excess TMA (Figure 3.5; Table 3.4, Expts. 37 and 38) an increase in particle number concentration, with great error, was observed in the presence of MaA compared to the base case with MSA, TMA and H₂O, perhaps indicating that TMA and/or the TMA-H₂O complex aided in growth of particles to detectable sizes. However, in previous studies of MSA, TMA and H₂O the MSA-H₂O complex was considered to be more important in particle formation and growth compared to the TMA-H₂O complex.[130, 133]
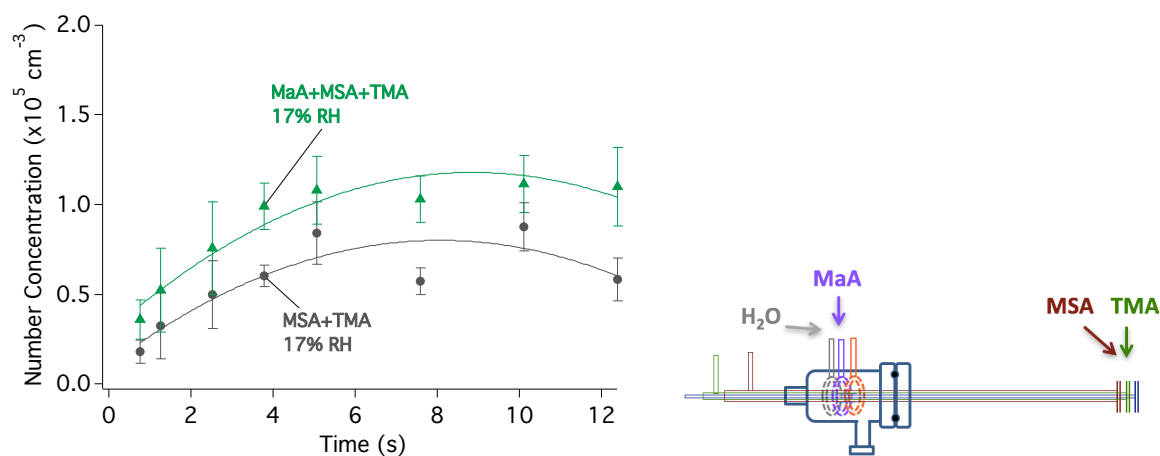
Figure 3.4 Particle number concentrations measured with the PSM with MSA (4 ppb), TMA (4 ppb, permeation tube), malonic acid (20 ppb) and water (17% RH) in the reactor where all reactants were added through the inlets as shown; errors (2σ) are from one minute sample time. Reaction times indicated in the figure corresponds to the time reactants interacted in the reactor, with t = 0 corresponding to the time MSA is introduced at spoke #1. Lines are intended to guide the eye. See Table 3.4, Expt. 39.
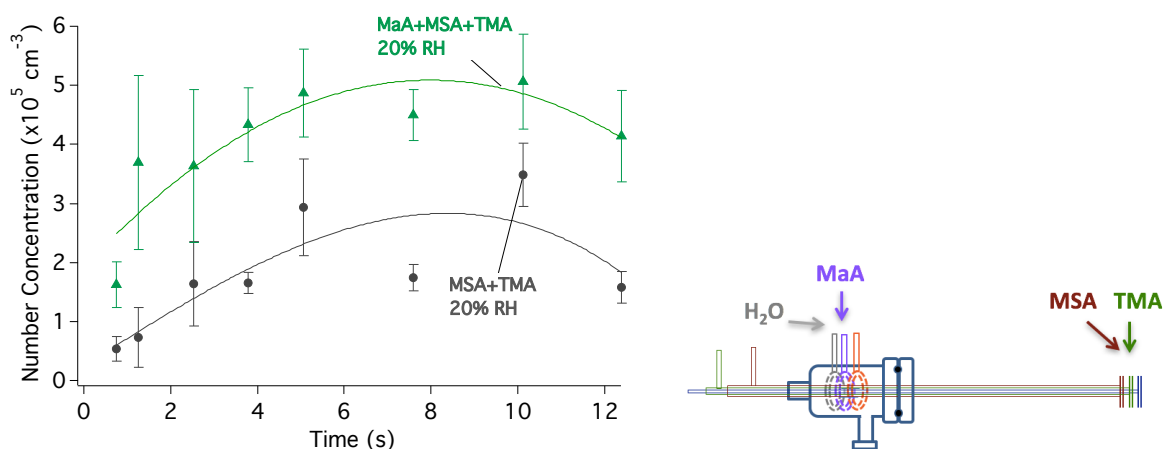
Figure 3.5 Particle number concentrations measured with the PSM with MSA (3 ppb), TMA (11 ppb, permeation tube), malonic acid (20 ppb) and water (20% RH) in the reactor where all reactants were added through the inlets as shown; errors (2σ) are from one minute sample time. Note that number concentrations for MaA + MSA + TMA 20% RH may be underestimated due to higher coincidence in particle counting from the CPC above 3×10^5 cm^{-3}. Reaction times indicated in the figure corresponds to the time reactants interacted in the reactor, with t = 0 corresponding to the time MSA is introduced at spoke #1. Lines are intended to guide the eye. See Table 3.4, Expt. 37.

Very preliminary results of experiments done with SuA are shown in Table 3.5. In the presence of SuA, particle formation is enhanced ($\geq$ 2 times more particles) under dry (Figure 3.6) and humid conditions. These early results suggest that the lower volatility of SuA may contribute to the more consistent enhancement observed compared to experiments done with MaA, but other properties, including molecular geometry, may also be important.
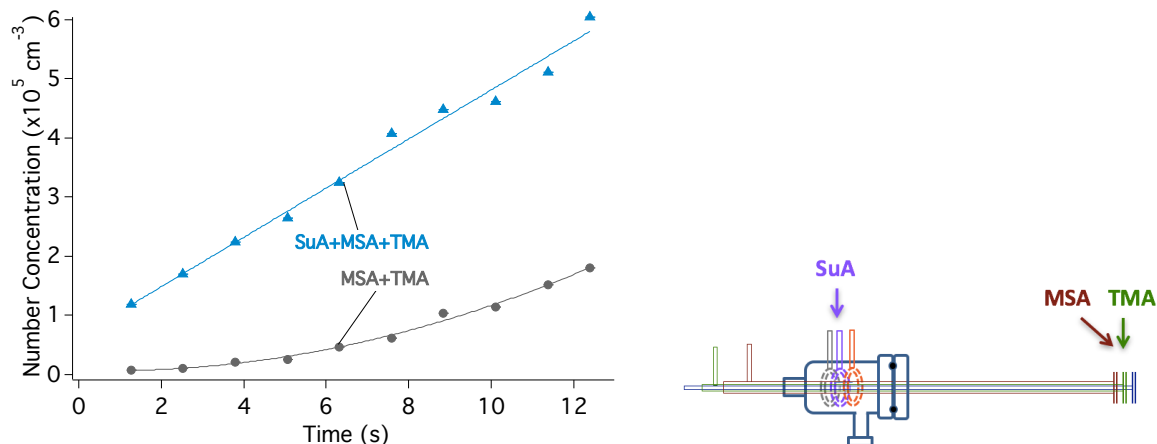
Figure 3.6 Particle number concentrations measured with the PSM with MSA (5.2 ppb), TMA (25 ppb, contaminated gas cylinder), succinic acid (0.2 ppm) in the reactor where all reactants were added through the inlets as shown; errors (2σ) are from one minute sample time. Note that number concentrations for SuA + MSA + TMA may be underestimated due to higher coincidence in particle counting from the CPC above 3×10^5 cm^{-3}. Reaction times indicated in the figure corresponds to the time reactants interacted in the reactor, with t = 0 corresponding to the time MSA is introduced at spoke #1. Lines are intended to guide the eye. See Table 3.5, Expt. 2.

Dr. Mychel Varner from the Gerber group calculated structures and energies of SuA, SuA-MSA and SuA-TMA shown in Figure 3.7. Unlike MaA, none of the four most stable conformational isomers of SuA have an internal hydrogen bond. In the SuA-MSA cluster, MSA forms two hydrogen bonds with one carboxylic group of SuA leaving two free oxygens on MSA, one free oxygen on SuA, and a free OH group on the other carboxylic group of SuA available for additional hydrogen bonding. Elm *et al.*[80] showed that dicarboxylic acids with a γ-carbonyl group (*e.g.* succinic acid) would best stabilize sulfuric acid and most likely lead to cluster formation. If, alternatively, MSA formed a hydrogen bond with each carboxylic group on SuA, similar to the SuA-H$_2$SO$_4$ cluster proposed by Elm *et al.*,[80] then there would still be hydrogen bonding opportunities available and the SuA-MSA cluster could continue to grow. In the SuA-TMA cluster, TMA hydrogen bonds to SuA and, though TMA has no hydrogen bonding sites left, there are two oxygens and one OH group on SuA available for growth. Experimental results

together with initial clusters calculated by the Gerber group and results from Elm *et al.*[80] support

that particle formation and growth with SuA should be more favorable than that with MaA.
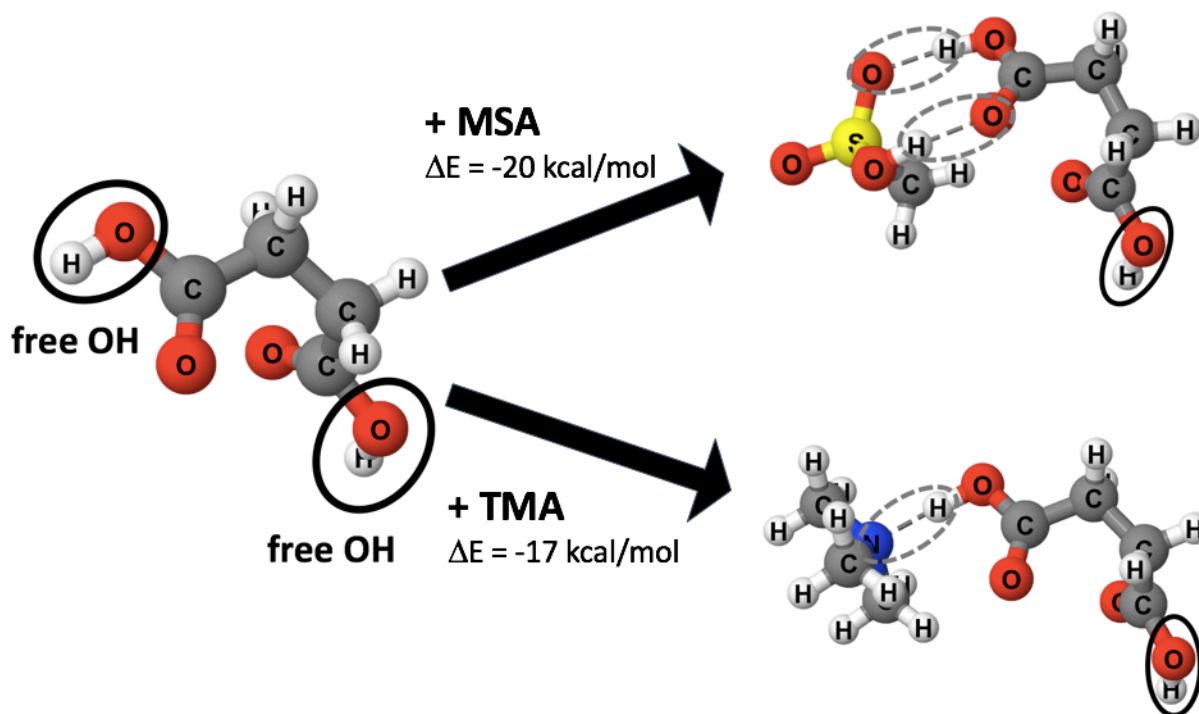
Figure 3.7 Structures and binding energies of SuA, SuA-MSA, and SuA-TMA calculated at the RIMP2/aug-cc-pV(D+d)Z level of theory by Dr. Mychel Varner from the Gerber group.

Table 3.5 Conditions and results for experiments done with MSA added through spoke #1, TMA (from the contaminated gas cylinder) added through spoke #2 and with and without succinic acid (SuA) added through ring #2.

Expt. #	Ring #1	Ring #2[a]	Spoke #1[b]	Spoke #2[b]	General Results	Conditioning Time (mins)
1a	dry air	dry air	6.2 ppb MSA	**25 ppb TMA**[c]	base case	
1b	dry air	0.2 ppm SuA	6.2 ppb MSA	**25 ppb TMA**	+[d]	24
2a	dry air	dry air	5.2 ppb MSA	**25 ppb TMA**	base case	
2b	dry air	0.2 ppm SuA	5.2 ppb MSA	**25 ppb TMA**	+	60
3a[e]	20% RH	dry air	5.6 ppb MSA	**18 ppb TMA**	base case	
3b	20% RH	0.2 ppm SuA	5.6 ppb MSA	**18 ppb TMA**	+	60
4a	20% RH	dry air	4.6 ppb MSA	**18 ppb TMA**	base case	
4b	20% RH	0.2 ppm SuA	4.6 ppb MSA	**18 ppb TMA**	+	120

Note: Only dry air was added through ring #3 and spoke #3.
[a] Succinic acid concentration is calculated from its vapor pressure at 343 K[159] taking into account dilution in the flow reactor. As discussed in the text, this is the maximum concentration of malonic acid during reaction.
[b] Concentrations of MSA and TMA are measured prior to their entrance to the reactor. These concentrations account for dilution in the reactor and, due to potential losses in the entrance lines, represent the maximum concentration of each species during reaction. Values are in bold-face font when in excess.
[c] Italicized entries indicate that the TMA source was the contaminated gas cylinder.
[d] "+" represents ≥ 2 times more particles were observed due to the added SuA.
[e] Blue highlight indicates experiment was done with water vapor.

3.3 EXPERIMENTAL IMPLICATIONS

Interpretation of these results must be made with extreme caution because of the great variability present during experiments. In addition to the different sources/purities of TMA, experiments were conducted with varying conditioning times of the reactor in the presence of the organic (MaA or SuA). Results are inconsistent from experiments where the system was conditioned with MaA, MSA and TMA (and water, if under humid conditions). In Chapters 4 and 5, measurements in the presence of the organic or another variable reactant are done immediately after the base case measurement is completed. It was determined that SuA could only be added

through the ring inlets. Succinic acid was likely lost along the spoke inlets, due to its low vapor pressure. Thus, in Chapters 4 and 5, the organic is always added through a ring inlet.

3.4 FUTURE DIRECTIONS

These experiments will need to be repeated with a non-contaminated source of TMA. Control experiments with MaA and TMA from a permeation tube and MaA and MSA should be done. Other orders of addition can be tested to determine if adding MaA or SuA, MSA and TMA in the rings and adding water through the spokes will affect particle growth. Since early results including SuA were done with excess TMA, it would be ideal to conduct additional experiments with excess MSA and equal concentrations of MSA and TMA.

CHAPTER 4   THE EFFECT OF OXALIC ACID ON THE REACTION OF MSA AND MA WITH AND WITHOUT WATER

Adapted from: K. D. Arquero, R. B. Gerber, and B. J. Finlayson-Pitts, "The Effect of Oxalic Acid on New Particle Formation from Methanesulfonic Acid, Methylamine, and Water" *Environmental Science and Technology* **2017**, 51, 2124 – 2130. Copyright 2017 by American Chemical Society.

4.1   RESEARCH GOALS

MSA and MA have been shown to more efficiently form particles with and without water vapor compared to dimethylamine, TMA, and ammonia.[131, 132] Here, the effect of OxA on the reaction of MSA and MA with and without water vapor was explored with the small volume aerosol flow reactor. OxA is the smallest dicarboxylic acid, is polar, has opportunities for hydrogen bonding and its vapor pressure (VP at 298 K = 1.4×10^{-2} Pa)[159] categorizes it as an IVOC.[154-157] The combination of these properties makes OxA an ideal candidate for studies of particle formation and growth. The results of this study, summarized in Tables 4.1 through 4.4, are presented in this chapter.

4.2   RESULTS AND DISCUSSION

In Figure 4.1, the data labelled 26% RH OxA + MA show the particle number concentration of water, OxA (17 ppb; 4×10^{11} cm^{-3}) and MA (890 ppt; 2×10^{10} cm^{-3}) compared to the base case, which contained only OxA and MA. At 890 ppt MA the number of particles formed is only a few per cm^3 without water vapor. With water vapor corresponding to 26% RH (1.6×10^{17} cm^{-3}), the particle number concentration increases by about an order of magnitude, but is still only tens

of particles cm^{-3}. At MA concentrations greater than ~9 ppb with a consistent 17 ppb of OxA

(Figure 4.2), the particle concentrations increase slightly to larger values with added water vapor

but the error bars are large, potentially due to the need for more conditioning with each increase

in MA.
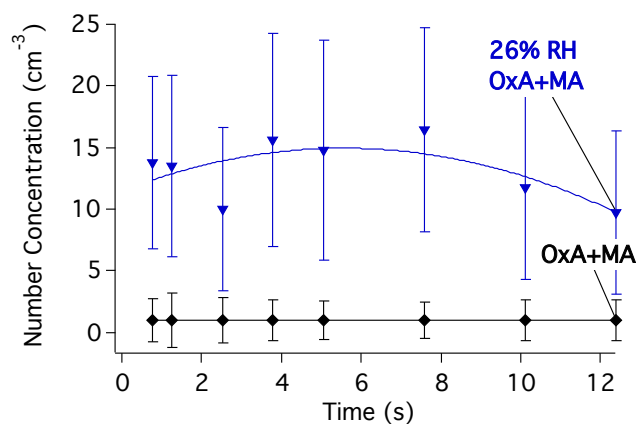
Figure 4.1 Number concentrations from the reaction of OxA (17 ppb) + MA (890 ppt) with and without water vapor (26% RH) measured with the CPC; errors (2σ) are from one minute sample time. Reaction times indicated in the figure corresponds to the time reactants interacted in the reactor, with t = 0 corresponding to the time at spoke #1. Lines intended to guide the eye. See Table 4.3, Expt. 31.
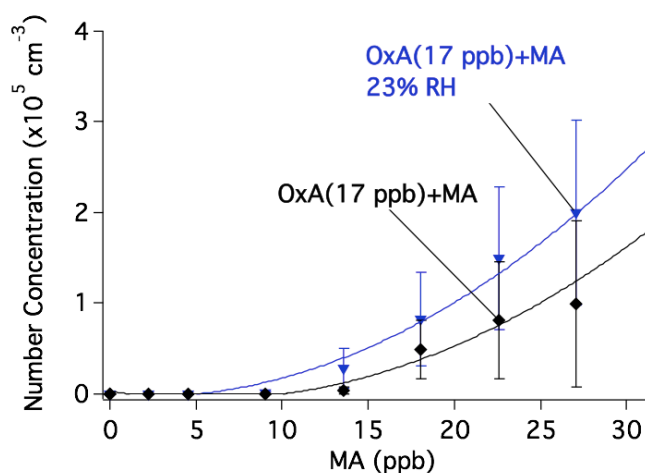
Figure 4.2 Number concentrations from the reaction of OxA (17 ppb) as a function of MA (0 – 32 ppb) with and without water vapor (23% RH) measured at 12.4 s reaction time with the CPC; errors (2σ) are from one minute sample time. Reaction times indicated in the figure corresponds to the time reactants interacted in the reactor, with t = 0 corresponding to the time at spoke #1. Lines intended to guide the eye. See Table 4.4, Expt. 40.

While proton transfer is expected between an acid and a base to form an ion pair, water is often required, even for strong acids. Tao et al.[73, 136] have shown that proton transfer to form an ion pair from one molecule of NH_3 with one molecule of H_2SO_4 occurs only if at least one water molecule is present, and for MSA, two water molecules are needed. Similar results were found with MSA and pyridine where proton transfer was observed only when one or two water molecules were present.[180] Theoretical calculations performed by Xu et al.[164] have shown that proton transfer from SuA to dimethylamine $((CH_3)_2NH)$ occurs with more than three water molecules present and that interactions between the acid and amine are strengthened by further hydration.

Theoretical calculations and structures done by Xu et al.[181] show a qualitative correlation between proton transfer in small clusters and experimental results presented here. There is no proton transfer in the OxA-MA cluster, but a proton transfer occurs in the OxA-MA-H_2O cluster and experimentally, particle formation is enhanced in the presence of water. This suggests that proton transfer may be important in stabilizing small clusters for particle formation and growth. A proton transfer is also observed for the OxA-MA dimer.[181] This supports the experimental observation of only a few particles formed from OxA-MA with MA concentrations < 9 ppb. To support particle formation from the OxA-MA dimer, a significant number of OxA-MA monomers would need to accumulate. However, OxA and MA are weakly bound by a single hydrogen bond (D_e = 15.97 kcal mol^{-1})[181] and might dissociate before a sufficient amount of monomers builds up. It may be that the critical number of OxA-MA monomers needed were formed at MA concentrations > 9 ppb, where, under dry conditions, particle formation was significant (Figure 4.2).

Theoretical calculations predict that OxA-dimethylamine,[163] OxA-ammonia,[161] and OxA-ammonia-H_2O[160, 162] clusters will be involved in particle formation. New particle formation from OxA and sulfuric acid with water[165] or ammonia[166] has also been predicted. However, if OxA and MA are representative of dicarboxylic acids and amines in air, then these reactions do not seem likely to contribute significantly to particle formation on their own at ambient RH with low concentrations of MA (< 9 ppb).

It has been shown that the reaction of MSA with MA forms particles efficiently and that the presence of water vapor greatly enhances both the number concentration (Figure 4.3) and diameters.[132] However, there are numerous organics in air, including dicarboxylic acids, which may contribute to stabilizing and growing small acid-amine clusters that lead to new particles more efficiently than the acid-amine combination alone.[63, 76-78, 82, 86-91] To probe this, experiments were done in which particles were formed from MSA-MA and then the effect of OxA was tested in the presence and absence of water vapor (Table 4.1).
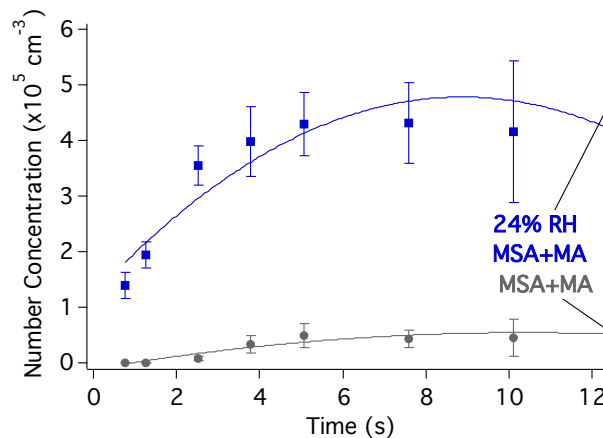
Figure 4.3 Number concentrations from the reaction of MSA (4 ppb) + MA (116 ppt) with and without water vapor (24% RH) measured with the CPC; errors (2σ) are from one minute sample time. Note that number concentrations for 24% RH MSA+MA may be underestimated due to higher coincidence in particle counting from the CPC above 3×10^5 cm^{-3}. Reaction times indicated in the figure corresponds to the time reactants interacted in the reactor, with t = 0 corresponding to the time MSA is introduced at spoke #1. Lines intended to guide the eye. See Table 4.1, Expt. 15.

Figure 4.4 shows a modest enhancement of new particle formation (< 1 order of magnitude) when only 17 ppb OxA is introduced to MSA and MA without water vapor. On the other hand, there is no significant change with OxA, MSA and MA in the presence of water vapor (Figure 4.5). Furthermore, Figure 4.6 shows size distributions from MSA + MA and OxA + MSA + MA without water (Figure 4.6 (a) and (b)) and with water (Figure 4.6 (c) and (d)) where there is no additional particle growth in the presence of OxA compared to the MSA + MA (+ H$_2$O) base case. In both dry and humid cases, OxA does not affect growth of particles beyond detectable sizes and particles are larger than 2.5 nm, consistent with the PSM and CPC yielding comparable results (Chapter 1, Section 1.3.3). Note that the concentrations of water vapor used in these experiments (20 − 40% RH) are much larger than the concentrations of OxA that can be added to the system, so a quantitative per-molecule comparison cannot be made between the roles of H$_2$O and OxA. OxA concentrations are limited by volatility, and reliably delivering water at ppb levels in this system is not feasible.
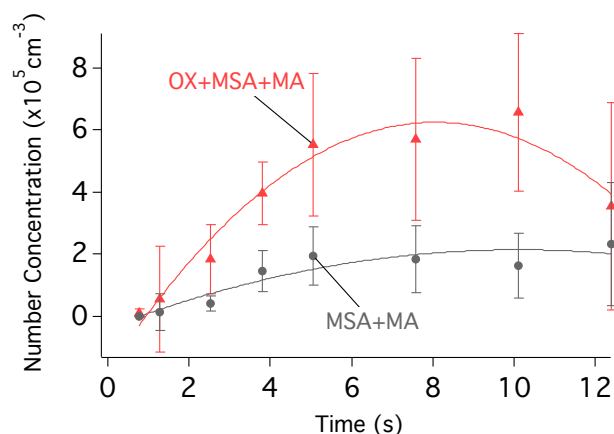
Figure 4.4 Number concentrations from the reaction of MSA (5 ppb) + MA (159 ppt) with and without OxA (17 ppb) measured with the PSM; errors (2σ) are from one minute sample time. Note that number concentrations for OxA+MSA+MA may be slightly underestimated due to higher coincidence in particle counting from the CPC above 3×10^5 cm^{-3}. Reaction times indicated in the figure corresponds to the time reactants interacted in the reactor, with t = 0 corresponding to the time MSA is introduced at spoke #1. Lines intended to guide the eye. See Table 4.1, Expt. 8.
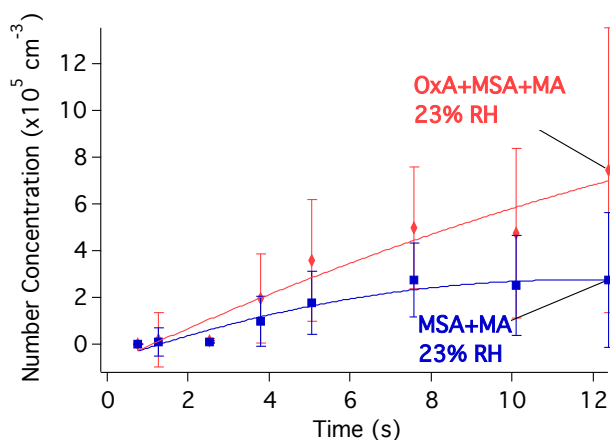
Figure 4.5 Number concentrations from the reaction of MSA (380 ppb) + MA (780 ppt) with and without OxA (17 ppb) in the presence of water vapor (23% RH) measured with the PSM; errors (2σ) are from one minute sample time. Note that number concentrations for OxA+MSA+MA 23% RH vapor may be slightly underestimated due to higher coincidence in particle counting from the CPC above 3×10^5 cm^{-3}. Reaction times indicated in the figure corresponds to the time reactants interacted in the reactor, with t = 0 corresponding to the time MSA is introduced at spoke #1. Lines intended to guide the eye. See Table 4.1, Expt. 3.
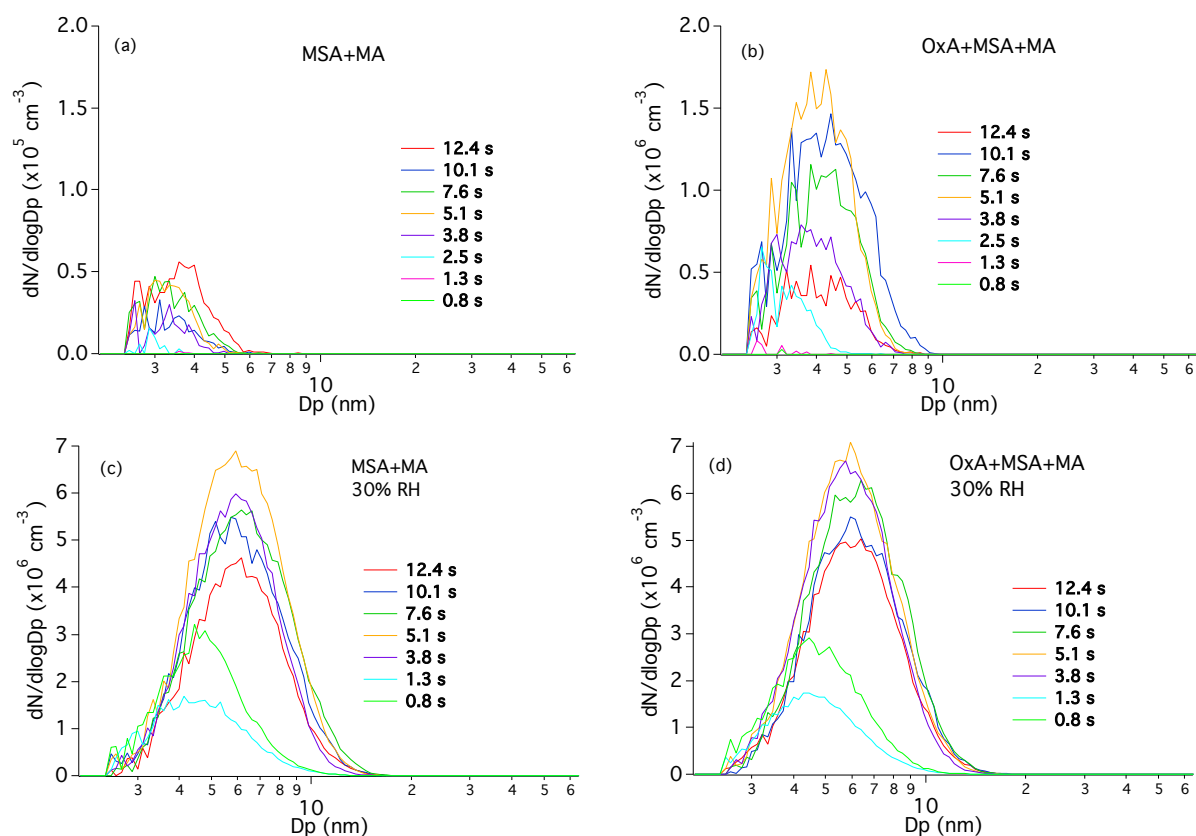
Figure 4.6 Typical size distributions from the reaction of (a) MSA (5 ppb) with MA (159 ppt) only and (b) in the presence of OxA (17 ppb) and from the reaction of (c) MSA (5 ppb) with MA (250 ppt) in the presence of water vapor (30% RH) and (d) in the presence of OxA (17 ppb) measured with the SMPS. Size distributions are averages of triplicate measurements, errors are ommitted for clarity. Reaction times indicated in the figure corresponds to the time reactants interacted in the reactor, with t = 0 corresponding to the time MSA is introduced at spoke #1. See Table 4.1, Expts. 8 and 1, respectively.

The data show that the MSA-amine reaction is the most important combination in this multi-component system, with both water vapor and OxA acting to increase particle formation from this acid-amine combination. Further confirmation of the critical role of MSA in particle formation is seen in Figure 4.7 and Figure 4.8 which MSA + OxA + MA is compared to the OxA-MA base case in the absence and presence of water vapor. In both cases, there is little particle formation from OxA + MA alone (MA concentrations were ≤ 9 ppb to minimize particle formation from OxA-MA). These experiments were performed on a freshly cleaned flow reactor

prior to exposure to MSA to examine the effect of the sulfur-based acid on particle formation. Some uptake of MSA on the unconditioned reactor walls may occur in competition with particle formation; note, however, that the configuration of the spokes through which MSA and MA are added (Figure 1.3) is such that they are rapidly mixed across the cross-sectional area of the flow reactor.
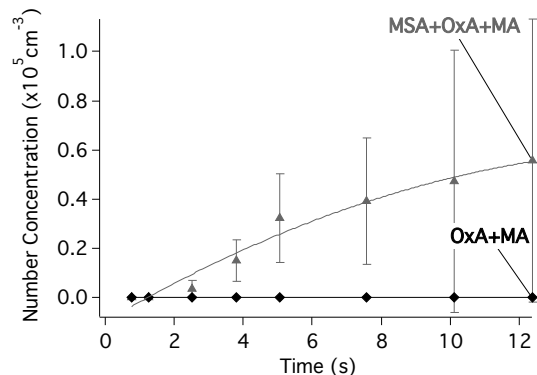
Figure 4.7 Number concentrations from the reaction of OxA (17 ppb) + MA (890 ppt) with and without MSA (9 ppb) measured with the CPC measured with the CPC; errors (2σ) are from one minute sample time. Reaction times indicated in the figure corresponds to the time reactants interacted in the reactor, with t = 0 corresponding to the time MSA is introduced at spoke #1. Lines intended to guide the eye. See Table 4.2, Expt. 19.
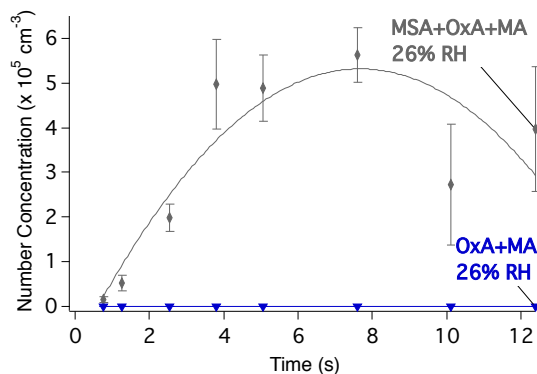
Figure 4.8 Number concentrations from the reaction of OxA (17 ppb) + MA (890 ppt) with and without MSA (620 ppt) in the presence of water (26% RH) measured with the CPC; errors (2σ) are from one minute sample time. Note that in number concentrations for MSA+(OxA+MA) 26% RH may be underestimated due to higher coincidence in particle counting from the CPC above 3×10^5 cm^{-3}. Reaction times indicated in the figure corresponds to the time reactants interacted in the reactor, with t = 0 corresponding to the time MSA is introduced at spoke #1. Lines intended to guide the eye. See Table 4.2, Expt. 17.

Multiple factors determine whether clusters will grow to detectable sizes in this system. As discussed in conjunction with the previous studies of particle formation from the reactions of MSA with amines, [130, 132, 133] the presence of hydrogen bonding sites in the small clusters may play a role through providing a mechanism for attracting and holding additional acid, base and water molecules. The fact that MSA (pK_a −1.9)[182] is so much more efficient than OxA (pK_{a1} 1.2, pK_{a2} 3.6)[183, 184] at forming particles with MA suggests that the strength of the acid-base interaction, *i.e.* the extent of proton transfer, may also be important. For example, Barsanti *et al.*[92] showed that the magnitude of the difference in pK_a, ΔpK_a, between an acid and base, influenced organic salt formation from an amine and acetic acid or pinic acid in an aqueous system. The ΔpK_a between MA (pK_a 10.6)[185] and OxA is 9.4 whereas the ΔpK_a between MA and MSA is 12.5. Calculations by Xu *et al.*[181] support a greater interaction between MSA and MA where a proton transfer is observed ($D_e$ = 18.15 kcal mol^{-1}) compared to OxA and MA where there is no proton transfer (D_e = 15.97 kcal mol^{-1}). Proton transfer to form an ion pair is also consistent with enhanced formation of particles in the MSA-amine system in the presence of water as experimentally observed in earlier studies.[130, 132, 133]

The extent of proton transfer to MA (measured by partial charge, δ) increases from δ = 0.83 in MSA-MA to δ = 0.87 in OxA-MSA-MA.[181] The fact that only 17 ppb OxA increases particle formation in the dry MSA-MA case (Figure 4.4) suggests that OxA plays a role similar to that of water, providing sites for additional attachment of MSA and amines to grow the cluster and enhancing proton transfer between MSA and MA as well.

The addition of water to the OxA-MSA-MA system greatly enhances particle formation (Figure 4.9), attributable to either or both of the following mechanisms: (1) increasing opportunities for hydrogen bonding or (2) promoting proton transfer. It is possible that both effects contribute to the increase in particle formation due to H_2O. Therefore, if water already promotes proton transfer between MSA and MA, then adding the much smaller amount of OxA (17 ppb) to the system at 23% RH (Figure 4.5) would not be expected to have significant impact. Such results highlight the complexity of particle formation in the atmosphere.
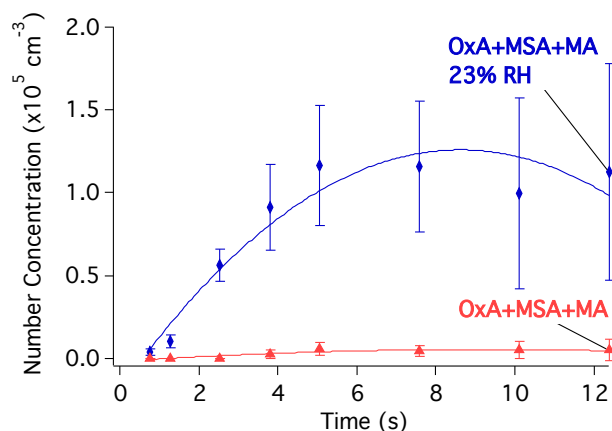
Figure 4.9 Number concentrations from the reaction of OxA (17 ppb) + MSA (0.9 ppb) + MA (47 ppt) with and without water (23% RH) measured with the CPC; errors (2σ) are from one minute sample time. Reaction times indicated in the figure corresponds to the time reactants interacted in the reactor, with t = 0 corresponding to the time MSA is introduced at spoke #1. Lines intended to guide the eye. See Table 4.3, Expt. 27.

Table 4.1 Conditions and results for MSA + MA and MSA + MA + H$_2$O experiments done with and without oxalic acid (OxA).

Expt.	Ring #1	Ring #2[a]	Spoke #1[b]	Spoke #2[b]	Degree of Enhancement due to Addition of OxA
			humid conditions		
1a	30% RH	dry air	**5 ppb MSA**	250 ppt MA	Base case
1b	30% RH	17 ppb OxA	**5 ppb MSA**	250 ppt MA	No change[c]
2a	34% RH	dry air	**4 ppb MSA**	64 ppt MA	Base case
2b	34% RH	17 ppb OxA	**4 ppb MSA**	64 ppt MA	No change
3a	23% RH	dry air	380 ppt MSA	**780 ppt MA**	Base case
3b	23% RH	17 ppb OxA	380 ppt MSA	**780 ppt MA**	No change
4a	22% RH	dry air	480 ppt MSA	**890 ppt MA**	Base case
4b	22% RH	17 ppb OxA	480 ppt MSA	**890 ppt MA**	+[d] (2 – 3 times more)
5a	18% RH	dry air	610 ppt MSA	**890 ppt MA**	Base case
5b	18% RH	17 ppb OxA	610 ppt MSA	**890 ppt MA**	No change
6a	24% RH	dry air	3 ppb MSA	2 ppb MA	Base case
6b	24% RH	17 ppb OxA	3 ppb MSA	2 ppb MA	No change
7a	24% RH	dry air	**3 ppb MSA**	47 ppt MA	Base case
7b	24% RH	17 ppb OxA	**3 ppb MSA**	47 ppt MA	No change
			dry conditions		
8a	dry air	dry air	**5 ppb MSA**	159 ppt MA	Base case
8b	dry air	17 ppb OxA	**5 ppb MSA**	159 ppt MA	+
9a	dry air	dry air	**7 ppb MSA**	190 ppt MA	Base case
9b	dry air	17 ppb OxA	**7 ppb MSA**	190 ppt MA	+
10a	dry air	dry air	**3 ppb MSA**	890 ppt MA	Base case
10b	dry air	17 ppb OxA	**3 ppb MSA**	890 ppt MA	+
11a	dry air	dry air	**8 ppb MSA**	890 ppt MA	Base case
11b	dry air	17 ppb OxA	**8 ppb MSA**	890 ppt MA	+
12a	dry air	dry air	**5 ppb MSA**	890 ppt MA	Base case
12b	dry air	17 ppb OxA	**5 ppb MSA**	890 ppt MA	+
13a	dry air	dry air	3 ppb MSA	2 ppb MA	Base case
13b	dry air	17 ppb OxA	3 ppb MSA	2 ppb MA	+
14a	dry air	dry air	**4 ppb MSA**	2 ppb MA	Base case
14b	dry air	17 ppb OxA	**4 ppb MSA**	2 ppb MA	+
15a	dry air	dry air	**4 ppb MSA**	116 ppt MA	Base case
15b	dry air	17 ppb OxA	**4 ppb MSA**	116 ppt MA	+
16a	dry air	dry air	**900 ppt MSA**	47 ppt MA	Base case
16b	dry air	17 ppb OxA	**900 ppt MSA**	47 ppt MA	+

Note: Only dry air was added through ring #3 and spoke #3

[a] Oxalic acid concentration is calculated from its vapor pressure at 303 K[159] taking into account dilution in the flow reactor. As discussed in the text, this is the maximum concentration of

oxalic acid during reaction.

[b] Concentrations of MSA and MA are measured prior to their entrance to the reactor. These concentrations account for dilution in the reactor and, due to potential losses in the entrance lines, represent the maximum concentration of each species during reaction. Values are in bold-face font when in excess.

[c] "No change" indicates < 2 times more particles were observed due to the added OxA.

[d] Enhancement of + represents ≥ 2 times more but < 1 order of magnitude more particles due to the added OxA.

Table 4.2 Conditions and results for experiments of OxA + MA and OxA + MA + H$_2$O with and without methanesulfonic acid (MSA).

Expt.	Ring #1	Ring #2[a]	Spoke #1[b]	Spoke #2 [b]	Degree of Enhancement due to Addition of MSA
			humid conditions		
17a	26% RH	17 ppb OxA	dry air	890 ppt MA	Base case
17b	26% RH	17 ppb OxA	620 ppt MSA	**890 ppt MA**	+ + +[c]
18a	23% RH	17 ppb OxA	dry air	466 ppt MA	Base case
18b	23% RH	17 ppb OxA	500 ppt MSA	466 ppt MA	+ + +
			dry conditions		
19a	dry air	17 ppb OxA	dry air	890 ppt MA	Base case
19b	dry air	17 ppb OxA	**9 ppb MSA**	890 ppt MA	+ + +
20a	dry air	17 ppb OxA	dry air	9 ppb MA	Base case
20b	dry air	17 ppb OxA	9 ppb MSA	9 ppb MA	+ + +

Note: Only dry air was added through ring #3 and spoke #3

[a] Oxalic acid concentration is calculated from its vapor pressure at 303 K[159] taking into account dilution in the flow reactor. This is the maximum concentration of oxalic acid during reaction.

[b] Concentrations of MSA and MA are measured prior to their entrance to the reactor. These concentrations account for dilution in the reactor and, due to potential losses in the entrance lines, represent the maximum concentration of each species during reaction. Values are in bold-face font when in excess.

[c] Enhancement of + + + represents ≥ 1 order of magnitude more particles due to the added MSA.

Table 4.3 Conditions and results for OxA + MSA + MA, MSA + MA, OxA + MA and OxA + MSA experiments done with and without water vapor.

Expt.	Ring #1	Ring #2[a]	Spoke #1[b]	Spoke #2[b]	Degree of Enhancement due to Addition of H_2O
21a	dry air	17 ppb OxA	600 ppt MSA	780 ppt MA	Base case
21b[c]	40% RH	17 ppb OxA	600 ppt MSA	780 ppt MA	+ + +[d]
22a	dry air	17 ppb OxA	**6 ppb MSA**	445 ppt MA	Base case
22b	20% RH	17 ppb OxA	**6 ppb MSA**	445 ppt MA	+ + +
23a	dry air	17 ppb OxA	**10 ppb MSA**	222 ppt MA	Base case
23b	22% RH	17 ppb OxA	**10 ppb MSA**	222 ppt MA	+ + +
24a	dry air	17 ppb OxA	**9 ppb MSA**	890 ppt MA	Base case
24b	23% RH	17 ppb OxA	**9 ppb MSA**	890 ppt MA	+ + +
25a	dry air	17 ppb OxA	3 ppb MSA	2 ppb MA	Base case
25b	24% RH	17 ppb OxA	3 ppb MSA	2 ppb MA	+ + +
26a	dry air	17 ppb OxA	**4 ppb MSA**	2 ppb MA	Base case
26b	24% RH	17 ppb OxA	**4 ppb MSA**	2 ppb MA	+ + +
27a	dry air	17 ppb OxA	**900 ppt MSA**	47 ppt MA	Base case
27b	24% RH	17 ppb OxA	**900 ppt MSA**	47 ppt MA	+ + +
28	varying RH	17 ppb OxA	dry air	dry air	+[e]
29	varying RH	17 ppb OxA	dry air	318 ppt MA	+
30	varying RH	17 ppb OxA	5 ppb MSA	dry air	+
31a	dry air	17 ppb OxA	dry air	890 ppt MA	Base case
31b	26% RH	17 ppb OxA	dry air	890 ppt MA	+
32a	dry air	17 ppb OxA	dry air	2 ppb MA	Base case
32b	21% RH	17 ppb OxA	dry air	2 ppb MA	+ + +
33a	dry air	9 ppb OxA	dry air	2 ppb MA	Base case
33b	24% RH	9 ppb OxA	dry air	2 ppb MA	+ + +
34a	dry air	17 ppb OxA	dry air	45 ppb MA	Base case
34b	22% RH	17 ppb OxA	dry air	45 ppb MA	+
35a	dry air	9 ppb OxA	dry air	45 ppb MA	Base case
35b	23% RH	9 ppb OxA	dry air	45 ppb MA	+ + +
36a	dry air	9 ppb OxA	dry air	9 ppb MA	Base case
36b	22% RH	9 ppb OxA	dry air	9 ppb MA	+ + +
37a	dry air	17 ppb OxA	dry air	446 ppt MA	Base case
37b	23% RH	17 ppb OxA	dry air	446 ppt MA	+
38a	dry air	dry air	**4 ppb MSA**	116 ppt MA	Base case
38b	24% RH	dry air	**4 ppb MSA**	116 ppt MA	+ + +

| 39a | dry air | dry air | **3 ppb MSA** | 47 ppt MA | Base case |
| 39b | 24% RH | dry air | **3 ppb MSA** | 47 ppt MA | + + + |

Note: Only dry air was added through ring #3 and spoke #3

[a] Oxalic acid concentration is calculated from its vapor pressure at 303 K[159] taking into account dilution in the flow reactor. This is the maximum concentration of oxalic acid during reaction.

[b] Concentrations of MSA and MA are measured prior to their entrance to the reactor. These concentrations account for dilution in the reactor and, due to potential losses in the entrance lines, represent the maximum concentration of each species during reaction. Values are in bold-face font when in excess.

[c] Blue highlight indicates experiment was done with water vapor.

[d] Enhancement of + + + represents $\geq$ 1 order of magnitude more particles due to the added H_2O.

[e] Enhancement of + represents $\geq$ 2 times more but < 1 order of magnitude more particles due to the added H_2O.

Table 4.4 Control experiments and results for the OxA, MSA, MA and H$_2$O system.

Expt.	Ring #1	Ring #2[a]	Spoke #1[b]	Spoke #2[b]	Result
40[c]	23% RH	17 ppb OxA	dry air	variable MA	significant particles with MA > 9 ppb
41	dry air	17 ppb OxA	dry air	890 ppt MA	no particles[d]
42	26% RH	17 ppb OxA	dry air	890 ppt MA	<<100 particles
43	dry air	17 ppb OxA	dry air	890 ppt MA	no particles
44	25% RH	17 ppb OxA	3 ppb MSA	dry air	<<100 particles

Note: Only dry air was added through ring #3 and spoke #3
[a] Oxalic acid concentration is calculated from its vapor pressure at 303 K[159] taking into account dilution in the flow reactor. This is the maximum concentration of oxalic acid during reaction.
[b] Concentrations of MSA and MA are measured prior to their entrance to the reactor. These concentrations account for dilution in the reactor and, due to potential losses in the entrance lines, represent the maximum concentration of each species during reaction.
[c] Blue highlight indicates experiment was done with water.
[d] No particles means < 10 particles cm^{-3} were measured.

4.3 ATMOSPHERIC IMPLICATIONS

Our studies show that OxA modestly enhances particle formation from the MSA-MA system but has no effect on MSA-MA-H$_2$O (Figure 4.10) because water at atmospherically relevant concentrations overwhelms the contribution of much smaller concentrations of organics. OxA and MA does not efficiently form particles even in the presence of water and are an unlikely source of atmospheric particles. Note that theoretical studies do predict particle formation from OxA and dimethylamine[163] or ammonia with[160, 162] and without[161] water. OxA, however, is only one of many organics found in air; other species individually or in concert might have a greater enhancement effect on particle formation. Understanding how acids, bases and water interact in the atmosphere on a molecular level is clearly important for the ability to accurately forecast particle formation at the regional and global scale.
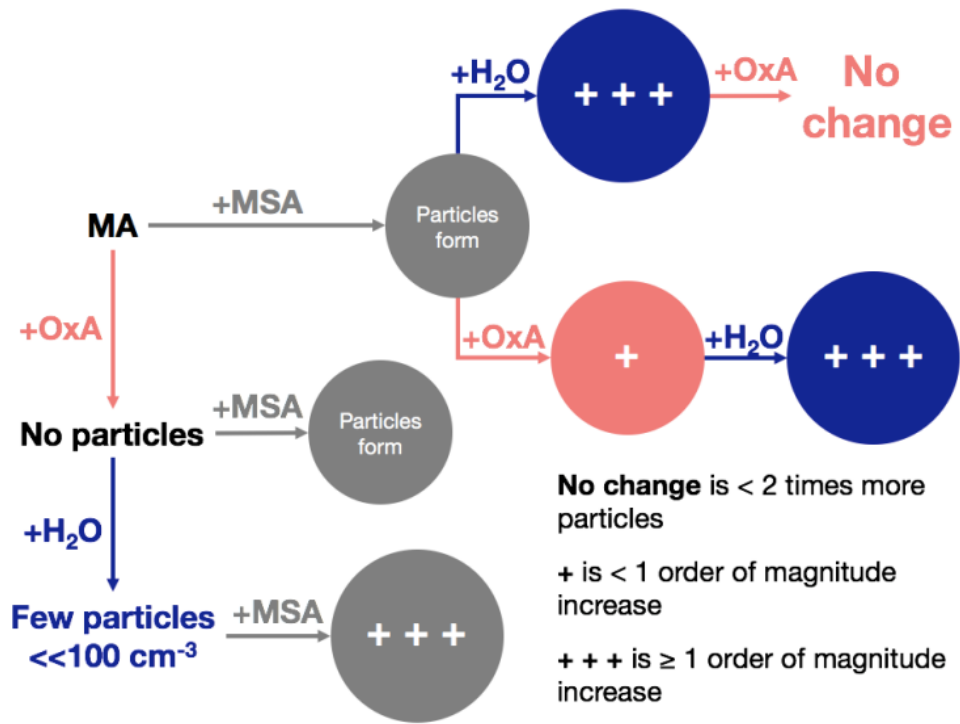
Figure 4.10 Summary of the overall results from experiments. Note this schematic is intended to show the net results of the presence of single components, not the experimental protocols.

CHAPTER 5   THE EFFECT OF OXALIC ACID ON THE REACTION OF MSA AND TMA WITH AND WITHOUT WATER

5.1   RESEARCH GOALS

The primary goal of this work is to determine the effect of OxA on the reaction of MSA and TMA under dry and humid conditions. Additionally, the impacts of amine structure and basicity on the OxA + amine, OxA + amine + H_2O, OxA + MSA + amine and OxA + MSA + amine + H_2O reactions are explored in comparison to the work done in Chapter 4 with MA. Tables 5.2 – 5.5 summarize all the results of this study, which are presented in this chapter. Results from laboratory experiments are presented along with theoretical calculations on structures of multi-component clusters comprised of OxA, MSA, TMA and H_2O.

5.2   RESULTS AND DISCUSSION

Previous studies of particle formation from reactions of MSA with amines have shown that basicity and hydrogen bonding capacity affect the growth of small clusters.[130, 132, 133] Furthermore, a qualitative correlation between particle formation and proton transfer in multi-component small clusters composed of MSA, MA, OxA and H_2O was proposed by Xu *et al*.[181] Hence, these three factors (basicity, proton transfer and hydrogen bonding capacity) will be considered in discussion of the correlation between the experimental data on particle formation and the theoretically predicted cluster properties. Although the size of these clusters is much

smaller than the smallest detectable particles measured in the lab, they provide a basis for greater insight into how/why particles form and grow in these systems.

5.2.1 Particle Formation from OxA and TMA in the absence and presence of H_2O

Figure 5.1 shows the number concentration of particles formed from OxA + TMA at 12.4 s reaction time in the absence (RH < 3%) and presence of water vapor (equivalent to 30% RH) as a function of TMA concentration. In the absence of water, no particles formed in the reaction of 17 ppb OxA with 0 – 9 ppb TMA. However, in the presence of water, some particle formation occurs, but less than 30 particles cm^{-3} were detected at all concentrations of TMA. This increase with H_2O is qualitatively similar to previously reported results for the reaction of 17 ppb OxA with 9 ppb MA where ~60 particles cm^{-3} were formed under dry conditions but in the presence of water, ~1500 particles cm^{-3} formed at 23% RH (Figure 4.2).[186] Thus, particle formation from the reaction of OxA with TMA is less efficient than the analogous system with MA, although neither forms a large number of particles and both are affected by the presence of water vapor. This comparison highlights the effect of amine structure on particle formation.
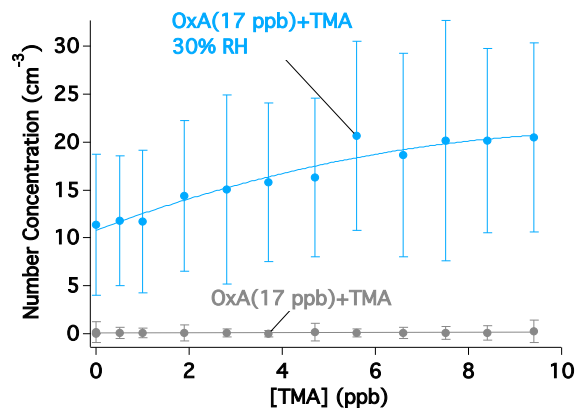
Figure 5.1 Number concentrations at 12.4 s reaction time comparing the base case reaction of OxA (17 ppb) with TMA (0 – 9 ppb) with and without water vapor (30% RH) measured with the CPC; errors (2σ) are from one minute of sample time with the CPC. Lines intended to guide the eye. See Table 5.5, Expts. 79, 83.

The most stable structures of OxA-TMA and OxA-TMA-H_2O are shown in Figure 5.2. In OxA-TMA, OxA transfers one proton to TMA, forming an ion pair $[HOOCCOO]^-[HN(CH_3)_3]^+$. TMA is a tertiary amine and once it accepts the proton from the acid it cannot participate in additional hydrogen bonding, only OxA can form hydrogen bonds with another reactant or cluster to grow. This may be the reason why detectable particles do not form efficiently from OxA and TMA under dry conditions (although the presence of stable smaller clusters is possible). Steric factors may also play a role. Proton transfer also occurs in the OxA-TMA-H_2O cluster and the partial charge on TMA is similar to that in the absence of water. i.e., $\delta = 0.82$ in OxA-TMA compared to $\delta = 0.84$ in OxA-TMA-H_2O. While there is essentially no increase in the extent of proton transfer with added water to OxA-TMA, the OxA-TMA-H_2O cluster (Figure 5.2b) can grow via hydrogen bonding to H_2O. Both systems can also grow if the internal hydrogen bond in OxA is broken. This is consistent with the experimental observation that a small number of particles is formed (< 30 particles cm^{-3}) in the presence of water.

The structures of OxA-MA with and without water reported by Xu *et al.*[181] are also shown in

Figure 5.2 to compare the effect of the nature of the amine on particle formation. There is no

proton transfer in the OxA-MA cluster, but with water the partial charge changes from $\delta = 0.13$

to $\delta = 0.80$ indicating a proton transfer occurs in the OxA-MA-H$_2$O cluster.[181] The difference of

whether or not a proton transfer occurs under dry conditions for MA versus TMA is mainly due

to the difference in basicity, where $\Delta G°_{MA}$ is 206.6 kcal mol^{-1} and $\Delta G°_{TMA}$ is 219.4 kcal mol^{-1}.[187]

This manifests itself in a shorter length of the hydrogen bond between the ion pair in the OxA-

TMA system (1.421 Å) compared to that in the OxA-MA system (1.551 Å). The binding energy

of OxA-TMA (Table 5.1) is also larger than for OxA-MA, 19.20 kcal mol^{-1} compared to 15.97

kcal mol^{-1}.[181] These calculations are consistent with TMA being a stronger base than MA, and

support proton transfer for TMA but not for MA.

In the presence of water, the acid transfers one proton to the base, and water is connected

through the hydrogen bond in the most stable structures of OxA-MA-H$_2$O and OxA-TMA-H$_2$O.

However, in the MA system, the three components form a cyclic structure (Figure 5.2d), which

is more stable than the open structure of the TMA system (Figure 5.2b). This stability of the MA

cluster is also reflected in the dissociation energies. The binding energies between water and the

ion pair are 11.33 kcal mol^{-1} for the MA system[181] and 9.62 kcal mol^{-1} for the TMA system, i.e.,

the interaction between water and the ion pair in the OxA-MA-H$_2$O cluster is somewhat stronger

than that in OxA-TMA-H$_2$O. The structure of the OxA-TMA-H$_2$O cluster (Figure 5.2b) shows

that hydrogen bonding can occur through water (and OxA if the internal hydrogen bond is

broken). For OxA-MA-H$_2$O (Figure 5.2d), there is an additional hydrogen bonding possibility at

the nitrogen. This is consistent with the experimental observation that at similar concentrations, MA is more efficient than TMA at forming particles with OxA both in dry and humid conditions.

In short, although proton transfer always takes place in the TMA system, it is likely that the ability to form hydrogen bonds determines whether the cluster can grow to detectable particle sizes and beyond. In any event, it is worth noting that the gas phase reaction of OxA and MA/TMA is not likely to be a significant source of particles at the low concentrations found in air, even in the presence of water. It should be noted that theoretical studies do predict participation of dry[161] and hydrated[160, 162] OxA-ammonia and OxA-dimethylamine[163] clusters in atmospheric nucleation as well as particle formation from OxA and sulfuric acid with water[165] or ammonia.[166]
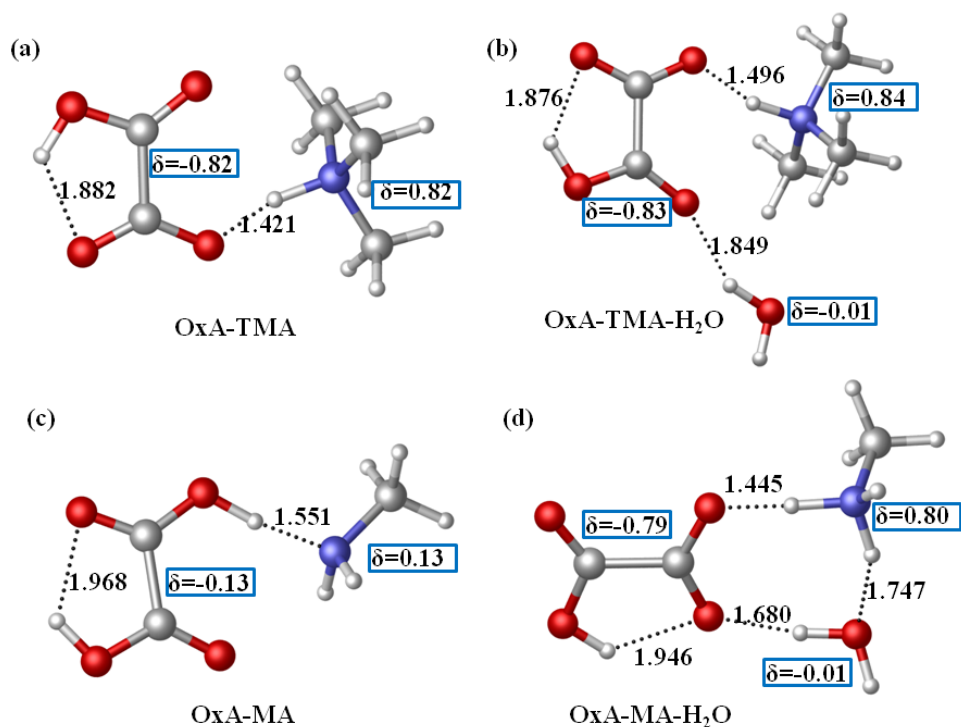
Figure 5.2 Key geometrical parameters (in angstroms) of the most stable structures of (a) OxA-TMA, (b) OxA-TMA-H$_2$O, (c) OxA-MA[181] and (d) OxA-MA-H$_2$O[181] clusters and partial charges δ (in atomic units) of each component calculated at the level of B3LYP-D3/aug-cc-pVDZ by Dr. Jing Xu from the Gerber group.

5.2.2 The effect of MSA on particle formation from OxA, TMA and H$_2$O

Compared to OxA + TMA alone, particle formation is enhanced by orders of magnitude due to the presence of MSA (Table 5.2) under both humid and dry conditions. For example, Figure 5.3 compares number concentrations in the absence and presence of MSA with the OxA + TMA + H$_2$O (30% RH) base case. This enhancement is not surprising given that MSA (pK$_a$ −1.9)[182] is a stronger acid than OxA (pK$_{a1}$ 1.2, pK$_{a2}$ 3.6).[183, 184] These results align with previous work that showed the greater the ΔpK$_a$ between an organic acid and an amine in the presence of water, the greater the extent of formation of the organic salt.[92] For MSA and TMA (pK$_a$ 9.76),[185] the ΔpK$_a$ is 11.7 whereas for OxA and TMA the ΔpK$_a$ is 8.6.
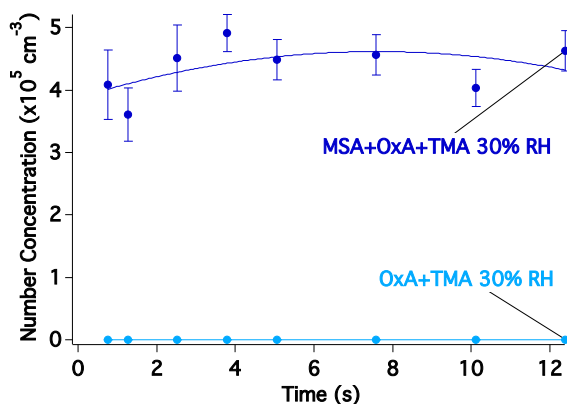
Figure 5.3 Number concentrations comparing the base case reaction of OxA (17 ppb) with TMA (4 ppb) at 30% RH with and without MSA (2.3 ppb) measured with the CPC; errors (2σ) are from one minute of sample time with the CPC. Reaction times indicated in the figure corresponds to the time reactants interacted in the reactor, with t = 0 corresponding to the time MSA is introduced at spoke #1. Lines intended to guide the eye. See Table 5.2, Expt. 1.

The structures of OxA-MSA-TMA and OxA-MSA-TMA-H$_2$O clusters are shown in Figure 5.4a,b. In both clusters, MSA transfers one proton to TMA, and OxA (and water, when present) connects to MSA through a hydrogen bond. The partial charges on MSA and OxA in the cluster without (Figure 5.4a) and with (Figure 5.4b) water are –0.79/–0.76 for MSA and –0.07/–0.08 for

OxA, respectively. In the OxA-MSA-TMA cluster, the transferred proton comes from MSA, not from OxA. Dissociation energies in Table 5.1 also show that MSA is more tightly bound ($D_e =$ 24.44 kcal mol^{-1} without H_2O and 24.73 kcal mol^{-1} with H_2O) than OxA ($D_e = 21.09$ kcal mol^{-1} without H_2O and 16.76 kcal mol^{-1} with H_2O). In addition, the dissociation energies for the binary system OxA-TMA ($D_e = 19.20$ kcal mol^{-1}) and MSA-TMA ($D_e = 22.56$ kcal mol^{-1}) support that MSA is a stronger acid than OxA. The added MSA increases the overall hydrogen bonding capacity to grow the clusters compared to the OxA-TMA (Figure 5.2a vs Figure 5.4a). In the case of the corresponding clusters with water, the water binds to the MSA (Figure 5.4b) rather than to the OxA (Figure 5.2b) which opens up an additional hydrogen bonding site on the OxA. These results show that in the competition between atmospheric acids, both acid strength, which affects extent of proton transfer to the base, and ability to form hydrogen bonds, influence particle formation from an acid and an amine in the absence and in the presence of water.
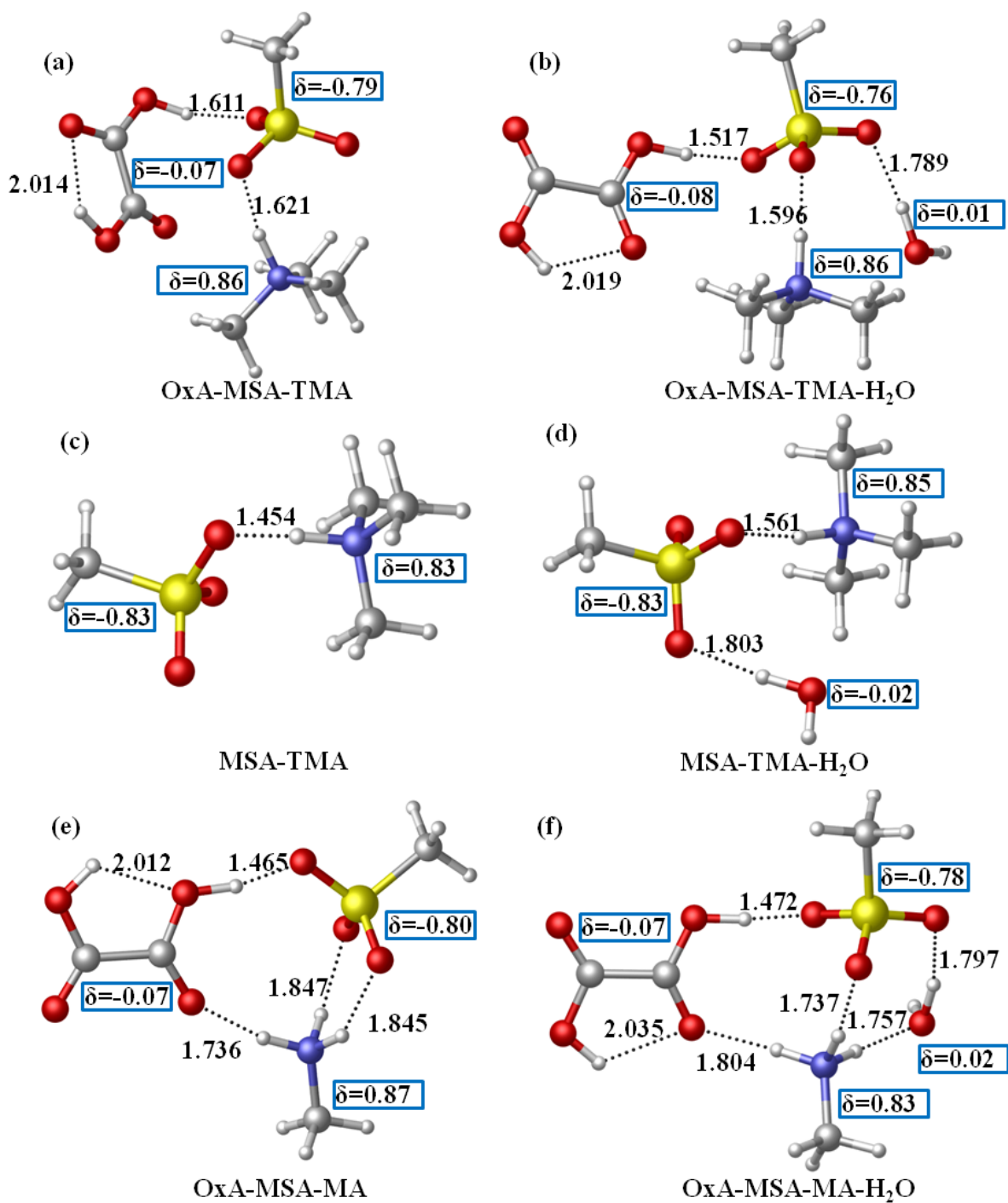
Figure 5.4 Key geometrical parameters (in angstroms) of most stable structures of (a) OxA-MSA-TMA, (b) OxA-MSA-TMA-H$_2$O, (c) MSA-TMA, (d) MSA-TMA-H$_2$O, (e) OxA-MSA-MA[181] and (f) OxA-MSA-MA-H$_2$O[181] clusters and partial charges **δ** (in atomic units) of each component calculated at the level of B3LYP-D3/aug-cc-pVDZ by Dr. Jing Xu of the Gerber group.

5.2.3 The effect of OxA on particle formation and growth with MSA and TMA with and without H_2O

Table 5.3 (Expts. 25 – 39) and Figure 5.5 – Figure 5.7 show that, without water vapor, the presence of OxA leads to larger particles compared to the MSA + TMA base case, but has a small effect on number concentration (≤ 2 times more particles). In some experiments the concentration of OxA was doubled to 34 ppb (Table 5.3, Expts. 38, 39), the maximum experimentally accessible concentration; however, this doubling did not result in additional significant growth in particle size. Neither was there enhancement of particle formation with the increased OxA concentration compared to the MSA + TMA base case or to experiments done with only 17 ppb OxA.

Dissociation energies (Table 5.1) show that the amount of energy required to remove MSA from OxA-MSA-TMA ($D_e = 24.44$ kcal mol^{-1}) is similar (within the calculation uncertainty) to that required to remove MSA from MSA-TMA (22.56 kcal mol^{-1}). Thus, the added OxA does not increase the stability of the MSA-TMA ion pair. For both MSA-TMA (Figure 5.4c) and OxA-MSA-TMA (Figure 5.4a) a proton transfer occurs from MSA to TMA. According to the partial charges (Figure 5.4a), OxA ($\delta = -0.07$) participates in the proton transfer to TMA, and plays a minor role compared to that of MSA ($\delta = -0.79$). However, a small increase in partial charge on TMA is observed with added OxA (from $\delta = 0.83$ in Figure 5.4c to 0.86 in Figure 5.4a) that may contribute to the small increase in particle number concentrations compared to the MSA + TMA base case (Figure 5.5 – Figure 5.7), as was shown with the OxA, MSA and MA system.[181] In OxA-MSA-TMA (Figure 5.4a), OxA connects with the ion pair through one hydrogen bond to the MSA, forming an open structure. The OxA-MSA-TMA cluster can grow to bigger sizes

through hydrogen bonding with the OxA or MSA. The ability to hydrogen bond through both OxA and MSA may yield larger sized clusters but such clusters are unwieldy and unlikely to pack efficiently, preventing a significant increase in particle number concentration, consistent with experimental observations.

In previous work on the effects of OxA on particle formation from MSA and MA, the addition of OxA did not affect particle size and had a modest effect on particle number concentrations (< 1 order of magnitude more particles) compared to the base case with MSA and MA without water vapor.[186] To elucidate the effect of the two different amines on particle formation, the structure of OxA-MSA-TMA is shown in Figure 5.4a and that of OxA-MSA-MA in Figure 5.4e. In the most stable structures of OxA-MSA-TMA and OxA-MSA-MA, the amine always accepts one proton from MSA, and the contribution of OxA ($\delta = -0.07$) to the proton transfer is the same. However, OxA forms a cyclic structure with MSA and MA (Figure 5.4e), and the energy required to remove MSA from the MSA-MA cluster (18.15 kcal mol^{-1})[181] is lower than that to remove MSA from the cyclic OxA-MSA-MA cluster (23.49 kcal mol^{-1}).[181] Thus, the presence of OxA in the MSA-MA system stabilizes the ionic cluster which correlates with the experimentally observed increase in particle number concentration.[181, 186]

In the two systems of MSA-MA and MSA-TMA, the effect of adding OxA produces different experimental results. For OxA-MSA-MA, the number of particles increases (within an order of magnitude), but particle sizes do not change. In the case of OxA-MSA-TMA, the particles grow to larger sizes, with only a slight increase ($\leq$ 2 times more particles) in number concentration.

Cluster geometry may explain this difference in formation and particle growth in the presence of OxA.

The initial structures in Figure 5.4 suggest that the cluster's geometry affects its ability to efficiently pack and subsequently impacts how clusters form particles and grow. The OxA-MSA-MA cluster (Figure 5.4e) is rigid and near-planar. As these OxA-MSA-MA clusters stack, the formed units are likely to be compact and relatively ordered, which would support strong dipole-dipole interactions between stacked units. The OxA-MSA-MA particles will be energetically stable, which is thermodynamically favorable for the formation of more particles. Considering the compact, rigid nature of the OxA-MSA-MA cluster, there is no reason to expect growth in particle size compared to the MSA-MA cluster. Figure 5.4a suggests that adding OxA to MSA-TMA, forms a "floppy" OxA-MSA-TMA cluster, with both OxA and TMA able to rotate about their respective hydrogen bonds with MSA. Such OxA-MSA-TMA units suggest significant probabilities of hydrogen bond formation with other such species, but these can be formed in different directions. These particles are somewhat disordered, probably not compact, and larger compared to MSA-TMA. The OxA-MSA-TMA particles are not expected to be very low in energy, since dipole-dipole interactions within each particle will be partly averaged out by the disorder and "floppiness." The increased probability of multidirectional hydrogen bonding on the OxA-MSA-TMA cluster is expected to result in significantly larger particles sizes, but not in an increased number of particles. Calculations for much larger clusters of OxA-MSA-MA and OxA-MSA-TMA are needed to test the above interpretation, but these are computationally demanding.
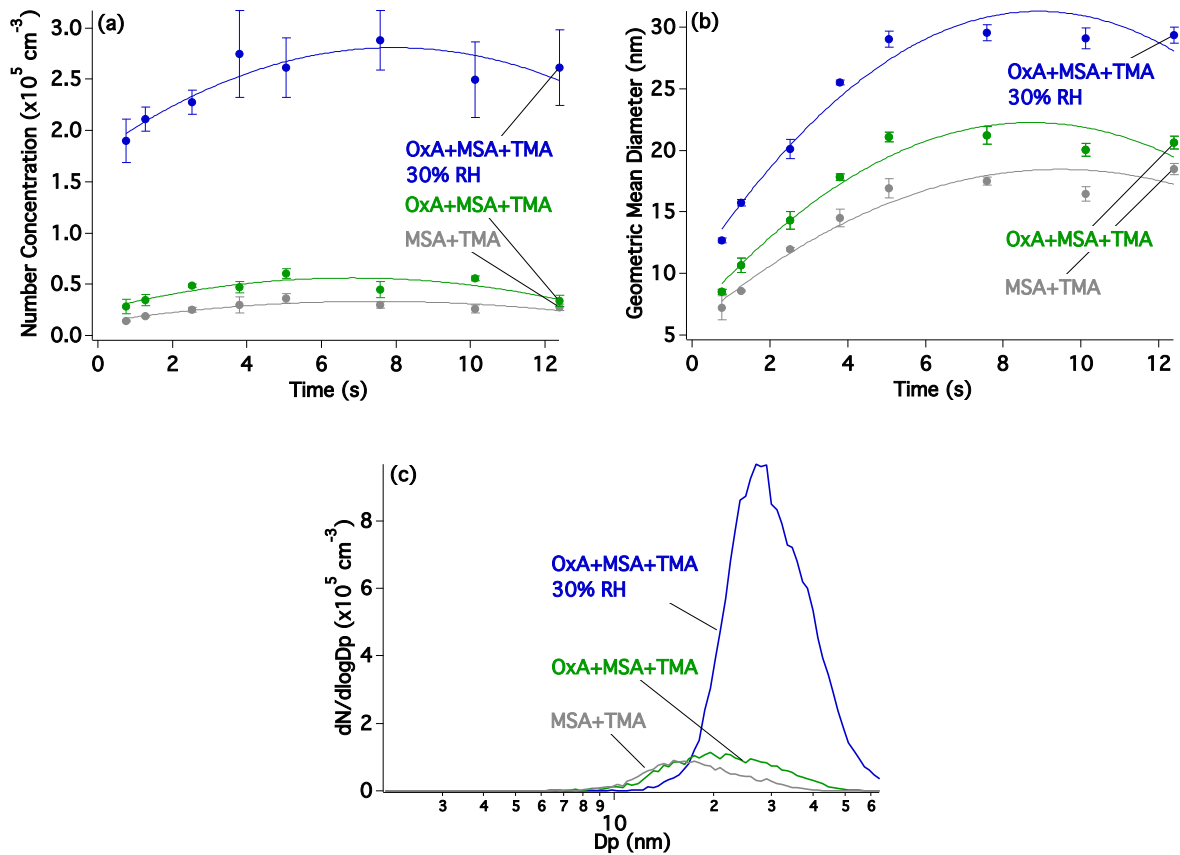
Figure 5.5 Comparison of (a) number concentrations (b) geometric mean diameters and (c) size distributions at 7.6 s reaction time of the base case reaction of excess MSA (5.3 ppb) with TMA (2.7 ppb) to those in the presence of OxA (17 ppb) and water vapor (30% RH) measured with the SMPS; errors (2σ) in (a) and (b) are from triplicate measurements with the SMPS; errors omitted in (c) for clarity. Reaction times indicated in the figure corresponds to the time reactants interacted in the reactor, with t = 0 corresponding to the time MSA is introduced at spoke #1. Lines in (a) and (b) are intended to guide the eye. See Table 5.3, Expt. 29 and Table 5.4, Expt. 60.
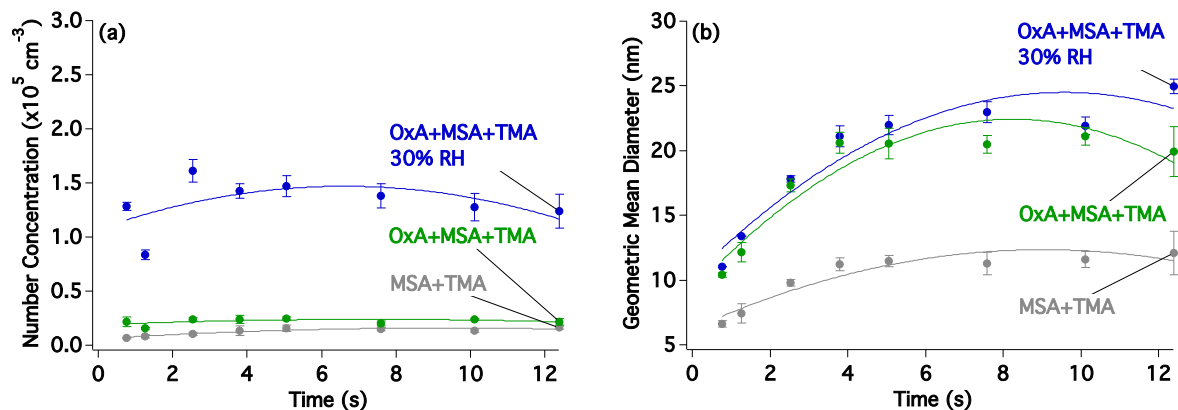
Figure 5.6 Comparison of (a) number concentrations and (b) geometric mean diameters of the base case reaction of MSA (2.1 ppb) with excess TMA (4 ppb) to those in the presence of OxA (17 ppb) and water vapor (30% RH) measured with the SMPS; errors (2σ) are from triplicate measurements with the SMPS. Reaction times indicated in the figure corresponds to the time reactants interacted in the reactor, with t = 0 corresponding to the time MSA is introduced at spoke #1. Lines intended to guide the eye. See Table 5.3, Expt. 31 and Table 5.4, Expt. 63.
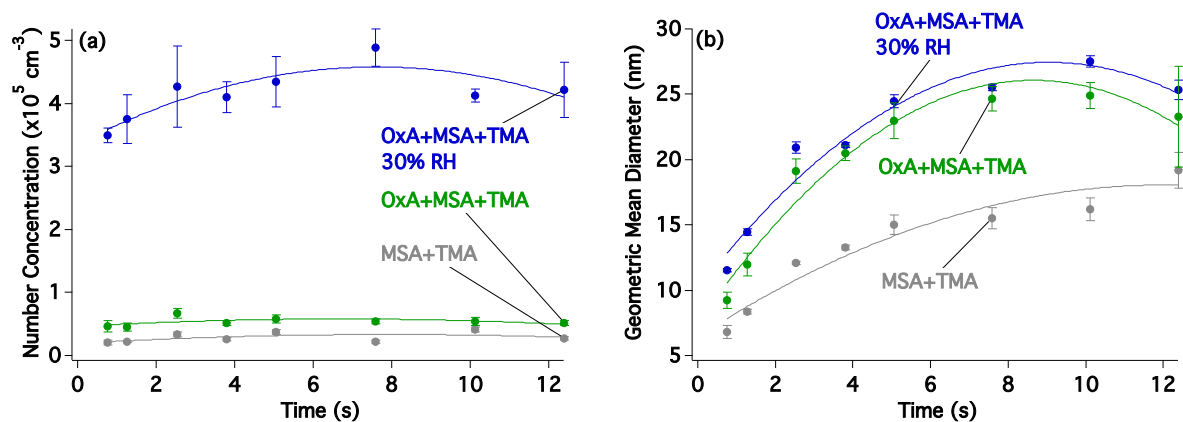
Figure 5.7 Comparison of (a) number concentrations and (b) geometric mean diameters of the base case reaction of approximately equal concentrations of MSA (3.6 ppb) and TMA (3.5 ppb) to those in the presence of OxA (17 ppb) and water vapor (30% RH) measured with the SMPS; errors (2σ) are from triplicate measurements with the SMPS. Reaction times indicated in the figure corresponds to the time reactants interacted in the reactor, with t = 0 corresponding to the time MSA is introduced at spoke #1. Lines intended to guide the eye. See Table 5.3, Expt. 34 and Table 5.4, Expt. 68.

As shown in Figure 5.8 – Figure 5.10 and Table 5.3 (Expts. 7 – 24) OxA has no effect on the

particle number concentration or size compared to the base case of MSA + TMA + H_2O (30%

RH, shown in light blue in Figure 5.8 – Figure 5.10) regardless of which reagent is in excess or if they are present at approximately equal concentrations. This is similar to the analogous MA system where OxA did not affect the MSA + MA + H$_2$O base case in number concentration or size.[186] The most stable structures of OxA-MSA-TMA-H$_2$O (Figure 5.4b) and OxA-MSA-MA-H$_2$O (Figure 5.4f) both show hydrogen bond capacity through the water and OxA molecules that should lead to particle formation and/or growth. Experimental limitations do not allow for equal amounts of OxA and water vapor to be introduced to the flow reactor. Even at the lowest RH (15% RH, 9.1×10^{16} cm^{-3}), there are five orders of magnitude more water molecules than OxA molecules (typical concentration 17 ppb, 4.2×10^{11} cm^{-3}), which overwhelms any contribution OxA has to particle formation and growth. Thus, the effect of OxA in the presence of water vapor, which is always present in the lower atmosphere in significant concentrations, is inconsequential in air.[186]
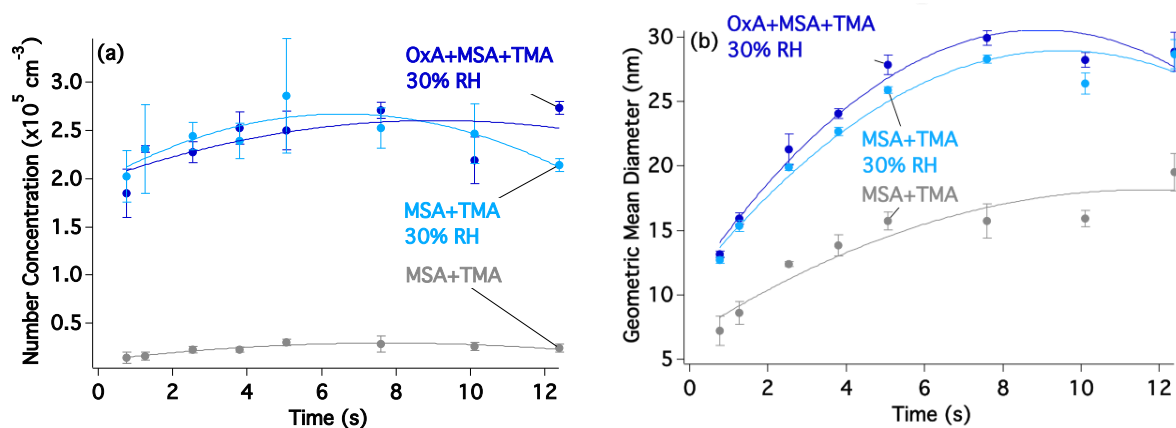
Figure 5.8 Comparison of (a) number concentrations and (b) geometric mean diameters of the base case reaction of excess MSA (5 ppb) with TMA (2.7 ppb) to those in the presence of water vapor (30% RH) and OxA (17 ppb) measured with the SMPS; errors (2σ) are from triplicate measurements with the SMPS. Reaction times indicated in the figure corresponds to the time reactants interacted in the reactor, with t = 0 corresponding to the time MSA is introduced at spoke #1. Lines intended to guide the eye. See Table 5.3, Expt. 9 and Table 5.4, Expt. 40.
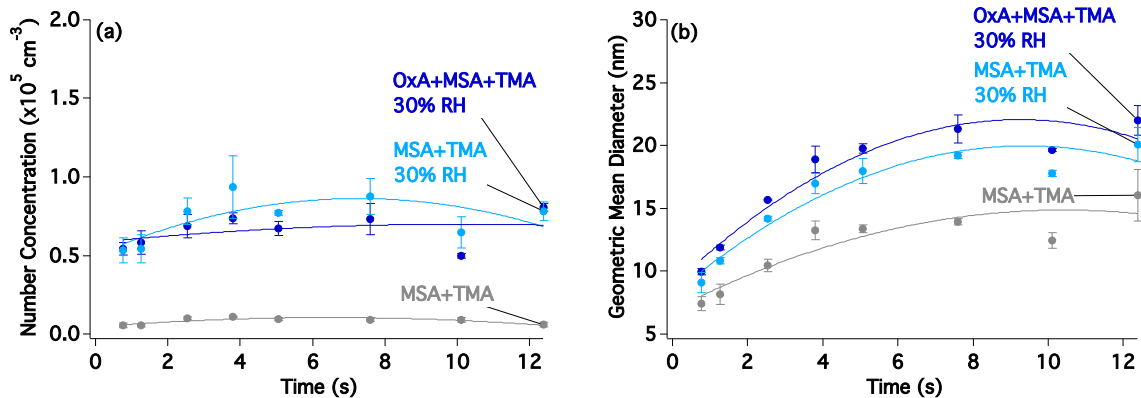
Figure 5.9 Comparison of (a) number concentrations and (b) geometric mean diameters of the base case reaction of MSA (2.1 ppb) with excess TMA (4 ppb) to those in the presence of water vapor (30% RH) and OxA (17 ppb) measured with the SMPS; errors (2σ) are from triplicate measurements with the SMPS. Reaction times indicated in the figure corresponds to the time reactants interacted in the reactor, with t = 0 corresponding to the time MSA is introduced at spoke #1. Lines intended to guide the eye. See Table 5.3, Expt. 12 and Table 5.4, Expt. 43.
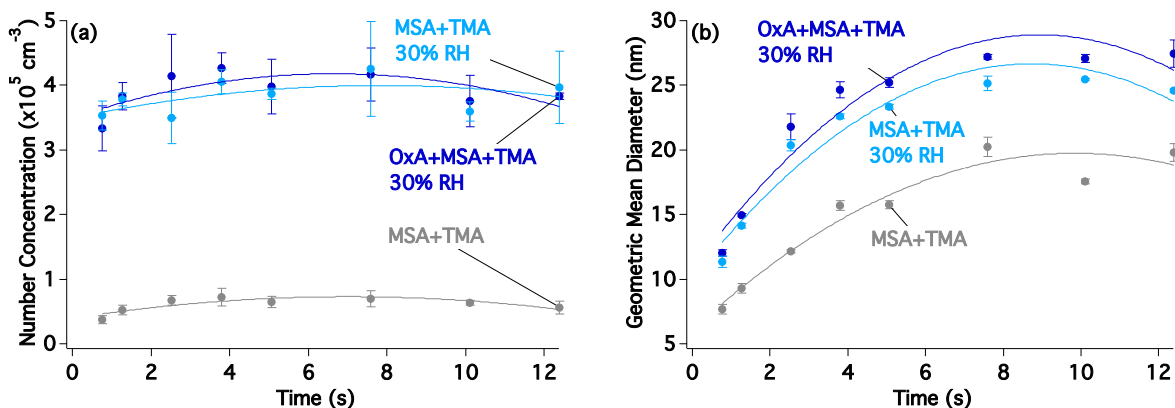
Figure 5.10 Comparison of (a) number concentrations and (b) geometric mean diameters of the base case reaction of approximately equal concentrations of MSA (3.2 ppb) with TMA (3.5 ppb) to those in the presence of water vapor (30% RH) and OxA (17 ppb) measured with the SMPS; errors (2σ) are from triplicate measurements with the SMPS. Reaction times indicated in the figure corresponds to the time reactants interacted in the reactor, with t = 0 corresponding to the time MSA is introduced at spoke #1. Lines intended to guide the eye. See Table 5.3, Expt. 19 and Table 5.4, Expt. 49.

5.2.4 The effect of H₂O on particle formation and growth

In agreement with previous studies of MSA-amine-H_2O,[130, 132, 133] Figure 5.8 – Figure 5.10

(Table 5.4, Expts. 40 – 55) show that water enhances particle formation and yields larger

81

particles in the MSA-TMA-H$_2$O system compared to the MSA + TMA base case. However,

water vapor alone does not grow OxA-MSA-TMA-H$_2$O particles (Table 5.4, Expts. 56 – 75) as

is evident in Figure 5.11, which shows number concentrations and particle sizes at different RHs.

Increasing RH has a significant effect on particle number but with similar concentrations of

MSA and TMA, particles did not grow larger.
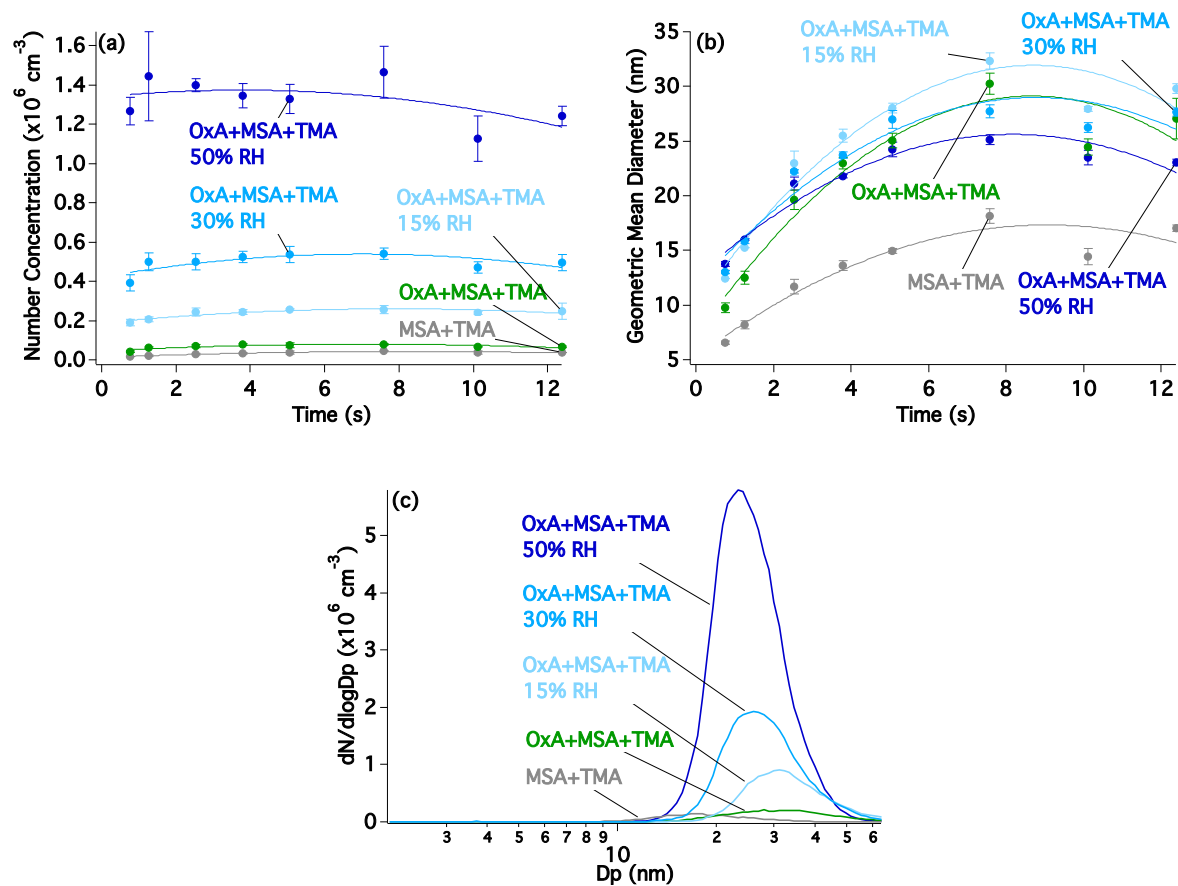
Figure 5.11 Comparison of (a) number concentrations, (b) geometric mean diameters, and (c) size distributions at 7.6 s reaction time of the base case reaction of approximately equal concentrations of MSA (3.8 ppb) with TMA (3.5 ppb) to those in the presence of OxA (17 ppb) and water vapor (15% RH, 30% RH, 50% RH) and measured with the SMPS; errors (2σ) in (a) and (b) are from triplicate measurements with the SMPS; errors omitted in (c) for clarity. Reaction times indicated in the figure corresponds to the time reactants interacted in the reactor, with t = 0 corresponding to the time MSA is introduced at spoke #1. Lines in (a) and (b) are intended to guide the eye. See Table 5.3, Expt. 36 and Table 5.4, Expts. 56, 70 and 74.

The only observation of particle growth with the addition of H_2O compared to the base case of OxA-MSA-TMA is shown in Figure 5.5b, c. Under conditions with excess MSA (Table 5.4, Expts. 59, 60), OxA-MSA-TMA-H_2O particles are larger compared to the base case without water, suggesting more efficient growth. Previous work showed that MSA and H_2O alone do not form particles efficiently[126-129] but studies when amines were added suggested that the MSA hydrate may play an important role in particle formation and growth.[133] This may also be the case in this study, in which the geometric mean diameter of OxA-MSA-TMA-H_2O particles in the presence of excess MSA (Figure 5.5) is larger by ~ 7 nm than when TMA is in excess (Figure 5.6), and the peak number concentration is slightly larger. A comparison of the OxA-MSA-TMA-H_2O data in Figure 5.8b to that in Figure 5.9b also suggests that excess MSA forms larger particles; thus, the geometric mean diameter of OxA-MSA-TMA-H_2O particles plateaus at ~30 nm in Figure 5.8b compared to ~20 nm in Figure 5.9b. (A cautionary note is that these experiments were carried out on different days so that direct quantitative comparisons are less certain).

The fact that particles are larger in excess MSA when all four components - MSA, TMA, OxA and H_2O - are present suggests that there are MSA hydrates left over in the gas phase once the limiting reagent TMA has reacted, and that these hydrates readily add to the OxA-MSA-TMA-H_2O clusters, resulting in particle growth. The increase in number concentration with increasing RH seen at approximately equal concentrations of MSA and TMA in the presence of OxA (Figure 5.11a,c) is likely due to a similar phenomenon; addition of the hydrates to the initial small, undetectable clusters to grow them into the detectable size range would manifest itself as an apparent increase in particle formation.

Table 5.1 Dissociation energies (D_e) calculated at the level of B3LYP-D3/aug-cc-pVDZ by Dr. Jing Xu from the Gerber group.

Systems	D_e (kcal mol^{-1})
OxA-TMA → OxA + TMA	19.20
MSA-TMA → MSA + TMA	22.56
OxA-TMA-H$_2$O → OxA-TMA + H$_2$O	9.62
MSA-TMA-H$_2$O → MSA-TMA + H$_2$O	14.23
OxA-MSA-TMA-H$_2$O → OxA-MSA-TMA + H$_2$O	9.91
OxA-MSA-TMA-H$_2$O → OxA-TMA-H$_2$O + MSA	24.73
OxA-MSA-TMA-H$_2$O → MSA-TMA-H$_2$O + OxA	16.76
OxA-MSA-TMA → MSA-TMA + OxA	21.09
OxA-MSA-TMA → OxA-TMA + MSA	24.44

Table 5.2 Conditions and results for OxA + TMA and OxA + TMA + H_2O experiments with and without MSA.

Expt.	Ring #1	Ring #2[a]	Spoke #1[b]	Spoke #2 [b]	Degree of Particle Formation Enhancement due to Addition of MSA
			humid conditions		
1a	30% RH	17 ppb OxA	dry air	4 ppb TMA[c]	base case
1b	30% RH	17 ppb OxA	2.3 ppb MSA	**4 ppb TMA**	+ + +
2a	29% RH	17 ppb OxA	dry air	1 ppb TMA	base case
2b	29% RH	17 ppb OxA	1.2 ppb MSA	1 ppb TMA	+ + +[d]
3a	30% RH	17 ppb OxA	dry air	0.2 ppb TMA	base case
3b	30% RH	17 ppb OxA	0.3 ppb MSA	0.2 ppb TMA	+ + +
			dry conditions		
4a	dry air	17 ppb OxA	dry air	2.7 ppb TMA	base case
4b	dry air	17 ppb OxA	**5 ppb MSA**	2.7 ppb TMA	+ + +
5a	dry air	17 ppb OxA	dry air	4 ppb TMA	base case
5b	dry air	17 ppb OxA	2.2 ppb MSA	**4 ppb TMA**	+ + +
6a	dry air	17 ppb OxA	dry air	3.5 ppb TMA	base case
6b	dry air	17 ppb OxA	4 ppb MSA	3.5 ppb TMA	+ + +

Note: Only dry air was added through ring #3 and spoke #3.
[a] The oxalic acid concentration, calculated from its vapor pressure at 303 K,[159] takes into account dilution in the flow reactor. This represents the maximum concentration achieved in the reaction.
[b] MSA and TMA concentrations are measured prior to their entrance to the reactor. These values account for dilution in the reactor, and are in bold-face font when in excess. These represent the maximum concentrations achieved in the reaction.
[c] 1 ppb = 2.48×10^{10} cm^{-3} at 1 atm and 294 K
[d] An enhancement of + + + represents > 10 times more particles due to the added MSA.

Table 5.3 Conditions and results for MSA + TMA and MSA + TMA + H$_2$O experiments with and without OxA.

Expt.	Ring #1	Ring #2[a]	Spoke #1[b]	Spoke #2[b]	Degree of Particle Formation Enhancement due to Addition of OxA	Particle growth?
			humid conditions			
7a	20% RH	dry air	**5.3 ppb MSA[c]**	2.6 ppb TMA	base case	base case
7b	20% RH	17 ppb OxA	**5.3 ppb MSA**	2.6 ppb TMA	no change[d]	X[e]
8a	20% RH	dry air	**5.5 ppb MSA**	2.6 ppb TMA	base case	base case
8b	20% RH	17 ppb OxA	**5.5 ppb MSA**	2.6 ppb TMA	no change	X
9a	30% RH	dry air	**5 ppb MSA**	2.7 ppb TMA	base case	base case
9b	30% RH	17 ppb OxA	**5 ppb MSA**	2.7 ppb TMA	no change	X
10a	30% RH	dry air	**5 ppb MSA**	2.7 ppb TMA	base case	base case
10b	30% RH	17 ppb OxA	**5 ppb MSA**	2.7 ppb TMA	no change	X
11a	30% RH	dry air	2.1 ppb MSA	**4 ppb TMA**	base case	base case
11b	30% RH	17 ppb OxA	2.1 ppb MSA	**4 ppb TMA**	no change	✓[f]
12a	30% RH	dry air	2.1 ppb MSA	**4 ppb TMA**	base case	base case
12b	30% RH	17 ppb OxA	2.1 ppb MSA	**4 ppb TMA**	no change	X
13a	30% RH	dry air	4.2 ppb MSA	**6 ppb TMA**	base case	base case
13b	30% RH	17 ppb OxA	4.2 ppb MSA	**6 ppb TMA**	no change	X
14a	30% RH	dry air	1.3 ppb MSA	**5 ppb TMA**	base case	base case
14b	30% RH	17 ppb OxA	1.3 ppb MSA	**5 ppb TMA**	no change	X
15a	15% RH	dry air	4.4 ppb MSA	3.2 ppb TMA	base case	base case
15b	15% RH	17 ppb OxA	4.4 ppb MSA	3.2 ppb TMA	no change	X

16a	15% RH	dry air	4 ppb MSA	3.5 ppb TMA	base case	base case
16b	15% RH	17 ppb OxA	4 ppb MSA	3.5 ppb TMA	no change	X
17a	29% RH	dry air	3.9 ppb MSA	3.7 ppb TMA	base case	base case
17b	29% RH	17 ppb OxA	3.9 ppb MSA	3.7 ppb TMA	no change	n/a [g]
18a	30% RH	dry air	3.1 ppb MSA	3.5 ppb TMA	base case	base case
18b	30% RH	17 ppb OxA	3.1 ppb MSA	3.5 ppb TMA	no change	X
19a	30% RH	dry air	3.2 ppb MSA	3.5 ppb TMA	base case	base case
19b	30% RH	17 ppb OxA	3.2 ppb MSA	3.5 ppb TMA	no change	X
20a	30% RH	dry air	3.6 ppb MSA	3.5 ppb TMA	base case	base case
20b	30% RH	34 ppb OxA	3.6 ppb MSA	3.5 ppb TMA	no change	X
21a	30% RH	dry air	3.4 ppb MSA	3.3 ppb TMA	base case	base case
21b	30% RH	34 ppb OxA	3.4 ppb MSA	3.3 ppb TMA	no change	X
22a	30% RH	dry air	3.1 ppb MSA	3.2 ppb TMA	base case	base case
22b	30% RH	34 ppb OxA	3.1 ppb MSA	3.2 ppb TMA	no change	X
23a	50% RH	dry air	3.7 ppb MSA	3.5 ppb TMA	base case	base case
23b	50% RH	17 ppb OxA	3.7 ppb MSA	3.5 ppb TMA	no change	X
24a	50% RH	dry air	2.7 ppb MSA	3.7 ppb TMA	base case	base case
24b	50% RH	17 ppb OxA	2.7 ppb MSA	3.7 ppb TMA	no change	X
dry conditions						
25a	dry air	dry air	**3.8 ppb MSA**	2.5 ppb TMA	base case	base case
25b	dry air	17 ppb OxA	**3.8 ppb MSA**	2.5 ppb TMA	no change	✓
26a	dry air	dry air	**4.7 ppb MSA**	2.5 ppb TMA	base case	base case
26b	dry air	17 ppb OxA	**4.7 ppb MSA**	2.5 ppb TMA	no change	✓
27a	dry air	dry air	**5.5 ppb MSA**	3.7 ppb TMA	base case	base case
27b	dry air	17 ppb OxA	**5.5 ppb MSA**	3.7 ppb TMA	no change	n/a
28a	dry air	dry air	**5 ppb MSA**	2.7 ppb TMA	base case	base case

28b	dry air	17 ppb OxA	**5 ppb MSA**	2.7 ppb TMA	no change	✓
29a	dry air	dry air	**5.3 ppb MSA**	2.7 ppb TMA	base case	base case
29b	dry air	17 ppb OxA	**5.3 ppb MSA**	2.7 ppb TMA	no change	✓
30a	dry air	dry air	4.6 ppb MSA	**9 ppb TMA**	base case	base case
30b	dry air	17 ppb OxA	4.6 ppb MSA	**9 ppb TMA**	+[h] (3 times more)	n/a
31a	dry air	dry air	2.1 ppb MSA	**4 ppb TMA**	base case	base case
31b	dry air	17 ppb OxA	2.1 ppb MSA	**4 ppb TMA**	no change	✓
32a	dry air	dry air	2.2 ppb MSA	**4 ppb TMA**	base case	base case
32b	dry air	17 ppb OxA	2.2 ppb MSA	**4 ppb TMA**	no change	✓
33a	dry air	dry air	3.5 ppb MSA	3.6 ppb TMA	base case	base case
33b	dry air	17 ppb OxA	3.5 ppb MSA	3.6 ppb TMA	no change	✓
34a	dry air	dry air	3.6 ppb MSA	3.5 ppb TMA	base case	base case
34b	dry air	17 ppb OxA	3.6 ppb MSA	3.5 ppb TMA	no change	✓
35a	dry air	dry air	3.2 ppb MSA	3.5 ppb TMA	base case	base case
35b	dry air	17 ppb OxA	3.2 ppb MSA	3.5 ppb TMA	no change	✓
36a	dry air	dry air	3.8 ppb MSA	3.5 ppb TMA	base case	base case
36b	dry air	17 ppb OxA	3.8 ppb MSA	3.5 ppb TMA	no change	✓
37a	dry air	dry air	3.7 ppb MSA	3.7 ppb TMA	base case	base case
37b	dry air	17 ppb OxA	3.7 ppb MSA	3.7 ppb TMA	no change	✓
38a	dry air	dry air	3.4 ppb MSA	3.5 ppb TMA	base case	base case
38b	dry air	34 ppb OxA	3.4 ppb MSA	3.5 ppb TMA	no change	✓
39a	dry air	dry air	3.5 ppb MSA	3.2 ppb TMA	base case	base case
39b	dry air	34 ppb OxA	3.5 ppb MSA	3.2 ppb TMA	no change	✓

Note: Only dry air was added through ring #3 and spoke #3.

[a] The oxalic acid concentration, calculated from its vapor pressure at 303 K,[159] takes into account dilution in the flow reactor. This represents the maximum concentration achieved in the reaction.

^b MSA and TMA concentrations are measured prior to their entrance to the reactor. These values account for dilution in the reactor, and are in bold-face font when in excess. These represent the maximum concentrations achieved in the reaction.

^c 1 ppb = 2.48×10^{10} cm^{-3} at 1 atm and 294 K

^d The designation, "no change" indicates $\leq$ 2 times more particles were observed due to the added OxA.

^e An "X" means particle growth compared to the base case was not observed.

^f A "✓" means particle growth compared to the base case was observed.

^g "n/a" means the reaction was not measured with the SMPS.

^h An enhancement of + represents > 2 times more but $\leq$ 4 times more particles due to the added OxA.

Table 5.4 Conditions and results for MSA + TMA and OxA + MSA + TMA experiments with and without water vapor.

Expt.	Ring #1	Ring #2[a]	Spoke #1[b]	Spoke #2[b]	Degree of Particle Formation Enhancement due to Addition of H_2O	Particle growth?
40a	dry air	dry air	**5 ppb MSA**[c]	2.7 ppb TMA	base case	base case
40b[d]	30% RH	dry air	**5 ppb MSA**	2.7 ppb TMA	+ +[e]	✓[f]
41a	dry air	dry air	**5 ppb MSA**	2.7 ppb TMA	base case	base case
41b	30% RH	dry air	**5 ppb MSA**	2.7 ppb TMA	+[g]	✓
42a	dry air	dry air	2.1 ppb MSA	**4 ppb TMA**	base case	base case
42b	30% RH	dry air	2.1 ppb MSA	**4 ppb TMA**	+ + +[h]	✓
43a	dry air	dry air	2.1 ppb MSA	**4 ppb TMA**	base case	base case
43b	30% RH	dry air	2.1 ppb MSA	**4 ppb TMA**	+ + (9 times more)	✓
44a	dry air	dry air	1.3 ppb MSA	**5 ppb TMA**	base case	base case
44b	30% RH	dry air	1.3 ppb MSA	**5 ppb TMA**	+ + +	✓
45a	dry air	dry air	4.4 ppb MSA	3.2 ppb TMA	base case	base case
45b	15% RH	dry air	4.4 ppb MSA	3.2 ppb TMA	+	✓
46a	dry air	dry air	4 ppb MSA	3.5 ppb TMA	base case	base case
46b	15% RH	dry air	4 ppb MSA	3.5 ppb TMA	+	✓
47a	dry air	dry air	3.9 ppb MSA	3.7 ppb TMA	base case	base case
47b	29% RH	dry air	3.9 ppb MSA	3.7 ppb TMA	+ +	n/a[i]
48a	dry air	dry air	3.1 ppb MSA	3.5 ppb TMA	base case	base case
48b	30% RH	dry air	3.1 ppb MSA	3.5 ppb TMA	+ + +	✓
49a	dry air	dry air	3.2 ppb MSA	3.5 ppb TMA	base case	base case
49b	30% RH	dry air	3.2 ppb MSA	3.5 ppb TMA	+ +	✓
50a	dry air	dry air	3.6 ppb MSA	3.5 ppb TMA	base case	base case
50b	30% RH	dry air	3.6 ppb MSA	3.5 ppb TMA	+ + +	✓
51a	dry air	dry air	3.4 ppb MSA	3.3 ppb TMA	base case	base case

51b	30% RH	dry air	3.4 ppb MSA	3.3 ppb TMA	+ +	✓
52a	dry air	dry air	3.1 ppb MSA	3.2 ppb TMA	base case	base case
52b	30% RH	dry air	3.1 ppb MSA	3.2 ppb TMA	+ +	✓
53a	dry air	dry air	2.9 ppb MSA	3.2 ppb TMA	base case	base case
53b	30% RH	dry air	2.9 ppb MSA	3.2 ppb TMA	+ +	✓
54a	dry air	dry air	3.7 ppb MSA	3.5 ppb TMA	base case	base case
54b	50% RH	dry air	3.7 ppb MSA	3.5 ppb TMA	+ + +	✓
55a	dry air	dry air	2.7 ppb MSA	3.7 ppb TMA	base case	base case
55b	50% RH	dry air	2.7 ppb MSA	3.7 ppb TMA	+ + +	✓
56a	dry air	17 ppb OxA	3.8 ppb MSA	3.5 ppb TMA	base case	base case
56b	15% RH	17 ppb OxA	3.8 ppb MSA	3.5 ppb TMA	+	X [j]
57a	dry air	17 ppb OxA	3.7 ppb MSA	3.7 ppb TMA	base case	base case
57b	15% RH	17 ppb OxA	3.7 ppb MSA	3.7 ppb TMA	no change	X
58a	dry air	17 ppb OxA	**5.5 ppb MSA**	3.7 ppb TMA	base case	base case
58b	29% RH	17 ppb OxA	**5 ppb MSA**	3.7 ppb TMA	+ +	n/a
59a	dry air	17 ppb OxA	**5 ppb MSA**	2.7 ppb TMA	base case	base case
59b	30% RH	17 ppb OxA	**5 ppb MSA**	2.7 ppb TMA	+ +	✓
60a	dry air	17 ppb OxA	**5.3 ppb MSA**	2.7 ppb TMA	base case	base case
60b	30% RH	17 ppb OxA	**5.3 ppb MSA**	2.7 ppb TMA	+ +	✓
61a	dry air	17 ppb OxA	2.2 ppb MSA	**4 ppb TMA**	base case	base case
61b	27% RH	17 ppb OxA	2.2 ppb MSA	**4 ppb TMA**	+ +	n/a
62a	dry air	17 ppb OxA	4.6 ppb MSA	**9 ppb TMA**	base case	base case
62b	28% RH	17 ppb OxA	4.6 ppb MSA	**9 ppb TMA**	+ +	n/a
63a	dry air	17 ppb OxA	2.1 ppb MSA	**4 ppb TMA**	base case	base case

63b	30% RH	17 ppb OxA	2.1 ppb MSA	**4 ppb TMA**	+ +	X
64a	dry air	17 ppb OxA	2.2 ppb MSA	**4 ppb TMA**	base case	base case
64b	30% RH	17 ppb OxA	2.2 ppb MSA	**4 ppb TMA**	+ +	X
65a	dry air	17 ppb OxA	2 ppb MSA	2 ppb TMA	base case	base case
65b	30% RH	17 ppb OxA	2 ppb MSA	2 ppb TMA	+ +	n/a
66a	dry air	17 ppb OxA	3.5 ppb MSA	3.6 ppb TMA	base case	base case
66b	30% RH	17 ppb OxA	3.5 ppb MSA	3.6 ppb TMA	+ +	X
67a	dry air	17 ppb OxA	4 ppb MSA	3.5 ppb TMA	base case	base case
67b	30% RH	17 ppb OxA	4 ppb MSA	3.5 ppb TMA	+ +	X
68a	dry air	17 ppb OxA	3.6 ppb MSA	3.5 ppb TMA	base case	base case
68b	30% RH	17 ppb OxA	3.6 ppb MSA	3.5 ppb TMA	+ +	X
69a	dry air	17 ppb OxA	3.2 ppb MSA	3.5 ppb TMA	base case	base case
69b	30% RH	17 ppb OxA	3.2 ppb MSA	3.5 ppb TMA	+ +	X
70a	dry air	17 ppb OxA	3.8 ppb MSA	3.5 ppb TMA	base case	base case
70b	30% RH	17 ppb OxA	3.8 ppb MSA	3.5 ppb TMA	+ +	X
71a	dry air	17 ppb OxA	3.7 ppb MSA	3.7 ppb TMA	base case	base case
71b	30% RH	17 ppb OxA	3.7 ppb MSA	3.7 ppb TMA	+	X
72a	dry air	34 ppb OxA	3.4 ppb MSA	3.5 ppb TMA	base case	base case
72b	30% RH	34 ppb OxA	3.4 ppb MSA	3.5 ppb TMA	+ + (6 times more)	X
73a	dry air	34 ppb OxA	3.5 ppb MSA	3.2 ppb TMA	base case	base case
73b	30% RH	34 ppb OxA	3.5 ppb MSA	3.2 ppb TMA	+ (4 times more)	X
74a	dry air	17 ppb OxA	3.8 ppb MSA	3.5 ppb TMA	base case	base case
74b	50% RH	17 ppb OxA	3.8 ppb MSA	3.5 ppb TMA	+ + +	X

75a	dry air	17 ppb OxA	3.7 ppb MSA	3.7 ppb TMA	base case	base case
75b	50% RH	17 ppb OxA	3.7 ppb MSA	3.7 ppb TMA	+ + (9 times more)	X

Note: Only dry air was added through ring #3 and spoke #3.

[a] The oxalic acid concentration, calculated from its vapor pressure at 303 K,[159] takes into account dilution in the flow reactor. This represents the maximum concentration achieved in the reaction.

[b] MSA and TMA concentrations are measured prior to their entrance to the reactor. These values account for dilution in the reactor, and are in bold-face font when in excess. These represent the maximum concentrations achieved in the reaction.

[c] 1 ppb = 2.48×10^{10} cm^{-3} at 1 atm and 294 K

[d] Blue highlight indicates experiment was done in the presence of water vapor.

[e] An enhancement of + + represents > 4 times more but ≤ 10 times more particles due to the added H_2O.

[f] A "✓" means particle growth compared to the base case was observed.

[g] An enhancement of + represents > 2 times more but ≤ 4 times more particles due to the added H_2O.

[h] An enhancement of + + + represents > 10 times more particles due to the added H_2O.

[i] "n/a" means the reaction was not measured with the SMPS.

[j] An "X" means particle growth compared to the base case was not observed.

Table 5.5 Control experiments and results for the OxA, MSA, TMA and water system.

Exp.	Ring #1	Ring #2[a]	Spoke #1	Spoke #2[b]	Results
76[c]	50% RH	dry air	dry air	dry air	<1000 particles
77	29% RH	17 ppb OxA	dry air	dry air	<100 particles
78	23% RH	17 ppb OxA	dry air	9 ppb TMA	<100 particles
79	30% RH	17 ppb OxA	dry air	0 – 9 ppb TMA	<100 particles
80	30% RH	17 ppb OxA	dry air	0.2 ppb TMA	<100 particles
81	30% RH	17 ppb OxA	dry air	4 ppb TMA	<100 particles
82	50% RH	17 ppb OxA	dry air	4 ppb TMA	<2000 particles
83	dry air	17 ppb OxA	dry air	0 – 9 ppb TMA	no particles
84	dry air	17 ppb OxA	dry air	0.2 ppb TMA	no particles
85	dry air	17 ppb OxA	dry air	4 ppb TMA	no particles
86	dry air	17 ppb OxA	dry air	4 ppb TMA	no particles
87	dry air	17 ppb OxA	dry air	9 ppb TMA	no particles

Note: Only dry air was added through ring #3 and spoke #3.
[a] The oxalic acid concentration, calculated from its vapor pressure at 303 K,[159] takes into account dilution in the flow reactor. This represents the maximum concentration achieved in the reaction.
[b] TMA concentrations are measured prior to their entrance to the reactor. These values account for dilution in the reactor. These represent the maximum concentrations achieved in the reaction.
[c] Experiment done on a dirty/used aerosol reactor, particles likely formed from degassing of reactants. No particles are formed with water vapor on a clean aerosol reactor.

5.3 ATMOSPHERIC IMPLICATIONS

Particle formation and growth from OxA, MSA, TMA and water are summarized schematically in Figure 5.12. Through comparing the results of OxA-MSA-amine-H_2O where the amine is either MA or TMA, we explore the effect of two kinds of bases on particle formation and growth. Basicity and hydrogen bonding capacity are used to explain how differences in amine structure affect particle formation and growth. Our results show that MA is more efficient than TMA at forming particles with OxA, which can be attributed mainly to the primary amine's greater capacity for hydrogen bonding, despite its lower basicity. Theoretically predicted proton transfer did not always correlate with experimentally observed particle formation in these studies of particles from TMA. For example, with the OxA-TMA cluster a proton transfer occurs but no particles were measured. Though the effect of OxA is likely overshadowed by water in the atmosphere, without water vapor OxA-MSA-TMA particles are larger than the MSA-TMA particles. For OxA-MSA-TMA, water enhanced particle number concentrations but larger OxA-MSA-TMA-H_2O particles were observed mainly in cases with excess MSA compared to the base case without H_2O, suggesting that the MSA hydrate is important for both nucleation and particle growth. Thus, the combination of laboratory experiments and theoretical calculations is a powerful approach to elucidate the processes of particle formation and growth.
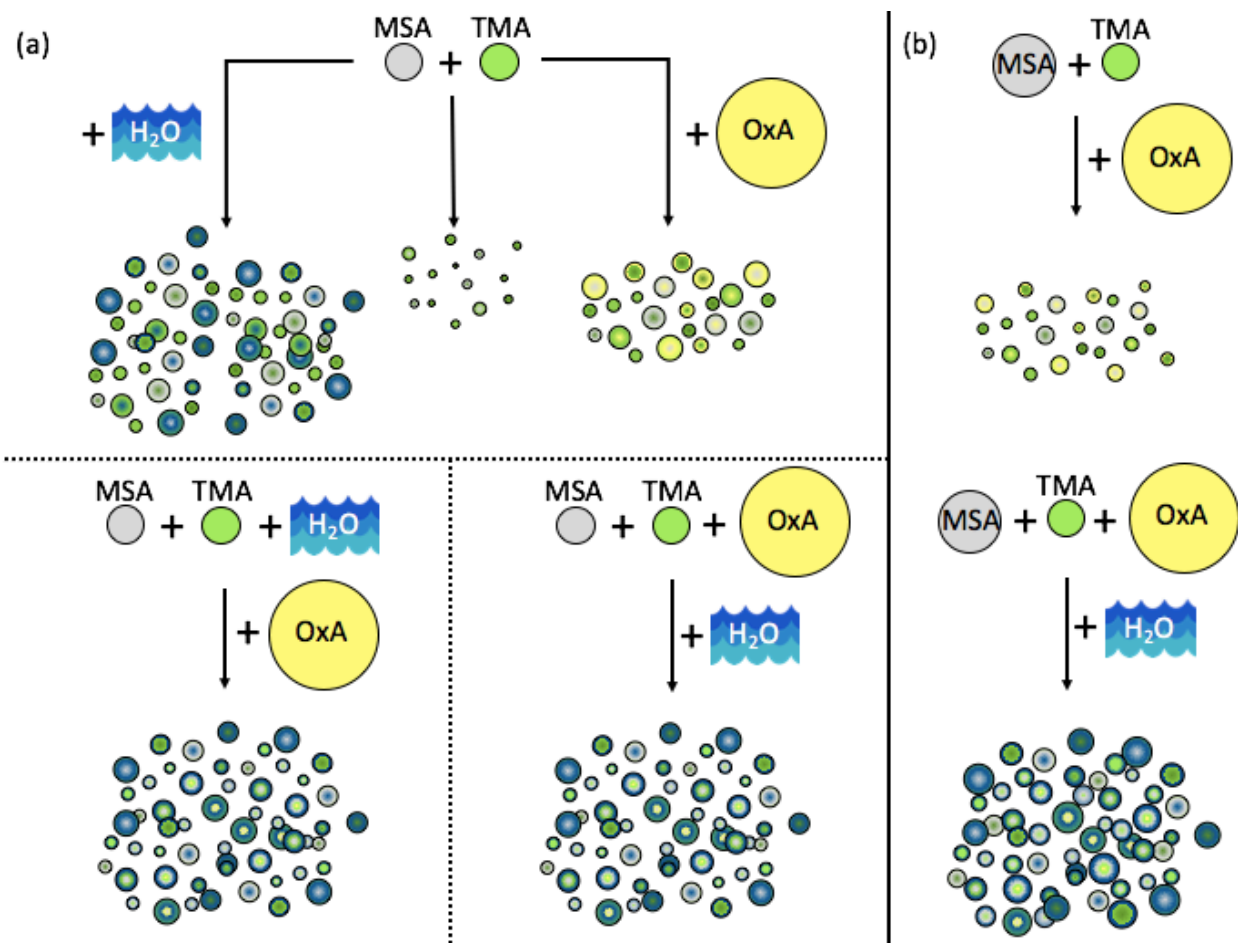
Figure 5.12 Schematic summary of experimental results to represent conditions with (a) equal concentrations of MSA and TMA and (b) with excess MSA. Note that this schematic is intended to show the net results of the addition of one selected gas phase species to its base case without that species.

CONCLUSIONS

Elucidating how particles form and grow in the atmosphere is important to fully understand the impact particles have on human health, the atmosphere and the climate. These laboratory studies, in collaboration with theoretical calculations completed by the Gerber group, suggest that proton transfer, hydrogen bonding and basicity all play a role in particle formation.

In the OxA-MA and OxA-MA-H_2O system, proton transfer correlated with particle formation. Few particles are formed from OxA-MA, where no proton transfer is observed. The presence of water promotes a proton transfer in the OxA-MA-H_2O cluster and results show particle formation is enhanced compared to OxA-MA. Particle formation from OxA and MA with and without water is more efficient compared to OxA and TMA with and without water. In this case, proton transfer did not correspond with particle formation and basicity is shown to be less important than hydrogen bonding capacity. MA is less basic than TMA but has more opportunities to hydrogen bond than TMA. Although theoretical studies predict otherwise, in these experimental studies there is no significant particle formation from dicarboxylic acids and amines with and without water. At atmospheric concentrations, the reaction of dicarboxylic acids, amines and water are an unlikely source of particles on their own.

Of the four organics investigated in this work, OxA had the most significant effect on particle formation and growth under dry conditions. With the MSA + MA system, OxA enhanced particle formation (< 1 order of magnitude more particles in the presence OxA) and did not grow particles to larger sizes. With the MSA + TMA system, OxA only slightly enhanced particle formation (≤ 2 times more particles in the presence OxA) but grew particles to larger sizes.

97

Here, amine structure influenced OxA-MSA-amine cluster geometry and ultimately determined whether growth in particle number or growth to larger particle sizes was more favorable.

There was no evidence of increased particle formation or particle growth in the presence of octanol, MaA or OxA under humid conditions compared to measurements of MSA, amine and H_2O. SuA was the exception and showed a slight enhancement (at least 2 times more particles) of new particle formation with water, which may be due to its low vapor pressure, its hydrogen bonding capacity or both. Since water is always present in the atmosphere it may overwhelm the effect of some organics. Results also suggest that water alone does not grow particles to larger sizes.

Coupling experimental results with theoretical calculations is a powerful approach. Theoretical calculations help expand interpretation of experimental results to give insight of the very initial stages of cluster formation. The results of this work can be implemented in atmospheric models to better predict particle impacts on a regional and global level.

REFERENCES

1.   Dockery, D. W.; Pope III, C. A.; Xu, X.; Spengler, J. D.; Ware, J. H.; Fay, M. E.; Ferris Jr., B. G.; Speizer, F. E., An association between air pollution and mortality in six US cities. *New Engl. J. Med.* **1993,** *329*, (24), 1753-1759.

2.   Feizabad, E.; Hossein-Nezhad, A.; Maghbooli, Z.; Ramezani, M.; Hashemian, R.; Moattari, S., Impact of air pollution on vitamin D deficiency and bone health in adolescents. *Arch. Osteoporos.* **2017,** *12*, (1), 34, DOI: 10.1007/s11657-017-0323-6.

3.   Giannadaki, D.; Lelieveld, J.; Pozzer, A., Implementing the US air quality standard for PM2.5 worldwide can prevent millions of premature deaths per year. *Environ. Health* **2016,** *15*, 88, DOI: 10.1186/s12940-016-0170-8.

4.   Lim, S. S.; Vos, T.; Flaxman, A. D.; Danaei, G.; Shibuya, K.; Adair-Rohani, H.; AlMazroa, M. A.; Amann, M.; Anderson, H. R.; Andrews, K. G., A comparative risk assessment of burden of disease and injury attributable to 67 risk factors and risk factor clusters in 21 regions, 1990–2010: a systematic analysis for the Global Burden of Disease Study 2010. *Lancet* **2013,** *380*, (9859), 2224-2260.

5.   Lelieveld, J.; Evans, J. S.; Fnais, M.; Giannadaki, D.; Pozzer, A., The contribution of outdoor air pollution sources to premature mortality on a global scale. *Nature* **2015,** *525*, (7569), 367-371.

6.   Plummer, L. E.; Carosino, C. M.; Bein, K. J.; Zhao, Y.; Willits, N.; Smiley-Jewell, S.; Wexler, A. S.; Pinkerton, K. E., Pulmonary inflammatory effects of source-oriented particulate matter from California's San Joaquin Valley. *Atmos. Environ.* **2015,** *119*, 174-181.

7.   Pope III, C. A.; Dockery, D. W., Health effects of fine particulate air pollution: lines that connect. *J. Air Waste Manage. Assoc.* **2006,** *56*, (6), 709-742.

8.   Pöschl, U.; Shiraiwa, M., Multiphase chemistry at the atmosphere–biosphere interface influencing climate and public health in the anthropocene. *Chem. Rev.* **2015,** *115*, (10), 4440-4475.

9.   Hinds, W. C., *Aerosol Technology: Properties, Behavior, and Measurement of Airborne Particles*. John Wiley & Sons: 2012.

10.   Singh, A.; Bloss, W. J.; Pope, F. D., 60 years of UK visibility measurements: impact of meteorology and atmospheric pollutants on visibility. *Atmos. Chem. Phys.* **2017,** *17*, (3), 2085-2101.

11.   Finlayson-Pitts, B. J.; Pitts Jr., J. N., *Chemistry of the Upper and Lower Atmosphere: Theory, Experiments, and Applications*. Academic Press: San Diego: 2000.

12.   Seinfeld, J. H.; Pandis, S. N., *Atmospheric Chemistry and Physics, A Wiley-Inter Science Publication*. John Wiley & Sons Inc, New York: 2006.

13.   Stocker, T. F.; Qin, D.; Plattner, G. K.; Tignor, M.; Allen, S. K.; Boschung, J.; Nauels, A.; Xia, Y.; Bex, B.; Midgley, B. M., *IPCC, 2013: Climate Change 2013: The Physical Science Basis. Contribution of Working Group I to the Fifth Assessment Report of the Intergovernmental Panel on Climate Change*. Cambridge University Press: 2013.

14.   Andreae, M.; Rosenfeld, D., Aerosol–cloud–precipitation interactions. Part 1. The nature and sources of cloud-active aerosols. *Earth-Sci. Rev.* **2008,** *89*, (1), 13-41.

15.   Farmer, D. K.; Cappa, C. D.; Kreidenweis, S. M., Atmospheric processes and their controlling influence on cloud condensation nuclei activity. *Chem. Rev.* **2015,** *115*, (10), 4199-4217.

16.   Hallquist, M.; Wenger, J. C.; Baltensperger, U.; Rudich, Y.; Simpson, D.; Claeys, M.; Dommen, J.; Donahue, N. M.; George, C.; Goldstein, A. H., The formation, properties and impact of secondary organic aerosol: current and emerging issues. *Atmos. Chem. Phys.* **2009,** *9*, (14), 5155-5236.

17.   Kanakidou, M.; Seinfeld, J. H.; Pandis, S. N.; Barnes, I.; Dentener, F. J.; Facchini, M. C.; Dingenen, R. V.; Ervens, B.; Nenes, A.; Nielsen, C. J., Organic aerosol and global climate modelling: a review. *Atmos. Chem. Phys.* **2005,** *5*, (4), 1053-1123.

18.   Lohmann, U.; Feichter, J., Global indirect aerosol effects: a review. *Atmos. Chem. Phys.* **2005,** *5*, (3), 715-737.

19.   Merikanto, J.; Spracklen, D. V.; Mann, G. W.; Pickering, S. J.; Carslaw, K. S., Impact of nucleation on global CCN. *Atmos. Chem. Phys.* **2009,** *9*, (21), 8601-8616.

20.   Berndt, T.; Böge, O.; Stratmann, F.; Heintzenberg, J.; Kulmala, M., Rapid formation of sulfuric acid particles at near-atmospheric conditions. *Science* **2005,** *307*, (5710), 698-700.

21.   Brus, D.; Neitola, K.; Hyvärinen, A.-P.; Petäjä, T.; Vanhanen, J.; Sipilä, M.; Paasonen, P.; Kulmala, M.; Lihavainen, H., Homogenous nucleation of sulfuric acid and water at close to atmospherically relevant conditions. *Atmos. Chem. Phys.* **2011,** *11*, (11), 5277-5287.

22.   Mirabel, P.; Katz, J. L., Binary homogeneous nucleation as a mechanism for the formation of aerosols. *J. Chem. Phys.* **1974,** *60*, (3), 1138-1144.

23.   Noppel, M.; Vehkamäki, H.; Kulmala, M., An improved model for hydrate formation in sulfuric acid–water nucleation. *J. Chem. Phys.* **2002,** *116*, (1), 218-228.

24.   Sipilä, M.; Berndt, T.; Petäjä, T.; Brus, D.; Vanhanen, J.; Stratmann, F.; Patokoski, J.; Mauldin, R. L.; Hyvärinen, A.-P.; Lihavainen, H., The role of sulfuric acid in atmospheric nucleation. *Science* **2010,** *327*, (5970), 1243-1246.

25.   Sorokin, A.; Vancassel, X.; Mirabel, P., Kinetic model for binary homogeneous nucleation in the H_2O–H_2SO_4 system: Comparison with experiments and classical theory of nucleation. *J. Chem. Phys.* **2005,** *123*, (24), 244508, DOI: 10.1063/1.2141511.

26.   Weber, R. J.; McMurry, P. H.; Eisele, F. L.; Tanner, D. J., Measurement of expected nucleation precursor species and 3-500-nm diameter particles at Mauna Loa observatory, Hawaii. *J. Atmos. Sci* **1995,** *52*, (12), 2242-2257.

27.   Weber, R. J.; Marti, J. J.; McMurry, P. H.; Eisele, F. L.; Tanner, D. J.; Jefferson, A., Measured atmospheric new particle formation rates: Implications for nucleation mechanisms. *Chem. Eng. Commun.* **1996,** *151*, (1), 53-64.

28.   Weber, R. J.; Chen, G.; Davis, D.; Mauldin, R. L.; Tanner, D. J.; Eisele, F. L.; Clarke, A. D.; Thornton, D. C.; Bandy, A. R., Measurements of enhanced H_2SO_4 and 3–4 nm particles near a frontal cloud during the First Aerosol Characterization Experiment (ACE 1). *J. Geophys. Res.* **2001,** *106*, (D20), 24107-24117.

29.   Bluth, G. J.; Doiron, S. D.; Schnetzler, C. C.; Krueger, A. J.; Walter, L. S., Global tracking of the SO_2 clouds from the June, 1991 Mount Pinatubo eruptions. *Geophys. Res. Lett.* **1992,** *19*, (2), 151-154.

30.   Smith, S. J.; Aardenne, J. v.; Klimont, Z.; Andres, R. J.; Volke, A.; Delgado Arias, S., Anthropogenic sulfur dioxide emissions: 1850–2005. *Atmos. Chem. Phys.* **2011,** *11*, (3), 1101-1116.

31.   Brus, D.; Hyvärinen, A. P.; Viisanen, Y.; Kulmala, M.; Lihavainen, H., Homogeneous nucleation of sulfuric acid and water mixture: experimental setup and first results. *Atmos. Chem. Phys.* **2010,** *10*, (6), 2631-2641.

32.   Benson, D. R.; Young, L. H.; Kameel, F. R.; Lee, S.-H., Laboratory-measured nucleation rates of sulfuric acid and water binary homogeneous nucleation from the $SO_2 + OH$ reaction. *Geophys. Res. Lett.* **2008,** *35*, (11), L11801, DOI: 10.1029/2008GL033387.

33.   Kuang, C.; McMurry, P. H.; McCormick, A. V.; Eisele, F. L., Dependence of nucleation rates on sulfuric acid vapor concentration in diverse atmospheric locations. *J. Geophys. Res.* **2008,** *113*, (D10), D10209, DOI: 10.1029/2007JD009253.

34.   Kulmala, M.; Vehkamäki, H.; Petäjä, T.; Dal Maso, M.; Lauri, A.; Kerminen, V.-M.; Birmili, W.; McMurry, P. H., Formation and growth rates of ultrafine atmospheric particles: a review of observations. *J. Aerosol Sci.* **2004,** *35*, (2), 143-176.

35.   Young, L.-H.; Benson, D. R.; Kameel, F. R.; Pierce, J. R.; Junninen, H.; Kulmala, M.; Lee, S.-H., Laboratory studies of H_2SO_4/H_2O binary homogeneous nucleation from the $SO_2 +$ OH reaction: evaluation of the experimental setup and preliminary results. *Atmos. Chem. Phys.* **2008,** *8*, (16), 4997-5016.

36.   Anderson, N.; Strader, R.; Davidson, C., Airborne reduced nitrogen: ammonia emissions from agriculture and other sources. *Environ. Int.* **2003,** *29*, (2), 277-286.

37.   Ge, X.; Wexler, A. S.; Clegg, S. L., Atmospheric amines–Part I. A review. *Atmos. Environ.* **2011,** *45*, (3), 524-546.

38.   Schade, G. W.; Crutzen, P. J., Emission of aliphatic amines from animal husbandry and their reactions: Potential source of N_2O and HCN. *J. Atmos. Chem.* **1995,** *22*, (3), 319-346.

39.   Sutton, M.; Dragosits, U.; Tang, Y.; Fowler, D., Ammonia emissions from non-agricultural sources in the UK. *Atmos. Environ.* **2000,** *34*, (6), 855-869.

40.   Mosier, A. R.; Andre, C. E.; Viets, F. G., Identification of aliphatic amines volatilized from cattle feedyard. *Environ. Sci. Technol.* **1973,** *7*, (7), 642-644.

41.   Almeida, J.; Schobesberger, S.; Kürten, A.; Ortega, I. K.; Kupiainen-Määttä, O.; Praplan, A. P.; Adamov, A.; Amorim, A.; Bianchi, F.; Breitenlechner, M., et al., Molecular understanding of sulphuric acid-amine particle nucleation in the atmosphere. *Nature* **2013,** *502*, (7471), 359-363.

42.   Ball, S. M.; Hanson, D. R.; Eisele, F. L.; McMurry, P. H., Laboratory studies of particle nucleation: Initial results for H_2SO_4, H_2O, and NH_3 vapors. *J. Geophys. Res.* **1999,** *104*, (D19), 23709-23718.

43.   Benson, D. R.; Erupe, M. E.; Lee, S.-H., Laboratory-measured H_2SO_4-H_2O-NH_3 ternary homogeneous nucleation rates: Initial observations. *Geophys. Res. Lett.* **2009,** *36*, (15), L15818, DOI: 10.1029/2009GL038728.

44.   Berndt, T.; Stratmann, F.; Sipilä, M.; Vanhanen, J.; Petäjä, T.; Mikkilä, J.; Grüner, A.; Spindler, G.; Mauldin III, L.; Curtius, J., et al., Laboratory study on new particle formation from the reaction OH + SO_2: influence of experimental conditions, H_2O vapour, NH_3 and the amine tert-butylamine on the overall process. *Atmos. Chem. Phys.* **2010,** *10*, (15), 7101-7116.

45.   Kirkby, J.; Curtius, J.; Almeida, J.; Dunne, E.; Duplissy, J.; Ehrhart, S.; Franchin, A.; Gagné, S.; Ickes, L.; Kürten, A., et al., Role of sulphuric acid, ammonia and galactic cosmic rays in atmospheric aerosol nucleation. *Nature* **2011,** *476*, (7361), 429-433.

46.   Anttila, T.; Vehkamäki, H.; Napari, I.; Kulmala, M., Effect of ammonium bisulphate formation on atmospheric water-sulphuric acid-ammonia nucleation. *Boreal Environ. Res.* **2005,** *10*, (6), 511-523.

47.   Yu, F., Effect of ammonia on new particle formation: A kinetic H_2SO_4-H_2O-NH_3 nucleation model constrained by laboratory measurements. *J. Geophys. Res.* **2006,** *111*, (D1), D01204, DOI: 10.1029/2005JD005968.

48.   Hanson, D. R.; McMurry, P. H.; Jiang, J.; Tanner, D. J.; Huey, L. G., Ambient pressure proton transfer mass spectrometry: detection of amines and ammonia. *Environ. Sci. Technol.* **2011,** *45*, (20), 8881-8888.

49.   VandenBoer, T. C.; Markovic, M. Z.; Petroff, A.; Czar, M. F.; Borduas, N.; Murphy, J. G., Ion chromatographic separation and quantitation of alkyl methylamines and ethylamines in atmospheric gas and particulate matter using preconcentration and suppressed conductivity detection. *J. Chromatogr. A* **2012,** *1252*, 74-83.

50.   VandenBoer, T. C.; Petroff, A.; Markovic, M. Z.; Murphy, J. G., Size distribution of alkyl amines in continental particulate matter and their online detection in the gas and particle phase. *Atmos. Chem. Phys.* **2011,** *11*, (9), 4319-4332.

51.   You, Y.; Kanawade, V. P.; De Gouw, J. A.; Guenther, A. B.; Madronich, S.; Sierra-Hernández, M.; Lawler, M.; Smith, J. N.; Takahama, S.; Ruggeri, G., Atmospheric amines and ammonia measured with a chemical ionization mass spectrometer (CIMS). *Atmos. Chem. Phys.* **2014,** *14*, (22), 12181-12194.

52.   Bzdek, B. R.; Ridge, D. P.; Johnston, M. V., Amine exchange into ammonium bisulfate and ammonium nitrate nuclei. *Atmos. Chem. Phys.* **2010,** *10*, (8), 3495-3503.

53.   Bzdek, B. R.; Ridge, D. P.; Johnston, M. V., Size-dependent reactions of ammonium bisulfate clusters with dimethylamine. *J. Phys. Chem. A* **2010,** *114*, (43), 11638-11644.

54.   DePalma, J. W.; Bzdek, B. R.; Doren, D. J.; Johnston, M. V., Structure and energetics of nanometer size clusters of sulfuric acid with ammonia and dimethylamine. *J. Phys. Chem. A* **2012,** *116*, (3), 1030-1040.

55.   DePalma, J. W.; Doren, D. J.; Johnston, M. V., Formation and growth of molecular clusters containing sulfuric acid, water, ammonia, and dimethylamine. *J. Phys. Chem. A* **2014,** *118*, (29), 5464-5473.

56.   Angelino, S.; Suess, D. T.; Prather, K. A., Formation of aerosol particles from reactions of secondary and tertiary alkylamines: Characterization by aerosol time-of-flight mass spectrometry. *Environ. Sci. Technol.* **2001,** *35*, (15), 3130-3138.

57.   Bzdek, B. R.; Ridge, D. P.; Johnston, M. V., Amine reactivity with charged sulfuric acid clusters. *Atmos. Chem. Phys.* **2011,** *11*, (16), 8735-8743.

58.   Erupe, M. E.; Viggiano, A. A.; Lee, S.-H., The effect of trimethylamine on atmospheric nucleation involving H_2SO_4. *Atmos. Chem. Phys.* **2011,** *11*, (10), 4767-4775.

59.   Freshour, N. A.; Carlson, K. K.; Melka, Y. A.; Hinz, S.; Panta, B.; Hanson, D. R., Amine permeation sources characterized with acid neutralization and sensitivities of an amine mass spectrometer. *Atmos. Meas. Tech.* **2014,** *7*, (10), 3611-3621.

60.   Glasoe, W. A.; Volz, K.; Panta, B.; Freshour, N.; Bachman, R.; Hanson, D. R.; McMurry, P. H.; Jen, C. N., Sulfuric acid nucleation: An experimental study of the effect of seven bases. *J. Geophys. Res.* **2015,** *120*, (5), 1933-1950.

61.   Jen, C. N.; McMurry, P. H.; Hanson, D. R., Stabilization of sulfuric acid dimers by ammonia, methylamine, dimethylamine, and trimethylamine. *J. Geophys. Res.* **2014,** *119*, (12), 7502-7514.

62.   Kurtén, T.; Loukonen, V.; Vehkamäki, H.; Kulmala, M., Amines are likely to enhance neutral and ion-induced sulfuric acid-water nucleation in the atmosphere more effectively than ammonia. *Atmos. Chem. Phys.* **2008,** *8*, (14), 4095-4103.

63.   Smith, J. N.; Barsanti, K. C.; Friedli, H. R.; Ehn, M.; Kulmala, M.; Collins, D. R.; Scheckman, J. H.; Williams, B. J.; McMurry, P. H., Observations of aminium salts in

atmospheric nanoparticles and possible climatic implications. *Proc. Natl. Acad. Sci. U.S.A.* **2010,** *107*, (15), 6634-6639.

64.   Yu, H.; McGraw, R. L.; Lee, S.-H., Effects of amines on formation of sub-3 nm particles and their subsequent growth. *Geophys. Res. Lett.* **2012,** *39*, (2), L02807, DOI: 10.1029/2011GL050099.

65.   Zollner, J. H.; Glasoe, W. A.; Panta, B.; Carlson, K. K.; McMurry, P. H.; Hanson, D. R., Sulfuric acid nucleation: power dependencies, variation with relative humidity, and effect of bases. *Atmos. Chem. Phys.* **2012,** *12*, (10), 4399-4411.

66.   DePalma, J. W.; Bzdek, B. R.; Ridge, D. P.; Johnston, M. V., Activation Barriers in the Growth of Molecular Clusters Derived from Sulfuric Acid and Ammonia. *J. Phys. Chem. A* **2014,** *118*, (49), 11547-11554.

67.   Kurtén, T.; Sundberg, M. R.; Vehkamäki, H.; Noppel, M.; Blomqvist, J.; Kulmala, M., Ab initio and density functional theory reinvestigation of gas-phase sulfuric acid monohydrate and ammonium hydrogen sulfate. *J. Phys. Chem. A* **2006,** *110*, (22), 7178-7188.

68.   McGrath, M. J.; Olenius, T.; Ortega, I. K.; Loukonen, V.; Paasonen, P.; Kurtén, T.; Kulmala, M.; Vehkamäki, H., Atmospheric Cluster Dynamics Code: a flexible method for solution of the birth-death equations. *Atmos. Chem. Phys.* **2012,** *12*, (5), 2345-2355.

69.   Ortega, I. K.; Kupiainen, O.; Kurtén, T.; Olenius, T.; Wilkman, O.; McGrath, M. J.; Loukonen, V.; Vehkamäki, H., From quantum chemical formation free energies to evaporation rates. *Atmos. Chem. Phys.* **2012,** *12*, (1), 225-235.

70.   Henschel, H.; Navarro, J. C. A.; Yli-Juuti, T.; Kupiainen-Määttä, O.; Olenius, T.; Ortega, I. K.; Clegg, S. L.; Kurtén, T.; Riipinen, I.; Vehkamäki, H., Hydration of atmospherically relevant molecular clusters: Computational chemistry and classical thermodynamics. *J. Phys. Chem. A* **2014,** *118*, (14), 2599-2611.

71.   Henschel, H.; Kurtén, T.; Vehkamäki, H., Computational Study on the Effect of Hydration on New Particle Formation in the Sulfuric Acid/Ammonia and Sulfuric Acid/Dimethylamine Systems. *J. Phys. Chem. A* **2016,** *120*, (11), 1886-1896.

72.   Kurtén, T.; Torpo, L.; Ding, C. G.; Vehkamäki, H.; Sundberg, M. R.; Laasonen, K.; Kulmala, M., A density functional study on water-sulfuric acid-ammonia clusters and implications for atmospheric cluster formation. *J. Geophys. Res.* **2007,** *112*, (D4), D04210, DOI: 10.1029/2006JD007391.

73.   Larson, L. J.; Largent, A.; Tao, F.-M., Structure of the sulfuric acid-ammonia system and the effect of water molecules in the gas phase. *J. Phys. Chem. A* **1999,** *103*, (34), 6786-6792.

74.   Loukonen, V.; Kurtén, T.; Ortega, I. K.; Vehkamäki, H.; Padua, A. A. H.; Sellegri, K.; Kulmala, M., Enhancing effect of dimethylamine in sulfuric acid nucleation in the presence of water–a computational study. *Atmos. Chem. Phys.* **2010,** *10*, (10), 4961-4974.

75.   Nadykto, A. B.; Yu, F.; Jakovleva, M. V.; Herb, J.; Xu, Y., Amines in the Earth's atmosphere: a density functional theory study of the thermochemistry of pre-nucleation clusters. *Entropy* **2011,** *13*, (2), 554-569.

76.   Metzger, A.; Verheggen, B.; Dommen, J.; Duplissy, J.; Prevot, A. S. H.; Weingartner, E.; Riipinen, I.; Kulmala, M.; Spracklen, D. V.; Carslaw, K. S., et al., Evidence for the role of organics in aerosol particle formation under atmospheric conditions. *Proc. Natl. Acad. Sci. U.S.A.* **2010,** *107*, (15), 6646-6651.

77.   Paasonen, P.; Nieminen, T.; Asmi, E.; Manninen, H. E.; Petäjä, T.; Plass-Dülmer, C.; Flentje, H.; Birmili, W.; Wiedensohler, A.; Horrak, U., et al., On the roles of sulphuric acid and

low-volatility organic vapours in the initial steps of atmospheric new particle formation. *Atmos. Chem. Phys.* **2010,** *10*, (22), 11223-11242.

78.   Riipinen, I.; Pierce, J. R.; Yli-Juuti, T.; Nieminen, T.; Hakkinen, S.; Ehn, M.; Junninen, H.; Lehtipalo, K.; Petäjä, T.; Slowik, J., et al., Organic condensation: a vital link connecting aerosol formation to cloud condensation nuclei (CCN) concentrations. *Atmos. Chem. Phys.* **2011,** *11*, 3865-3878.

79.   Jimenez, J. L.; Canagaratna, M. R.; Donahue, N. M.; Prevot, A. S. H.; Zhang, Q.; Kroll, J. H.; DeCarlo, P. F.; Allan, J. D.; Coe, H.; Ng, N. L., et al., Evolution of organic aerosols in the atmosphere. *Science* **2009,** *326*, (5959), 1525-1529.

80.   Elm, J.; Myllys, N.; Kurten, T., What Is Required for Highly Oxidized Molecules To Form Clusters with Sulfuric Acid? *J. Phys. Chem. A* **2017,** *121*, (23), 4578-4587.

81.   Bianchi, F.; Tröstl, J.; Junninen, H.; Frege, C.; Henne, S.; Hoyle, C. R.; Molteni, U.; Herrmann, E.; Adamov, A.; Bukowiecki, N., et al., New particle formation in the free troposphere: A question of chemistry and timing. *Science* **2016,** *352*, (6289), 1109-1112.

82.   Ehn, M.; Thornton, J. A.; Kleist, E.; Sipilä, M.; Junninen, H.; Pullinen, I.; Springer, M.; Rubach, F.; Tillmann, R.; Lee, B., et al., A large source of low-volatility secondary organic aerosol. *Nature* **2014,** *506*, (7489), 476-479.

83.   Jokinen, T.; Berndt, T.; Makkonen, R.; Kerminen, V.-M.; Junninen, H.; Paasonen, P.; Stratmann, F.; Herrmann, H.; Guenther, A. B.; Worsnop, D. R., et al., Production of extremely low volatile organic compounds from biogenic emissions: Measured yields and atmospheric implications. *Proc. Natl. Acad. Sci. U.S.A.* **2015,** *112*, (23), 7123-7128.

84.   Kirkby, J.; Duplissy, J.; Sengupta, K.; Frege, C.; Gordon, H.; Williamson, C.; Heinritzi, M.; Simon, M.; Yan, C.; Almeida, J., et al., Ion-induced nucleation of pure biogenic particles. *Nature* **2016,** *533*, (7604), 521-526.

85.   Tröstl, J.; Chuang, W. K.; Gordon, H.; Heinritzi, M.; Yan, C.; Molteni, U.; Ahlm, L.; Frege, C.; Bianchi, F.; Wagner, R., et al., The role of low-volatility organic compounds in initial particle growth in the atmosphere. *Nature* **2016,** *533*, (7604), 527-531.

86.   Kulmala, M.; Kontkanen, J.; Junninen, H.; Lehtipalo, K.; Manninen, H. E.; Nieminen, T.; Petäjä, T.; Sipilä, M.; Schobesberger, S.; Rantala, P., et al., Direct observations of atmospheric aerosol nucleation. *Science* **2013,** *339*, (6122), 943-946.

87.   O'Dowd, C. D.; Aalto, P.; Hmeri, K.; Kulmala, M.; Hoffmann, T., Aerosol formation: Atmospheric particles from organic vapours. *Nature* **2002,** *416*, (6880), 497-498.

88.   Riccobono, F.; Schobesberger, S.; Scott, C. E.; Dommen, J.; Ortega, I. K.; Rondo, L.; Almeida, J.; Amorim, A.; Bianchi, F.; Breitenlechner, M., et al., Oxidation products of biogenic emissions contribute to nucleation of atmospheric particles. *Science* **2014,** *344*, (6185), 717-721.

89.   Riipinen, I.; Yli-Juuti, T.; Pierce, J. R.; Petäjä, T.; Worsnop, D. R.; Kulmala, M.; Donahue, N. M., The contribution of organics to atmospheric nanoparticle growth. *Nat. Geosci.* **2012,** *5*, (7), 453-458.

90.   Zhang, R.; Suh, I.; Zhao, J.; Zhang, D.; Fortner, E. C.; Tie, X.; Molina, L. T.; Molina, M. J., Atmospheric new particle formation enhanced by organic acids. *Science* **2004,** *304*, (5676), 1487-1490.

91.   Zhang, R.; Wang, L.; Khalizov, A. F.; Zhao, J.; Zheng, J.; McGraw, R. L.; Molina, L. T., Formation of nanoparticles of blue haze enhanced by anthropogenic pollution. *Proc. Natl. Acad. Sci. U.S.A.* **2009,** *106*, (42), 17650-17654.

92.   Barsanti, K. C.; McMurry, P. H.; Smith, J. N., The potential contribution of organic salts to new particle growth. *Atmos. Chem. Phys.* **2009,** *9*, (9), 2949-2957.

93.	Yli-Juuti, T.; Barsanti, K.; Hildebrandt Ruiz, L.; Kieloaho, A.-J.; Makkonen, U.; Petäjä, T.; Ruuskanen, T.; Kulmala, M.; Riipinen, I., Model for acid-base chemistry in nanoparticle growth (MABNAG). *Atmos. Chem. Phys.* **2013,** *13*, (24), 12507-12524.

94.	Quinn, P. K.; Miller, T. L.; Bates, T. S.; Ogren, J. A.; Andrews, E.; Shaw, G. E., A 3-year record of simultaneously measured aerosol chemical and optical properties at Barrow, Alaska. *J. Geophys. Res.* **2002,** *107*, (D11), 4130, DOI: 10.1029/2001JD001248.

95.	Willis, M. D.; Burkart, J.; Thomas, J. L.; Köllner, F.; Schneider, J.; Bozem, H.; Hoor, P. M.; Aliabadi, A. A.; Schulz, H.; Herber, A. B., Growth of nucleation mode particles in the summertime Arctic: a case study. *Atmos. Chem. Phys.* **2016,** *16*, (12), 7663-7679.

96.	Berresheim, H.; Huey, J. W.; Thorn, R. P.; Eisele, F. L.; Tanner, D. J.; Jefferson, A., Measurements of dimethyl sulfide, dimethyl sulfoxide, dimethyl sulfone, and aerosol ions at Palmer Station, Antarctica. *J. Geophys. Res.* **1998,** *103*, (D1), 1629-1637.

97.	Facchini, M. C.; Decesari, S.; Rinaldi, M.; Carbone, C.; Finessi, E.; Mircea, M.; Fuzzi, S.; Moretti, F.; Tagliavini, E.; Ceburnis, D., et al., Important source of marine secondary organic aerosol from biogenic amines. *Environ. Sci. Technol.* **2008,** *42*, (24), 9116-9121.

98.	Froyd, K. D.; Murphy, D. M.; Sanford, T. J.; Thomson, D. S.; Wilson, J. C.; Pfister, L.; Lait, L., Aerosol composition of the tropical upper troposphere. *Atmos. Chem. Phys.* **2009,** *9*, (13), 4363-4385.

99.	Hopkins, R. J.; Desyaterik, Y.; Tivanski, A. V.; Zaveri, R. A.; Berkowitz, C. M.; Tyliszczak, T.; Gilles, M. K.; Laskin, A., Chemical speciation of sulfur in marine cloud droplets and particles: Analysis of individual particles from the marine boundary layer over the California current. *J. Geophys. Res.* **2008,** *113*, (D4), D04209, DOI: 10.1029/2007JD008954.

100.	Kerminen, V.; Aurela, M.; Hillamo, R. E.; Virkkula, A., Formation of particulate MSA: deductions from size distribution measurements in the Finnish Arctic. *Tellus B* **1997,** *49*, (2), 159-171.

101.	Kolaitis, L. N.; Bruynseels, F. J.; Van Grieken, R. E.; Andreae, M. O., Determination of methanesulfonic acid and non-sea-salt sulfate in single marine aerosol particles. *Environ. Sci. Technol.* **1989,** *23*, (2), 236-240.

102.	Legrand, M.; Pasteur, E. C., Methane sulfonic acid to non-sea-salt sulfate ratio in coastal Antarctic aerosol and surface snow. *J. Geophys. Res.* **1998,** *103*, (D9), 10991-11006.

103.	Sorooshian, A.; Padró, L. T.; Nenes, A.; Feingold, G.; McComiskey, A.; Hersey, S. P.; Gates, H.; Jonsson, H. H.; Miller, S. D.; Stephens, G. L., On the link between ocean biota emissions, aerosol, and maritime clouds: Airborne, ground, and satellite measurements off the coast of California. *Global Biogeochem. Cy.* **2009,** *23*, (4), GB4007, DOI: 10.1029/2009GB003464.

104.	Zorn, S. R.; Drewnick, F.; Schott, M.; Hoffmann, T.; Borrmann, S., Characterization of the South Atlantic marine boundary layer aerosol using an aerodyne aerosol mass spectrometer. *Atmos. Chem. Phys.* **2008,** *8*, (16), 4711-4728.

105.	Crippa, M.; El Haddad, I.; Slowik, J. G.; DeCarlo, P. F.; Mohr, C.; Heringa, M. F.; Chirico, R.; Marchand, N.; Sciare, J.; Baltensperger, U., Identification of marine and continental aerosol sources in Paris using high resolution aerosol mass spectrometry. *J. Geophys. Res.* **2013,** *118*, (4), 1950-1963.

106.	Gaston, C. J.; Pratt, K. A.; Qin, X.; Prather, K. A., Real-time detection and mixing state of methanesulfonate in single particles at an inland urban location during a phytoplankton bloom. *Environ. Sci. Technol.* **2010,** *44*, (5), 1566-1572.

107.   Ge, X.; Zhang, Q.; Sun, Y.; Ruehl, C. R.; Setyan, A., Effect of aqueous-phase processing on aerosol chemistry and size distributions in Fresno, California, during wintertime. *Environ. Chem.* **2012,** *9*, (3), 221-235.

108.   Huffman, J. A.; Docherty, K. S.; Aiken, A. C.; Cubison, M. J.; Ulbrich, I. M.; DeCarlo, P. F.; Sueper, D.; Jayne, J. T.; Worsnop, D. R.; Ziemann, P. J., Chemically-resolved aerosol volatility measurements from two megacity field studies. *Atmos. Chem. Phys.* **2009,** *9*, (18), 7161-7182.

109.   Setyan, A.; Zhang, Q.; Merkel, M.; Knighton, W. B.; Sun, Y.; Song, C.; Shilling, J. E.; Onasch, T. B.; Herndon, S. C.; Worsnop, D. R., Characterization of submicron particles influenced by mixed biogenic and anthropogenic emissions using high-resolution aerosol mass spectrometry: results from CARES. *Atmos. Chem. Phys.* **2012,** *12*, (17), 8131-8156.

110.   Barnes, I.; Hjorth, J.; Mihalopoulos, N., Dimethyl sulfide and dimethyl sulfoxide and their oxidation in the atmosphere. *Chem. Rev.* **2006,** *106*, (3), 940-975.

111.   Hatakeyama, S.; Okuda, M.; Akimoto, H., Formation of sulfur dioxide and methanesulfonic acid in the photooxidation of dimethyl sulfide in the air. *Geophys. Res. Lett.* **1982,** *9*, (5), 583-586.

112.   Patroescu, I.; Barnes, I.; Becker, K.; Mihalopoulos, N., FT-IR product study of the OH-initiated oxidation of DMS in the presence of NO_x. *Atmos. Environ.* **1998,** *33*, (1), 25-35.

113.   Tyndall, G. S.; Ravishankara, A., Atmospheric oxidation of reduced sulfur species. *Int. J. Chem. Kinet.* **1991,** *23*, (6), 483-527.

114.   Saltzman, E. S.; Savoie, D. L.; Prospero, J. M.; Zika, R. G., Methanesulfonic acid and non-sea-salt sulfate in Pacific air: Regional and seasonal variations. *J. Atmos. Chem.* **1986,** *4*, (2), 227-240.

115.   Saltzman, E. S.; Savoie, D. L.; Zika, R. G.; Prospero, J. M., Methane sulfonic acid in the marine atmosphere. *J. Geophys. Res.* **1983,** *88*, (C15), 10897-10902.

116.   Watts, S. F., The mass budgets of carbonyl sulfide, dimethyl sulfide, carbon disulfide and hydrogen sulfide. *Atmos. Environ.* **2000,** *34*, (5), 761-779.

117.   Trabue, S.; Scoggin, K.; Mitloehner, F.; Li, H.; Burns, R.; Xin, H., Field sampling method for quantifying volatile sulfur compounds from animal feeding operations. *Atmos. Environ.* **2008,** *42*, (14), 3332-3341.

118.   Van den Velde, S.; Nevens, F.; van Steenberghe, D.; Quirynen, M., GC–MS analysis of breath odor compounds in liver patients. *J. Chromatogr. B* **2008,** *875*, (2), 344-348.

119.   Berresheim, H.; Eisele, F. L.; Tanner, D. J.; McInnes, L. M.; Ramsey-Bell, D. C.; Covert, D. S., Atmospheric sulfur chemistry and cloud condensation nuclei (CCN) concentrations over the northeastern Pacific coast. *J. Geophys. Res.* **1993,** *98*, (D7), 12701-12711.

120.   Berresheim, H.; Adam, M.; Monahan, C.; O'Dowd, C. D.; Plane, J. M. C.; Bohn, B.; Rohrer, F., Missing SO_2 oxidant in the coastal atmosphere?–observations from high-resolution measurements of OH and atmospheric sulfur compounds. *Atmos. Chem. Phys.* **2014,** *14*, (22), 12209-12223.

121.   Berresheim, H.; Elste, T.; Tremmel, H. G.; Allen, A. G.; Hansson, H. C.; Rosman, K.; Dal Maso, M.; Mäkelä, J. M.; Kulmala, M.; O'Dowd, C. D., Gas-aerosol relationships of H_2SO_4, MSA, and OH: Observations in the coastal marine boundary layer at Mace Head, Ireland. *J. Geophys. Res.* **2002,** *107*, (D19), 8100, DOI: 10.1029/2000JD000229.

122.   Eisele, F. L.; Tanner, D. J., Measurement of the gas phase concentration of H_2SO_4 and methane sulfonic acid and estimates of H_2SO_4 production and loss in the atmosphere. *J. Geophys. Res.* **1993,** *98*, (D5), 9001-9010.

123.   Mauldin, R. L.; Cantrell, C. A.; Zondlo, M.; Kosciuch, E.; Eisele, F. L.; Chen, G.; Davis, D.; Weber, R. J.; Crawford, J.; Blake, D., et al., Highlights of OH, H_2SO_4 and methane sulfonic acid measurements made aboard the NASA P-3B during Transport and Chemical Evolution over the Pacific. *J. Geophys. Res.* **2003,** *108*, (D20), 8796, DOI: 10.1029/2003JD003410.

124.   Mauldin, R. L.; Tanner, D. J.; Heath, J. A.; Huebert, B. J.; Eisele, F. L., Observations of H_2SO_4 and MSA during PEM-Tropics-A. *J. Geophys. Res.* **1999,** *104*, (D5), 5801-5816.

125.   Perraud, V.; Horne, J. R.; Martinez, A. S.; Kalinowski, J.; Meinardi, S.; Dawson, M. L.; Wingen, L. M.; Dabdub, D.; Blake, D. R.; Gerber, R. B., et al., The future of airborne sulfur-containing particles in the absence of fossil fuel sulfur dioxide emissions. *Proc. Natl. Acad. Sci. U.S.A.* **2015,** *112*, (44), 13514-13519.

126.   Kreidenweis, S. M.; Flagan, R. C.; Seinfeld, J. H.; Okuyama, K., Binary nucleation of methanesulfonic acid and water. *J. Aerosol Sci.* **1989,** *20*, (5), 585-607.

127.   Kreidenweis, S. M.; Seinfeld, J. H., Nucleation of sulfuric acid-water and methanesulfonic acid-water solution particles: implications for the atmospheric chemistry of organosulfur species. *Atmos. Environ.* **1988,** *22*, (2), 283-296.

128.   Wyslouzil, B. E.; Seinfeld, J. H.; Flagan, R. C.; Okuyama, K., Binary nucleation in acid–water systems. II. Sulfuric acid–water and a comparison with methanesulfonic acid–water. *J. Chem. Phys.* **1991,** *94*, (10), 6842-6850.

129.   Wyslouzil, B. E.; Seinfeld, J. H.; Flagan, R. C.; Okuyama, K., Binary nucleation in acid–water systems. I. Methanesulfonic acid–water. *J. Chem. Phys.* **1991,** *94*, (10), 6827-6841.

130.   Chen, H.; Ezell, M. J.; Arquero, K. D.; Varner, M. E.; Dawson, M. L.; Gerber, R. B.; Finlayson-Pitts, B. J., New particle formation and growth from methanesulfonic acid, trimethylamine and water. *Phys. Chem. Chem. Phys.* **2015,** *17*, (20), 13699-13709.

131.   Chen, H.; Finlayson-Pitts, B. J., New Particle Formation from Methanesulfonic Acid and Amines/Ammonia as a Function of Temperature. *Environ. Sci. Technol.* **2017,** *51*, (1), 243-252.

132.   Chen, H.; Varner, M. E.; Gerber, R. B.; Finlayson-Pitts, B. J., Reactions of methanesulfonic acid with amines and ammonia as a source of new particles in air. *J. Phys. Chem. B* **2016,** *120*, (8), 1526-1536.

133.   Dawson, M. L.; Varner, M. E.; Perraud, V.; Ezell, M. J.; Gerber, R. B.; Finlayson-Pitts, B. J., Simplified mechanism for new particle formation from methanesulfonic acid, amines, and water via experiments and ab initio calculations. *Proc. Natl. Acad. Sci. U.S.A.* **2012,** *109*, (46), 18719-18724.

134.   Bork, N.; Elm, J.; Olenius, T.; Vehkamäki, H., Methane sulfonic acid-enhanced formation of molecular clusters of sulfuric acid and dimethyl amine. *Atmos. Chem. Phys.* **2014,** *14*, (22), 12023-12030.

135.   Hanson, D. R., Mass Accommodation of H_2SO_4 and CH_3SO_3H on Water− Sulfuric Acid Solutions from 6% to 97% RH. *J. Phys. Chem. A* **2005,** *109*, (31), 6919-6927.

136.   Li, S.; Zhang, L.; Qin, W.; Tao, F.-M., Intermolecular structure and properties of the methanesulfonic acid–ammonia system in small water clusters. *Chem. Phys. Lett.* **2007,** *447*, (1), 33-38.

137.   Napari, I.; Kulmala, M.; Vehkamäki, H., Ternary nucleation of inorganic acids, ammonia, and water. *J. Chem. Phys.* **2002,** *117*, (18), 8418-8425.

138.   Kesselmeier, J.; Staudt, M., Biogenic volatile organic compounds (VOC): An overview on emission, physiology and ecology. *J. Atmos. Chem.* **1999,** *33*, (1), 23-88.

139.   König, G.; Brunda, M.; Puxbaum, H.; Hewitt, C. N.; Duckham, S. C.; Rudolph, J., Relative contribution of oxygenated hydrocarbons to the total biogenic VOC emissions of

selected mid-European agricultural and natural plant species. *Atmos. Environ.* **1995,** *29*, (8), 861-874.

140.   Donaldson, D.; Anderson, D., Adsorption of atmospheric gases at the air− water interface. 2. C1− C4 alcohols, acids, and acetone. *J. Phys. Chem. A* **1999,** *103*, (7), 871-876.

141.   Chebbi, A.; Carlier, P., Carboxylic acids in the troposphere, occurrence, sources, and sinks: A review. *Atmos. Environ.* **1996,** *30*, (24), 4233-4249.

142.   Ho, K. F.; Lee, S. C.; Ho, S. S. H.; Kawamura, K.; Tachibana, E.; Cheng, Y.; Zhu, T., Dicarboxylic acids, ketocarboxylic acids, α-dicarbonyls, fatty acids, and benzoic acid in urban aerosols collected during the 2006 Campaign of Air Quality Research in Beijing (CAREBeijing-2006). *J. Geophys. Res.* **2010,** *115*, (D19), D19312, DOI: 10.1029/2009JD013304.

143.   Kawamura, K.; Ikushima, K., Seasonal changes in the distribution of dicarboxylic acids in the urban atmosphere. *Environ. Sci. Technol.* **1993,** *27*, (10), 2227-2235.

144.   Kawamura, K.; Kaplan, I. R., Motor exhaust emissions as a primary source for dicarboxylic acids in Los Angeles ambient air. *Environ. Sci. Technol.* **1987,** *21*, (1), 105-110.

145.   Kawamura, K.; Kasukabe, H.; Barrie, L. A., Source and reaction pathways of dicarboxylic acids, ketoacids and dicarbonyls in arctic aerosols: One year of observations. *Atmos. Environ.* **1996,** *30*, (10), 1709-1722.

146.   Kawamura, K.; Kasukabe, H.; Yasui, O.; Barrie, L. A., Production of dicarboxylic acids in the arctic atmosphere at polar sunrise. *Geophys. Res. Lett.* **1995,** *22*, (10), 1253-1256.

147.   Kawamura, K.; Sakaguchi, F., Molecular distributions of water soluble dicarboxylic acids in marine aerosols over the Pacific Ocean including tropics. *J. Geophys. Res.* **1999,** *104*, (D3), 3501-3509.

148.   Kawamura, K.; Yasui, O., Diurnal changes in the distribution of dicarboxylic acids, ketocarboxylic acids and dicarbonyls in the urban Tokyo atmosphere. *Atmos. Environ.* **2005,** *39*, (10), 1945-1960.

149.   Kerminen, V.-M.; Ojanen, C.; Pakkanen, T.; Hillamo, R.; Aurela, M.; Meriläinen, J., Low-molecular-weight dicarboxylic acids in an urban and rural atmosphere. *J. Aerosol Sci.* **2000,** *31*, (3), 349-362.

150.   Khwaja, H. A., Atmospheric concentrations of carboxylic acids and related compounds at a semiurban site. *Atmos. Environ.* **1995,** *29*, (1), 127-139.

151.   Limbeck, A.; Puxbaum, H.; Otter, L.; Scholes, M. C., Semivolatile behavior of dicarboxylic acids and other polar organic species at a rural background site (Nylsvley, RSA). *Atmos. Environ.* **2001,** *35*, (10), 1853-1862.

152.   Sempére, R.; Kawamura, K., Comparative distributions of dicarboxylic acids and related polar compounds in snow, rain and aerosols from urban atmosphere. *Atmos. Environ.* **1994,** *28*, (3), 449-459.

153.   Narukawa, M.; Kawamura, K.; Takeuchi, N.; Nakajima, T., Distribution of dicarboxylic acids and carbon isotopic compositions in aerosols from 1997 Indonesian forest fires. *Geophys. Res. Lett.* **1999,** *26*, (20), 3101-3104.

154.   Donahue, N. M.; Chuang, W.; Epstein, S. A.; Kroll, J. H.; Worsnop, D. R.; Robinson, A. L.; Adams, P. J.; Pandis, S. N., Why do organic aerosols exist? Understanding aerosol lifetimes using the two-dimensional volatility basis set. *Environ. Chem.* **2013,** *10*, (3), 151-157.

155.   Donahue, N. M.; Epstein, S. A.; Pandis, S. N.; Robinson, A. L., A two-dimensional volatility basis set: 1. organic-aerosol mixing thermodynamics. *Atmos. Chem. Phys.* **2011,** *11*, (7), 3303-3318.

156.   Donahue, N. M.; Kroll, J. H.; Pandis, S. N.; Robinson, A. L., A two-dimensional volatility basis set–Part 2: Diagnostics of organic-aerosol evolution. *Atmos. Chem. Phys.* **2012,** *12*, (2), 615-634.

157.   Donahue, N. M.; Ortega, I. K.; Chuang, W.; Riipinen, I.; Riccobono, F.; Schobesberger, S.; Dommen, J.; Baltensperger, U.; Kulmala, M.; Worsnop, D. R., et al., How do organic vapors contribute to new-particle formation? *Faraday Discuss.* **2013,** *165*, 91-104.

158.   Nasirzadeh, K.; Neueder, R.; Kunz, W., Vapor pressure determination of the aliphatic C5 to C8 1-alcohols. *J. Chem. Eng. Data* **2006,** *51*, (1), 7-10.

159.   Bilde, M.; Barsanti, K.; Booth, M.; Cappa, C. D.; Donahue, N. M.; Emanuelsson, E. U.; McFiggans, G.; Krieger, U. K.; Marcolli, C.; Tropping, D., et al., Saturation vapor pressures and transition enthalpies of low-volatility organic molecules of atmospheric relevance: From dicarboxylic acids to complex mixtures. *Chem. Rev.* **2015,** *115*, (10), 4115-4156.

160.   Peng, X.-Q.; Huang, T.; Miao, S.-K.; Chen, J.; Wen, H.; Feng, Y.-J.; Hong, Y.; Wang, C.-Y.; Huang, W., Hydration of oxalic acid–ammonia complex: atmospheric implication and Rayleigh-scattering properties. *RSC Advances* **2016,** *6*, (52), 46582-46593.

161.   Peng, X.-Q.; Liu, Y.-R.; Huang, T.; Jiang, S.; Huang, W., Interaction of gas phase oxalic acid with ammonia and its atmospheric implications. *Phys. Chem. Chem. Phys.* **2015,** *17*, (14), 9552-9563.

162.   Weber, K. H.; Liu, Q.; Tao, F.-M., Theoretical study on stable small clusters of oxalic acid with ammonia and water. *J. Phys. Chem. A* **2014,** *118*, (8), 1451-1468.

163.   Chen, J.; Jiang, S.; Liu, Y.-R.; Huang, T.; Wang, C.-Y.; Miao, S.-K.; Wang, Z.-Q.; Zhang, Y.; Huang, W., Interaction of oxalic acid with dimethylamine and its atmospheric implications. *RSC Advances* **2017,** *7*, (11), 6374-6388.

164.   Xu, W.; Zhang, R., A theoretical study of hydrated molecular clusters of amines and dicarboxylic acids. *J. Chem. Phys.* **2013,** *139*, (6), 064312, DOI: 10.1063/1.4817497.

165.   Miao, S.-K.; Jiang, S.; Chen, J.; Ma, Y.; Zhu, Y.-P.; Wen, Y.; Zhang, M.-M.; Huang, W., Hydration of a sulfuric acid–oxalic acid complex: acid dissociation and its atmospheric implication. *RSC Advances* **2015,** *5*, (60), 48638-48646.

166.   Xu, W.; Zhang, R., Theoretical investigation of interaction of dicarboxylic acids with common aerosol nucleation precursors. *J. Phys. Chem. A* **2012,** *116*, (18), 4539-4550.

167.   Müller, C.; Iinuma, Y.; Karstensen, J.; van Pinxteren, D.; Lehmann, S.; Gnauk, T.; Herrmann, H., Seasonal variation of aliphatic amines in marine sub-micrometer particles at the Cape Verde islands. *Atmos. Chem. Phys.* **2009,** *9*, (24), 9587-9597.

168.   van Pinxteren, M.; Fiedler, B.; van Pinxteren, D.; Iinuma, Y.; Körtzinger, A.; Herrmann, H., Chemical characterization of sub-micrometer aerosol particles in the tropical Atlantic Ocean: marine and biomass burning influences. *J. Atmos. Chem.* **2015,** *72*, (2), 105-125.

169.   Ezell, M. J.; Chen, H.; Arquero, K. D.; Finlayson-Pitts, B. J., Aerosol fast flow reactor for laboratory studies of new particle formation. *J. Aerosol Sci.* **2014,** *78*, 30-40.

170.   Dawson, M. L.; Perraud, V.; Gomez, A.; Arquero, K. D.; Ezell, M. J.; Finlayson-Pitts, B. J., Measurement of gas-phase ammonia and amines in air by collection onto an ion exchange resin and analysis by ion chromatography. *Atmos. Meas. Tech.* **2014,** *7*, (8), 2733-2744.

171.   Giechaskiel, B.; Wang, X.; Gilliland, D.; Drossinos, Y., The effect of particle chemical composition on the activation probability in n-butanol condensation particle counters. *J. Aerosol Sci.* **2011,** *42*, (1), 20-37.

172.   Hermann, M.; Wehner, B.; Bischof, O.; Han, H.-S.; Krinke, T.; Liu, W.; Zerrath, A.; Wiedensohler, A., Particle counting efficiencies of new TSI condensation particle counters. *J. Aerosol Sci.* **2007,** *38*, (6), 674-682.

173.   Kangasluoma, J.; Kuang, C.; Wimmer, D.; Rissanen, M. P.; Lehtipalo, K.; Ehn, M.; Worsnop, D. R.; Wang, J.; Kulmala, M.; Petäjä, T., Sub-3 nm particle size and composition dependent response of a nano-CPC battery. *Atmos. Meas. Tech.* **2014,** *7*, (3), 689-700.

174.   Kulmala, M.; Mordas, G.; Petäjä, T.; Grönholm, T.; Aalto, P. P.; Vehkamäki, H.; Hienola, A. I.; Herrmann, E.; Sipilä, M.; Riipinen, I., The condensation particle counter battery (CPCB): A new tool to investigate the activation properties of nanoparticles. *J. Aerosol Sci.* **2007,** *38*, (3), 289-304.

175.   Mordas, G.; Manninen, H.; Petäjä, T.; Aalto, P.; Hämeri, K.; Kulmala, M., On operation of the ultra-fine water-based CPC TSI 3786 and comparison with other TSI models (TSI 3776, TSI 3772, TSI 3025, TSI 3010, TSI 3007). *Aerosol Sci. Technol.* **2008,** *42*, (2), 152-158.

176.   TSI, Inc. Model 3776 Ultrafine Condensation Particle Counter Operation and Service Manual. P/N 1980522, Revision B, April 2006.

177.   Chen, L.; Ma, Y.; Guo, Y.; Zhang, C.; Liang, Z.; Zhang, X., Quantifying the effects of operational parameters on the counting efficiency of a condensation particle counter using response surface Design of Experiments (DoE). *J. Aerosol Sci.* **2017,** *106*, 11-23.

178.   Hermann, M.; Wiedensohler, A., Counting efficiency of condensation particle counters at low-pressures with illustrative data from the upper troposphere. *J. Aerosol Sci.* **2001,** *32*, (8), 975-991.

179.   Stolzenburg, M. R.; McMurry, P. H., An ultrafine aerosol condensation nucleus counter. *Aerosol Sci. Technol.* **1991,** *14*, (1), 48-65.

180.   Lehtonen, O.; Hartikainen, J.; Rissanen, K.; Ikkala, O.; Pietilä, L.-O., Hydrogen bonding and protonation in acid–base complexes: Methanesulfonic acid-pyridine. *J. Chem. Phys.* **2002,** *116*, (6), 2417-2424.

181.   Xu, J.; Finlayson-Pitts, B. J.; Gerber, R. B., Proton Transfer in Mixed Clusters of Methanesulfonic Acid, Methylamine, and Oxalic Acid: Implications for Atmospheric Particle Formation. *J. Phys. Chem. A* **2017,** *121*, (12), 2377-2385.

182.   Patai, S., *Chemistry of Sulphinic Acids, Esters and Their Derivatives*. Wiley: 1990.

183.   Liptak, M. D.; Shields, G. C., Experimentation with different thermodynamic cycles used for pKa calculations on carboxylic acids using complete basis set and Gaussian-n models combined with CPCM continuum solvation methods. *Int. J. Quantum Chem.* **2001,** *85*, (6), 727-741.

184.   Serjeant, E. P.; Dempsey, B., *Ionisation Constants of Organic Acids in Aqueous Solution*. Pergamon: 1979; Vol. 23.

185.   Hall Jr., H. K., Correlation of the base strengths of amines1. *J. Am. Chem. Soc.* **1957,** *79*, (20), 5441-5444.

186.   Arquero, K. D.; Gerber, R. B.; Finlayson-Pitts, B. J., The Role of Oxalic Acid in New Particle Formation from Methanesulfonic Acid, Methylamine, and Water. *Environ. Sci. Technol.* **2017,** *51*, (4), 2124-2130.

187.   Weast, R. C.; Astle, M. J.; Beyer, W. H., *CRC Handbook of Chemistry and Physics*. CRC Press Boca Raton, FL: 1988; Vol. 69.